1-1-2012

Inducible Deletion of Dicer or Drosha Reveals Multiple Functions for miRNAs in Postnatal Epidermis and Hair Follicles

Monica Teta
University of Pennsylvania, Monica_Teta@comcast.net

Inducible Deletion of Dicer or Drosha Reveals Multiple Functions for miRNAs in Postnatal Epidermis and Hair Follicles

Abstract

miRNAs make up one of the most abundant classes of regulatory molecules as each miRNA is estimated to regulate hundreds of mRNAs. The repressive effects on individual target mRNAs are typically relatively mild and the deletion of individual or even multiple related miRNAs often results in subtle phenotypes. Changes in the miRNA expression profiles of multiple tumor samples, including melenoma and epithelial skin cancers, suggest a widespread alteration in miRNA networks during tumorigenesis. Similarily, miRNA networks are essential for the development of multiple systems, including the hair follicle. Although a few epidermal miRNAs have been studied in adult skin, global miRNA loss has not been evaluated. Two key endonucleases, Dicer and Drosha, are required for miRNA biogenesis; however both enzymes have miRNA-independent functions of processing siRNA or preribosomal RNAs, respectively. To elucidate miRNA function in adult skin, we generated mice with inducible epidermal deletion of each endonuclease and assayed for shared phenotypes. Deletion of *Dicer* or *Drosha* in adult life resulted exclusively in a shared spectrum of phenotypes, indicating that their major function is in miRNA biogenesis, rather than in non-miRNA dependent roles. Interestingly neither enzyme was necessary to maintain resting hair follicles, but both were required during distinct phases of adult hair follicle growth: for the viability of the transient amplifying population; for normal hair shaft formation; and for initiation of hair follicle regression. After prolonged loss of either enzyme, follicular degradation occurred concomitantly with epidermal thickening and dermal inflammation, suggesting additional miRNA roles in hair follicle maintenance and epidermal homeostasis. Analysis of miR-205 targets, a miRNA highly expressed throughout the hair follicle growth cycle, revealed significantly increased levels of Zeb2, and E2F1 in *Dicer* mutant skin suggesting that deregulation of these factors may contribute to *Dicer* and *Drosha* mutant phenotypes, facilitating future studies of their regulation and function in the skin. These results demonstrate specific requirements for miRNAs in maintaining the ability of adult hair follicles to grow and regenerate, and indicate that Drosha and Dicer dependent miRNAs play multiple roles at successive time points of the hair follicle growth cycle.

Degree Type
Dissertation

Degree Name
Doctor of Philosophy (PhD)

Graduate Group
Cell & Molecular Biology

First Advisor
Sarah E. Millar

Second Advisor
Edward E. Morrisey

Keywords
Dicer, Drosha, epidermis, hair follicle, microRNA, skin

Subject Categories
Biology

INDUCIBLE DELETION OF DICER OR DROSHA REVEALS MULTIPLE

FUNCTIONS FOR MIRNAS IN POSTNATAL EPIDERMIS AND HAIR FOLLICLES

Monica Teta

A DISSERTATION

in

Cell and Molecular Biology

Presented to the Faculties of the University of Pennsylvania

in

Partial Fulfillment of the Requirements for the

Degree of Doctor of Philosophy

2012

Supervisor of Dissertation

_____

Sarah E. Millar, Professor of Dermatology

Graduate Group Chairperson

_____

Daniel S. Kessler, Associate Professor of Cell and Developmental Biology

Dissertation Committee

Edward E. Morrisey, Professor of Medicine

George Cotsarelis, Milton Bixler Hartzell Professor of Dermatology

Stephen DiNardo, Professor of Cell and Developmental Biology

Andrei Thomas-Tikhonenko, Associate Professor, Pathology and Laboratory Medicine

DEDICATION

I dedicate this body of work to my grandfather, parents, siblings and friends who stood, and continue to stand with me during the most humble and most exuberant moments of my career.

AKNOWLEDGMENTS

Personal

I have had the very good fortune to work alongside many wonderful people, who also happen to be superb biologists. I have benefited from their kindness and wisdom, more then they may know. With gracious appreciation, I would like to thank: Dr. Doug Cavener, Dr. Barbra McGrath and Amy Frank from the Pennsylvania State University –without your patience and guidance I may not have stepped into this wonderful career so gracefully; Drs. Jake Kushner, Alan Diehl, Peter Kline and Changhong Li, from my early days at The Children's Hospital of Philadelphia –your support and encouragement allowed me to 'aim for the stars'; Dr. Thomas Andl, Dr. Denise Gay, Dr. Fang Liu and Cynthia Douglas–you were pillars of strength when experiments failed and I sought redirection. Finally, I would like to thank my thesis mentor, Dr. Sarah Millar, and my committee members, Drs. Ed Morrisey, George Cotsarelis, Steve DiNardo, and Andrei Thomas-Tikhonenko, -your gentle criticism and collegial advice have propelled me to higher standards.

Academic

ABSTRACT

INDUCIBLE DEPLETION OF DICER OR DROSHA REVEALS MULTIPLE

FUNCTIONS FOR MIRNAS IN POSTNATAL EPIDERMIS AND HAIR FOLLICLES

Monica Teta

Sarah E. Millar

miRNAs make up one of the most abundant classes of regulatory molecules as each

miRNA is estimated to regulate hundreds of mRNAs. The repressive effects on

individual target mRNAs are typically relatively mild and the deletion of individual or

even multiple related miRNAs often results in subtle phenotypes. Changes in the miRNA

expression profiles of multiple tumor samples, including melenoma and epithelial skin

cancers, suggest a widespread alteration in miRNA networks during tumorigenesis.

Similarily, miRNA networks are essential for the development of multiple systems,

including the hair follicle. Although a few epidermal miRNAs have been studied in adult

skin, global miRNA loss has not been evaluated. Two key endonucleases, Dicer and

Drosha, are required for miRNA biogenesis; however both enzymes have miRNA-

independent functions of processing siRNA or preribosomal RNAs, respectively. To

elucidate miRNA function in adult skin, we generated mice with inducible epidermal

deletion of each endonuclease and assayed for shared phenotypes. Deletion of *Dicer* or

Drosha in adult life resulted exclusively in a shared spectrum of phenotypes, indicating

that their major function is in miRNA biogenesis, rather than in non-miRNA dependent

roles. Interestingly neither enzyme was necessary to maintain resting hair follicles, but

both were required during distinct phases of adult hair follicle growth: for the viability of the transient amplifying population; for normal hair shaft formation; and for initiation of hair follicle regression. After prolonged loss of either enzyme, follicular degradation occurred concomitantly with epidermal thickening and dermal inflammation, suggesting additional miRNA roles in hair follicle maintenance and epidermal homeostasis. Analysis of miR-205 targets, a miRNA highly expressed throughout the hair follicle growth cycle, revealed significantly increased levels of Zeb2, and E2F1 in *Dicer* mutant skin suggesting that deregulation of these factors may contribute to *Dicer* and *Drosha* mutant phenotypes, facilitating future studies of their regulation and function in the skin. These results demonstrate specific requirements for miRNAs in maintaining the ability of adult hair follicles to grow and regenerate, and indicate that Drosha and Dicer dependent miRNAs play multiple roles at successive time points of the hair follicle growth cycle.

TABLE OF CONTENTS

CHAPTER TWO. Dicer and Drosha are required in the embryonic hair follicle growth
cycle for hair shaft formation, transition into catagen and maintenance of hair follicle
structures.

CHAPTER FIVE. Analysis of Notch signaling and selected epithelial miR-205 targets in Dicer control and mutant skin

CHAPTER SIX. Conclusion

LIST OF FIGURES

LIST OF FIGURES
(continued)

CHAPTER ONE

Introduction

1.1 Development and maintenance of adult epidermis

The first epidermal markers, keratin 14 (KRT14) and keratin 5 (KRT5) are expressed on day 9.5 of mouse embryonic development, at the single-layered ectodermal stage (Byrne et al. 1994). By embryonic day 14.5, the single-celled germinal layer stratifies, forming a basal progenitor layer and a spinous layer. Once keratinocytes leave the basal layer and differentiate, they discontinue KRT5 and KRT14 production, instead expressing keratin1 (KRT1) and keratin 10 (KRT10) (Byrne et al. 1994). Progeny of the spinous layer migrate upward and differentiate, forming the granular layer. As the granular keratinocytes age, they continue to migrate upward and undergo programmed cell death, releasing their nucleus and cytoplasmic organelles. The compacted layer of dead cells and keratin is cross-linked to form a protective cornified layer, which provides the vital barrier function of the skin (Michel et al., 1988). The cornified layer is open to the external environment, and it is continually shed and replaced throughout life (Figure 1.1). Therefore, epidermal maintenance requires the continuous production of keratinocytes, making the epidermis an ideal model system for studying cell renewal and differentiation.

A number of factors regulate the transition of a basal cell to a suprabasal cell. In the adult, the basal layer is believed to be a niche for the interfollicular epidermal stem cell population (Bickenbach and Mackenzie, 1984; Jones et al., 1995; Potten and Morris, 1988). The transcription factor p63 is necessary for epidermal development, as it is

expressed just prior to KRT5 and KRT14 expression and is required for epidermal stratification (Mills et al., 1999; Yang et al., 1999). In the adult, p63 expression remains in the basal layer of the epidermis and plays roles in cell proliferation and survival (Trong and Kavari, 2007; Senoo et al 2007). During development, Notch receptors 1, 2, 3, and the ligand Jagged 1 are expressed in the suprabasal layers of the developing epidermis, while the ligand Jagged 2 is expressed in the basal layer (Powell et al. 1998; Pan et al. 2004). Activated Notch1 promotes differentiation of the spinous layer and represses p63 and integrin expression (Blanpain and Fuchs, 2009; Moriyama et al., 2008). Recent evidence suggests that activated Notch3 and asymmetric cell division also act in a common pathway to promote the embryonic basal to suprabasal transition (Williams et al., 2011). In the adult, loss of Notch results in hyperproliferation and expansion of basal keratinocytes into the suprabasal layers. Conversely, overexpression of Notch 1 in the granular layer promotes granular keratinocyte differentiation, consistant with a role for Notch1 in adult epidermis in repressing basal fate and promoting suprabasal differentiation (Rangarajan et al. 2001; Nickoloff et al. 2002; Nicolas et al. 2003; Uyttendaele et al. 2004). These studies indicate that the regulation of Notch and p63 localization is essential for epidermal stratification, and adult epidermal homeostasis.

1.2 Enzymatic roles of Dicer and Drosha in miRNA biogenesis

MicroRNAs (miRNAs) are small, endogenously expressed, non-coding RNAs that constitute one of the most abundant classes of gene-regulatory molecules. Nearly one third of all human genes are estimated to be regulated by miRNAs and over one hundred miRNAs are expressed in embryonic skin (Andl et al., 2006; Bartel, 2004; Siomi and Siomi 2010; Yi et al. 2009). MiRNAs are transcribed from the genome by polymerase II as single stranded RNA, termed primary precursor for miRNA (pri-miRNA) (Cai et al., 2004; Lee et al., 2004). The pri-miRNA self-base pairs to form a hairpin-like secondary structure that is processed in a stepwise manner by the RNase III endonucleases Drosha and Dicer (Lee et al., 2003; Lee et al., 2002). MiRNA processing first occurs in the nucleus, as the nuclear enzyme complex Drosha-DGCR8 cleaves the pri-miRNA hairpin at the intersection of single and double stranded RNA (Gregory et al., 2004; Lee et al., 2003). The DGCR8 co-factor is responsible for recognizing and binding the ssRNA that flanks the dsRNA stem of the pri-miRNA, allowing for Drosha to specifically cleave at this site (Han et al., 2006). This results in a smaller hairpin-like intermediate referred to as a precursor miRNA (pre-RNA). The pre-RNA is then recognized by the Exportin5 machinery and is exported out into the cytoplasm where it is accessible by Dicer and its cofactors TRBP and PACT (Lee et al., 2006). TRBP and PACT are not required for pre-miRNA recognition and cleavage, but they increase miRNA accumulation (Lee et al., 2006). The Dicer PAZ-domain and surrounding amino acids form a binding pocket, which anchors the two-base 3' overhang of the pre-miRNA and binds 7-nucleotides within the pre-miRNA phosphodiester backbone (Ma et al., 2004). As a result the pre-

miRNA is cleaved 19-22 nucleotides from the end of the hairpin-like structure, releasing an miRNA duplex that consists of both the guide and passenger miRNA strands (Grishok et al., 2001; Hutvagner et al., 2001; Ketting et al., 2001).

The miRNA duplex is further processed by argonaute 2 (Ago2), an endonuclease and helicase, that recognizes the cleaved miRNA duplex and typically degrades the passenger strand (Liu et al., 2004; Meister et al., 2004; Song et al., 2004). Ago2 along with the mature miRNA then combines with other members of the RISC complex and targets mRNAs for degradation or translational inhibition, with the former occurring more frequently in mammals (Olsen and Ambros, 1999) (Figure 1.2). A single miRNA can repress the production of hundreds of proteins, but the repression is typically relatively mild (Mourelatos, 2008). Furthermore, single or compound miRNA depletion often results in subtle phenotypes that sometimes require the onset of stress such as tissue injury.

In addition to miRNA processing, both Drosha and Dicer have alternate functions. Although Drosha is predominantly known for cleaving miRNAs, Drosha is also present in the nucleoli during S-phase and has been shown to process pre-ribosomal RNAs (Wu et al., 2000). Dicer processes endogenous siRNAs as well as miRNAs, and may even be capable of cleaving miRNA-mRNA duplexes (Bergeron et al., 2010).

1.3 Constitutive epidermal deletion of *Dicer* and *DGCR8* affects postnatal epidermal maintenance

Components of the miRNA biogenesis pathway were independently knocked out in murine epidermis by our lab and the Fuchs lab. Using the Keratin 14 promoter to drive Cre expression constitutively, *Dicer* or *DGCR8* was effectively depleted in the basal layer of the epidermis from embryonic day eleven onward. *Dicer* mutant mice were viable at birth, but did not grow at the same rate as littermate controls. Most mutant mice did not survive past postnatal day seven, possibly due to Keratin 14 promoter activity driving Cre expression in the esophogous and forestomach, although a skin barrier defect was not ruled out. Histology from skin biopsies taken at postnatal day one revealed a normal and intact epidermis, appropriately expressing stratification markers. Interestingly, epidermal Keratin 15, which is expressed in the epidermis at PD1 and is a marker for adult hair follicle stem cells, was lost in the *Dicer* mutant, although the significance of this is not known. Histology at PD7 showed a thickened epidermis, as well as evaginations of dermal cells surrounded by epidermal keratinocytes. Further immunostaining revealed a hyperproliferative basal layer and increased expression of Keratin 17, an epidermal hyperproliferation marker. Conversely Notch1 expression was reduced in comparison to control epidermis. Based on these data, we concluded that while Dicer is not required for epidermal stratification, it appears to have roles in regulating basal keratinocyte proliferation (Andl et al 2006). It was not known whether Dicer has similar roles in adult epidermis, or whether it is strictly required during embryogenesis.

Similarly depletion of DGCR8, a co-factor of Drosha, resulted in epidermal

hyperproliferation, but did not produce defects in epidermal stratification (Yi et al.,

2009). Both *Dicer* and *DGCR8* loss also resulted in expansion of the stem cell-like

marker p63 into the suprabasal layers. Because loss of both components of miRNA

biogenesis resulted in similar epidermal phenotypes, this suggested that miRNAs are

necessary for suppression of epidermal proliferation. In this thesis, I investigate whether

miRNAs are also required for epidermal homeostasis postnatally, and whether Dicer and

Drosha have divergent roles in adult epidermis.

1.4 Embryonic hair germ formation and postnatal hair follicle development

Hair follicles develop during embryogenesis via interactions between the epithelium and

underlying fibroblasts. A dermal signal initiates an epidermal thickening called the hair

placode, and the hair placode in turn promotes the clustering of mesenchymal cells

beneath it. As the mesenchymal cells condense forming a "dermal condensate" they in

turn signal to the placode, causing it to proliferate and invaginate into the dermis forming

a hair germ. As the hair germ develops it produces a transient amplifying population,

known as the matrix. Signaling from dermal condensate stimulates these cells to divide

and differentiate, producing the hair shaft and layered structures that are necessary for

hair shaft support and production, collectively known as the inner root sheath (IRS)

(Millar, 2002). The outer layer of epidermal cells that surrounds the hair follicle forms

the outer root sheath (ORS), and like the epidermis expresses the keratin pair, KRT5 and

KRT14. Hair follicle development is complete when the nascent hair follicles grow

down into the dermis and enter the subdermal fat layer (Figure 1.3). BMP signaling

promotes matrix cell differentiation, and Notch signaling is required for hair shaft and

IRS cell maintenance (Pan et al., 2004).

1.5 The adult hair follicle growth cycle

In adult skin the dermal condensate (see Chapter 1.4) remains closely associated with the

hair follicle, and is known as the dermal papilla (DP). However, although the uppermost

portion of the hair follicle, including the bulge region, is permanently maintained, the

lower epithelial hair follicle undergoes cycles of degeneration and regeneration. This is

referred to as the hair follicle growth cycle and consists of three main phases: a growth

phase (anagen); a regression phase (catagen); and a resting phase (telogen) (Dry, 1926;

Muller-Rover et al., 2001) (Figure 1.4). To maintain these cycles of regeneration, it is

necessary that hair follicles contain a dedicated stem cell population. Hair follicle stem

cells reside in the permanent bulge region of the follicle.

The hair follicle bulge is made up of two distinct populations of cells, a basal layer

present in both the neonate and the adult, and a suprabasal layer that forms only after the

first postnatal hair cycle is initiated (Blanpain et al., 2004). Cells of the bulge express

keratin 15 (KRT15) (Liu et al., 2003), S100A4 (Ito and Kizawa, 2001) and CD34 (Morris

et al., 2004; Tumbar et al., 2004), in addition to outer root sheath markers, including

KRT5 and KRT14. Recent evidence indicates that the bulge is a heterogeneous cell

population, containing cells that support the stem cell niche in addition to stem cells (Hsu

et al., 2011) Unlike epidermal progenitors, which are largely believed to be unipotent,

hair follicle stem cells are capable of producing sebaceous glands and epidermal cells

when transplanted, or in vivo after skin injury (Ito et al., 2005; Levy et al., 2005). Under normal conditions, hair follicle stem cell activity occurs only at the onset of the hair follicle growth phase (anagen).

Once hair follicles develop and reach the end of the growth cycle, proliferation stops and the lower two thirds of the follicle undergo apoptosis in a process known as catagen. The DP and the epithelial follicle regress toward the epidermis (catagen) leaving only the permanent upper structures of the hair follicle including the bulge stem cell compartment (Lindner et al., 1997).   The hair follicle stem cells cease to proliferate by mid anagen and remain quiescent until the onset of a new anagen phase (Cotsarelis et al., 1990; Wilson et al., 1994a; Wilson et al., 1994b). Hair follicles undergo a resting period (telogen) for scarcely a day in young mice but remain in telogen for prolonged periods in older mice. Although the factors that maintain the bulge during these periods have not been fully evaluated, signaling that re-initiates stem cell division is believed to occur from dermal cells (Cotsarelis et al., 1990; Oliver and Jahoda, 1988; Plikus et al., 2008; Reynolds and Jahoda, 1992). Stem cell progeny then migrate downward to form a new matrix population that both surrounds the dermal papilla and differentiates to produce a new IRS and hair shaft (Fuchs, 2007; Millar, 2002; Oshima et al., 2001). The new hair shaft replaces the old one and the hair follicle remains in the growth phase until catagen is initiated again.

To maintain hair follicle cycling throughout the lifespan of the animal, many signaling factors are necessary for the transition and maintenance of the different phases. For

instance timing of the induction of catagen determines how long follicles remain in anagen and the length of the hair shaft. FGF5 activation has been implicated in catagen initiation, as FGF5 is upregulated late in anagen (Rosenquist and Martin, 1996) and loss of FGF5 results in delayed catagen and a phenotype of long hair (the angora phenotype). The EGF signaling family may also be involved in catagen induction, as mice expressing a skin specific, dominant negative EGFR mutation fail to enter catagen and remain in an aberrant anagen stage (Murillas et al., 1995). Beta-catenin signaling and sonic hedgehog signaling are both indispensible for the initiation of a new growth phase (Lo Celso et al., 2004; Van Mater et al., 2003; Callahan et al., 2004; Mill et al., 2003), and bone morphogenetic protein signaling is required for differentiation of the hair shaft and inner root sheath and restricts hair follicle stem cells from proliferating during the resting phase (Andl et al., 2004) Kobielak, K. et al., 2007.). Although we know which pathways are necessary for particular phases of the hair follicle growth cycle, the regulatory pathways responsible for the cyclical initiation and restriction of these signaling molecules must be as intricate as the hair follicle growth cycle itself. The factors that protect the permanent upper hair follicle, including the hair follicle bulge cell population, from destruction and that maintain them during rest are also vital. For instance, adult stem cells are prone to DNA damage since they self-renew for extended periods of time and Bcl-2, an anti-apoptotic factor, is expressed at higher levels in the bulge compared to epidermal progenitor cells (Sotiropoulou et al. 2010). The transient amplifying matrix population of the hair follicle must maintain high proliferation rates to quickly produce the lower hair follicle after rest. Therefore, the hair follicle matrix must also be under significant stress

from telomere shortening, oxidative damage or errors accumulated during DNA synthesis; however the factors that protect this compartment remain unknown.

1.6 *Dicer* and *DGCR8* are required for the completion of hair follicle development

In addition to epidermal hyperproliferation, our lab and others have shown that skin-specific depletion of *Dicer* or *DGCR8* during development results in abrogated hair follicle growth (Andl et al., 2006, Yi et al., 2006). Using the Keratin 14 promoter to drive Cre expression constitutively in the epidermis, *Dicer* or *DGCR8* was effectively depleted from embryonic day eleven onward. Neither *Dicer* nor *DGCR8* mutant mice ever produce a normal coat of hair. Histology from *Dicer* mutant skin at postnatal day one showed that hair follicles had developed but were smaller and less proliferative then controls. By postnatal day seven hair follicles became missangled and produced defective hair shafts that never penetrated the epidermis. Matrix cell proliferation was markedly decreased as indicated by fewer ki67 or phosphohistone H3 positive cells, and cell death was observed in mutant hair follicle bulbs. In situ hybridization for Notch1 revealed reduced Notch1 mRNA levels in the hair follicles, as well as the epidermis.

Skin specific deletion of DGCR8 also resulted in abrogated hair follicle downgrowth and cell death in both hair germs and more mature hair follicle bulbs. The similar hair follicle phenotypes resulting from constitutive epidermal deletion of *Dicer* and *DGCR8* indicated that these defects are predominantly due to miRNA depletion rather than non-miRNA functions of Drosha or Dicer. In this thesis I will address whether miRNAs are required

10

for cyclical hair growth in the adult in addition to functions in hair follicle morphogenesis.

1.7 MiRNA expression and function in the skin

Dicer and Drosha are expressed throughout all skin lineages, suggesting miRNA biogenesis occurs universally in the skin (Yi et al. 2009). Over 100 miRNAs are expressed in embryonic skin, including at least fifteen that are most highly expressed specifically in embryonic epidermis and absent in the hair follicle germ, and six miRNAs that are expressed specifically in developing hair follicles and absent in the epidermis (Andl et al. 2006; Yi et al. 2006). The function of only a few of these miRNAs has been revealed through in vivo loss or gain of function studies. Many miRNAs belong to redundant or partially redundant families so that depletion of a single miRNA may not necessarily reveal its functions. Indeed, RNA regulation may be even more complex as members from different families may share the same mRNA target. Some miRNAs lie within other genes, which can present a technical challenge in knocking out the miRNA and not the gene in which it resides (Kuhnert et al., 2008). Nevertheless, the functions of a few miRNAs have been uncovered in the skin.

In the epidermis, miR-203 is normally expressed in the suprabasal layer and has been shown to repress expression of the proliferative basal cell protein ΔNp63α. When miR-203 is prematurely expressed in the basal layer, the epidermis loses its proliferative potential; conversely when miR-203 is inhibited with a miR-203 antagonist, p63 is expressed inappropriately in the suprabasal compartment resulting in hyperproliferation

of the epidermis (Yi et al. 2008). It has also been shown that miR34a and miR34c, which are expressed in suprabasal epidermal layers, repress the cell cycle proteins cyclin D1 and cyclin dependent kinase 4. In the basal layer p63 represses miR34a and miR34c in the basal compartment, resulting in expression of cyclin D1 and cyclin dependent kinase 4 and allowing for basal cell cycle progression (Antonini et al. 2010). Lastly, overexpression of miR-125b, which is modestly expressed in the basal epidermal layer, leads to a thicker epidermis, suggesting miR-125b may also have roles in regulating epidermal progenitor cells (Zhang et al. 2011). Although other miRNAs have been implicated to have functions in adult epidermis based on tumor expression data, or over expression in certain disease states, to date none of these have been stringently tested in vivo (Braig et al.2010; Chen et al.2010; Satzger et al.2010; Sonkoly et al., 2007; Yu et al., 2008).

To date, only two miRNAs have been implicated in normal hair follicle cycling. The miRNA miR-31, is normally upregulated during anagen and downregulated again during catagen and telogen. Injection of the miR-31 antagonist suggests that miR-31 is necessary for promoting anagen, as hair follicle growth is accelerated in miR-31 inhibited skin (Mardaryev et al. 2010). MiR-125b is normally upregulated in the bulge, but becomes downregulated as stem cell progeny differentiate. When miR-125b is inappropriately expressed in the stem cell progeny in vivo, differentiation of the hair follicle and sebaceous gland is diminished, possibly due to loss of Vitamin D Receptor expression, which is believed to be a direct target of miR-125b in keratinocyes (Mardaryev et al. 2011). Given that at least six miRNAs are differentially expressed in

the hair follicle and that the cyclical expression of many signaling molecules is necessary for the hair follicle growth cycle, it is likely that additional miRNAs are involved in preventing or fine-tuning signaling activity

1.8 Figures and Legends

Figure 1.1 Epidermal development
Schematic representing the process of epidermal development. The germinal layer of the ectoderm stratifies giving rise to the basal and spinous layers. The spinous layer then stratifies producing the granular layer. Finally the cells of the granular layer terminally differentiate forming the cornified layer, and are replenished by continuing basal proliferation and differentiation throughout adult life.

Figure 1.1 Epidermal development
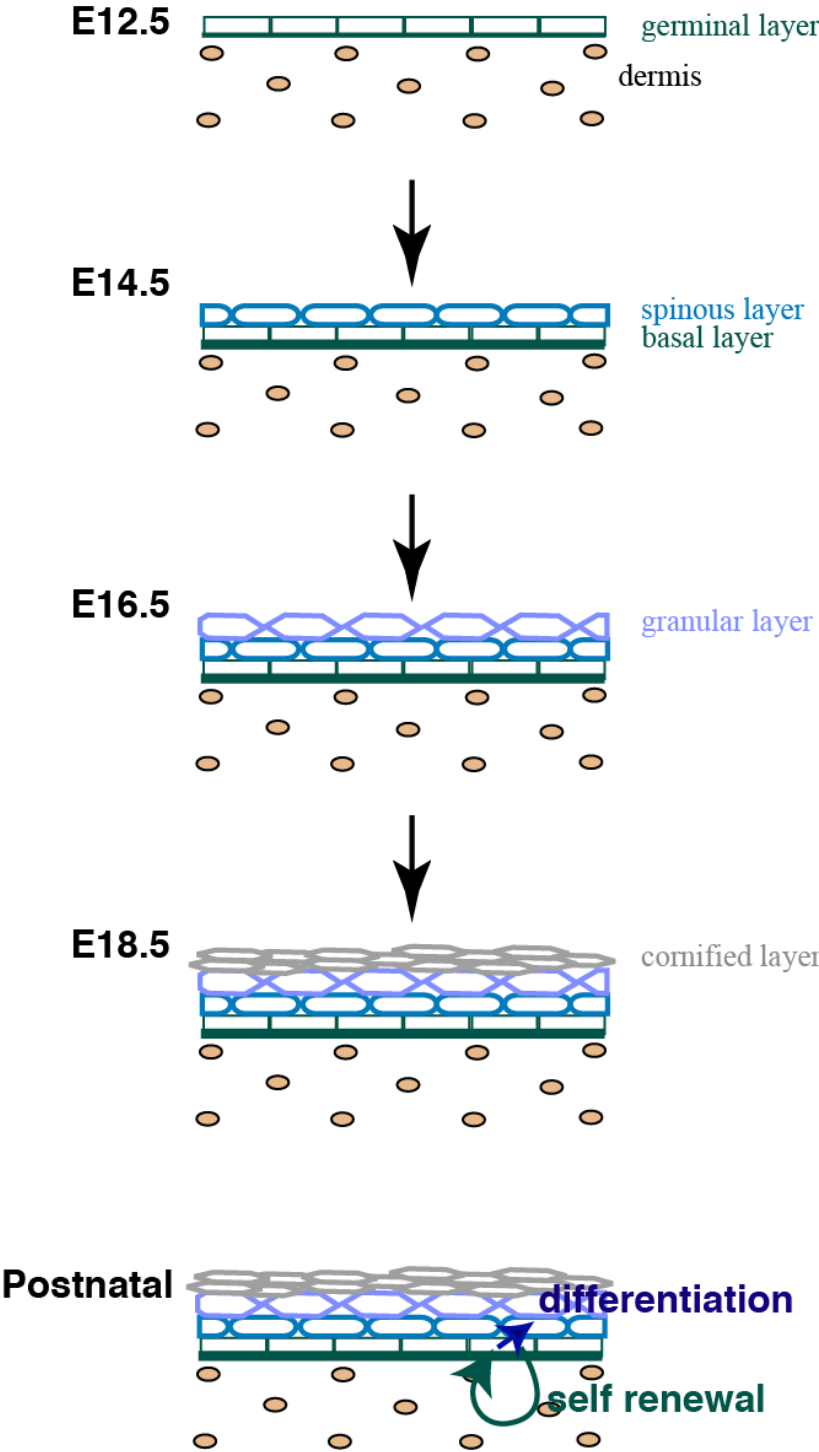
Figure 1.2 The miRNA biogenesis pathway

Diagram showing the steps and components of the miRNA biogenesis pathway. A pri-miRNA is processed into pre-miRNA by Drosha in the nucleus. The pre-miRNA is exported into the cytoplasm by the Exportin5 machinery, where it is cleaved by Dicer, generating a miRNA duplex which is further processed to yield the mature miRNA. The mature miRNA then combines with other proteins to form the RISC complex which targets the mRNA for translational inhibition and/or degradation.

Figure 1.2 The miRNA biogenesis pathway
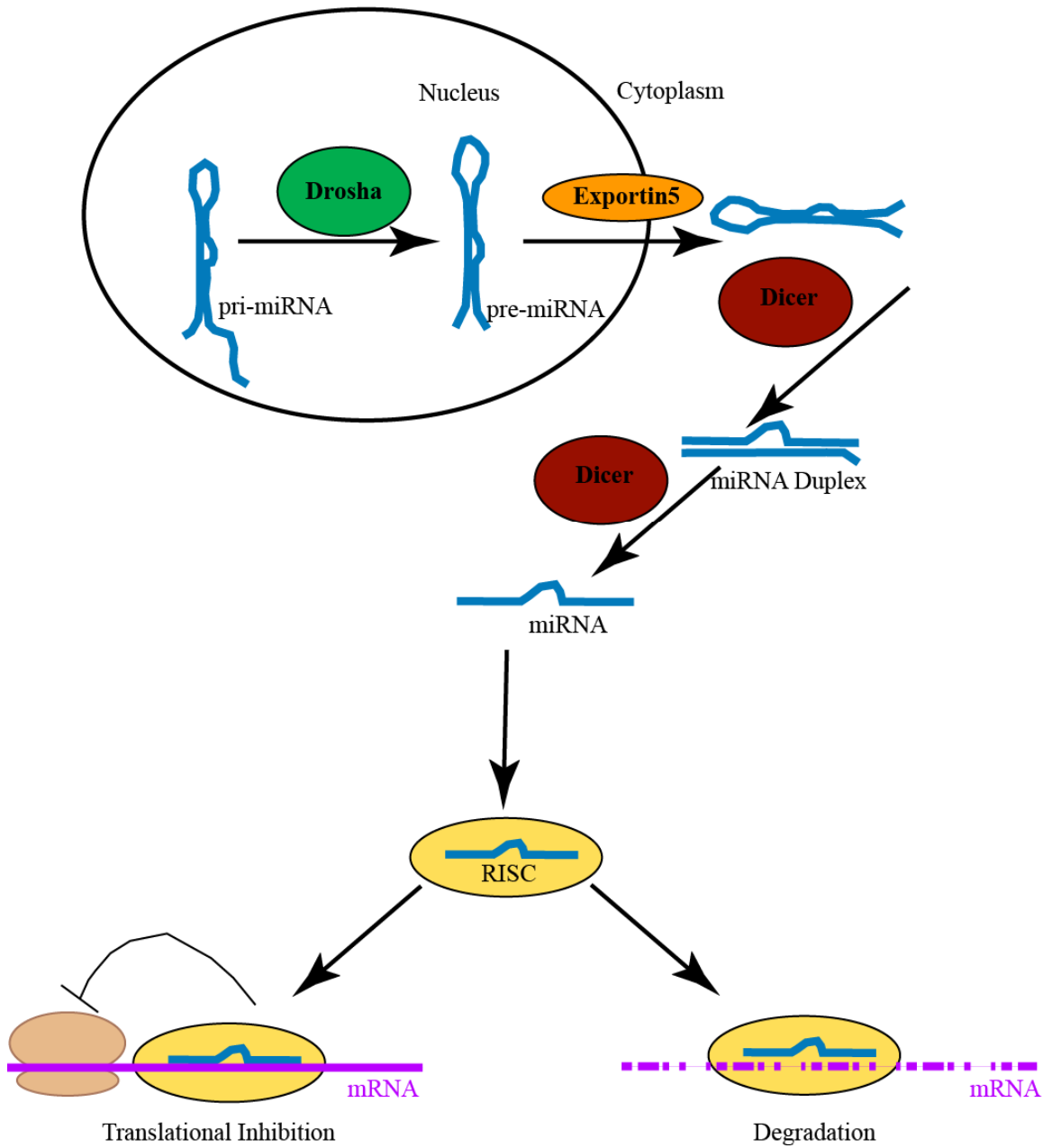
Figure 1.3 Hair follicle development
Schematic depiction of hair germ and hair follicle development. The dermis signals to epidermal cells stimulating development of hair placodes, which in turn promote formation of mesenchymal condensates. The dermal condensate signals the placode to proliferate and invaginate into the dermis, forming the hair germ. The hair germ develop further to form the stem cell compartment (bulge), a transient amplifying population (matrix), the hair shaft, and the inner root sheath. The outer layer of cells that surround the hair follicle forms the outer root sheath, and the dermal condensate develops into the dermal papilla. ORS, outer root sheath; HS, hair shaft; IRS, inner root sheath; DP, dermal papilla; SB, sebaceous gland.

Figure 1.3 Hair follicle development
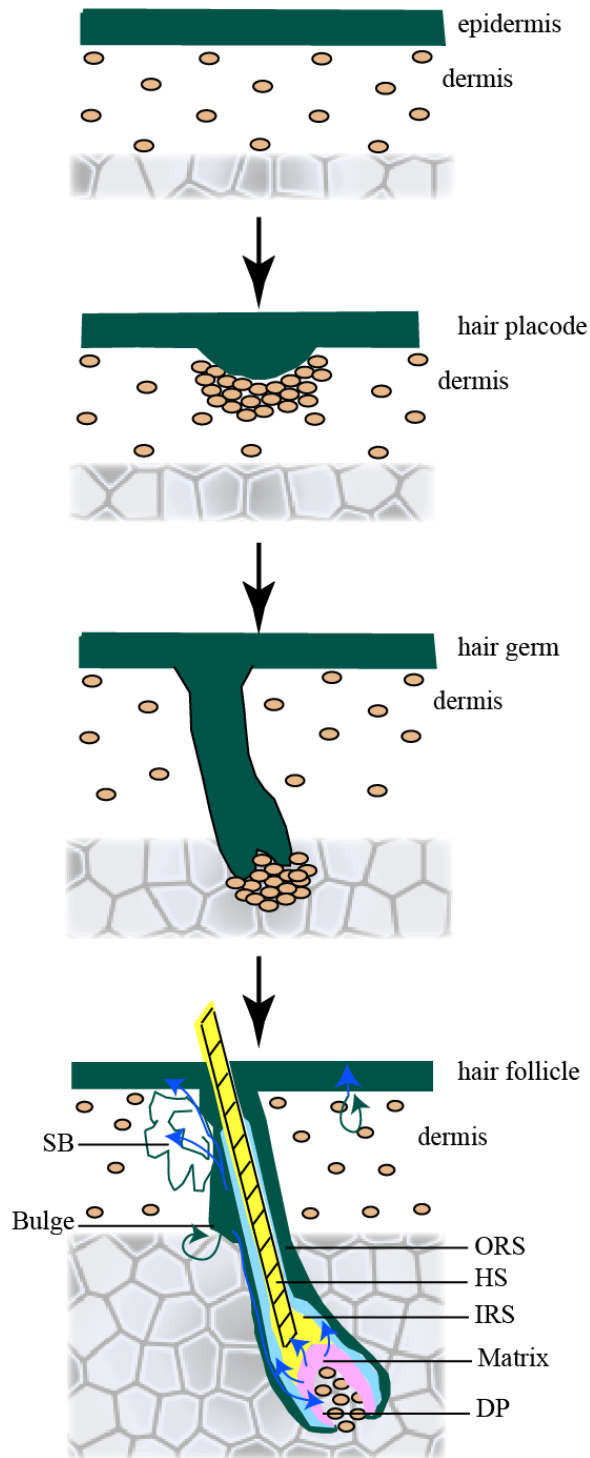
Figure 1.4 The hair follicle growth cycle
Schematic representing the stages of the hair follicle growth cycle. Telogen, upper left: Hair follicles remain at rest and hair follicle stem cells are quiescent. Anagen, right: Hair follicle stem cells are activated transiently, and stem cell progeny produce the structures necessary to generate a new hair shaft. Catagen, bottom: Hair follicles undergo programmed degradation and regress toward the epidermis.

Figure 1.4 The hair follicel growth cycle
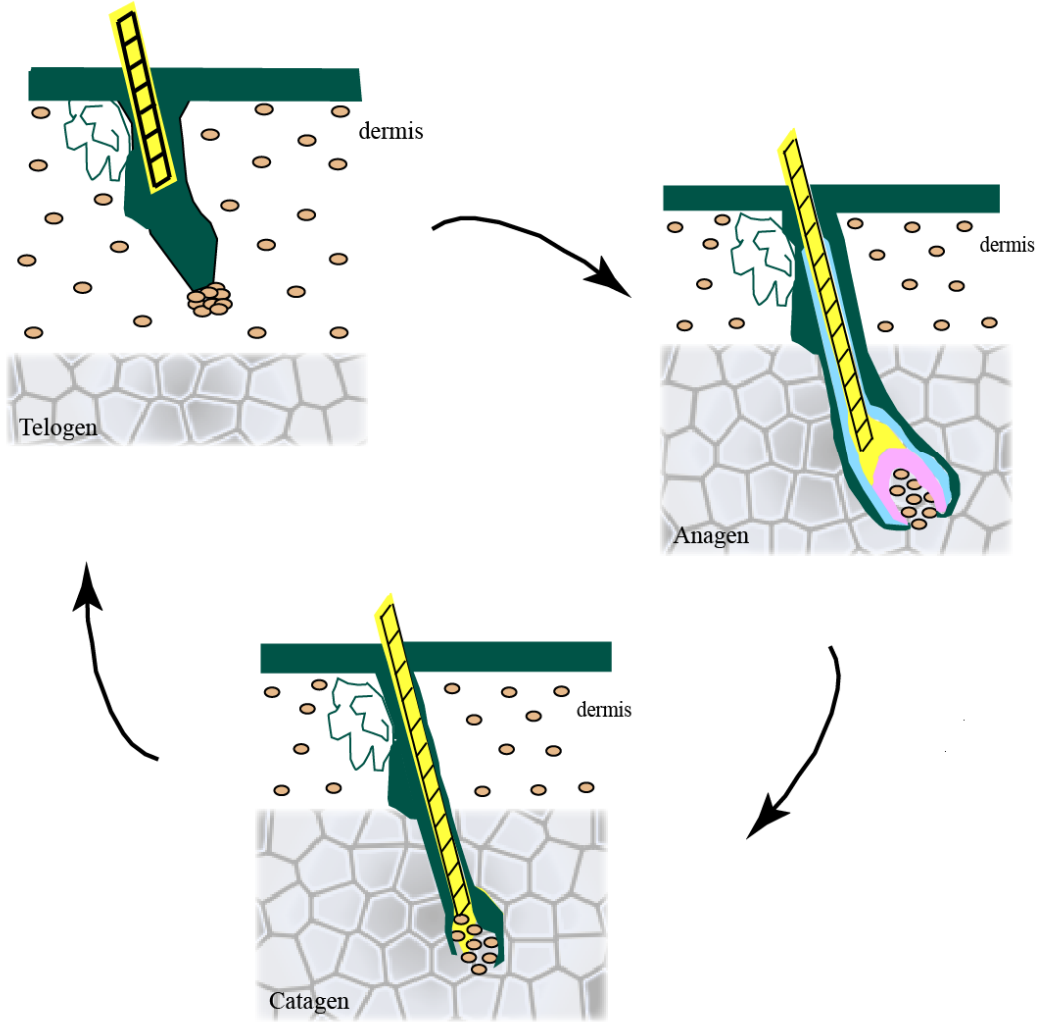
dermis

Telogen

dermis

Anagen

dermis

Catagen

21

CHAPTER TWO.

Dicer and Drosha are required in the embryonic hair follicle growth cycle

for hair shaft formation, transition into catagen and maintenance of hair follicle

structures.

2.1 Abstract

In adult skin, hair follicles are not simply maintained but are cyclically regenerated. This is known as the hair follicle growth cycle and consists of three main phases: growth (anagen), regression (catagen), and rest (telogen). Constitutive epidermal deletion of two members of the miRNA biogenesis pathway, Dicer and DGCR8, a cofactor of Drosha, revealed that these factors are required for completion of hair follicle morphogenesis. Based on these phenotypes and the functions of miRNAs in regulating a large number of mammalian genes, I hypothesized that miRNAs are also important during the postnatal hair follicle growth cycle. To address this we generated epidermal-specific, inducible *Dicer* and *Drosha* mutant mice. Here I show that both Dicer and Drosha are required postnatally for normal hair shaft formation and regression, and for the maintenance of hair follicle structures, and their associated stem cells. I found that levels of EGFR and Notch1 are reduced at early time points following deletion and may contribute to observed hair shaft phenotypes and failed hair follicle maintenance. Similar phenotypes were observed in *Dicer* and *Drosha* mutants, suggesting that they resulted from miRNA depletion. Consistant with this, several direct targets of the highly expressed epithelial-specific miRNA miR-205 were upregulated in Dicer and Drosha mutant skin.

2.2 Introduction

Hair follicles start to form at E14 of mouse embryogenesis, from thickenings of surface

ectoderm that proliferate to produce a hair germ, which then grows downward into the

skin. Around birth, rapidly proliferating matrix cells in the hair bulb begin to

differentiate to form an inner root sheath (IRS), and hair shaft (Millar 2002). Embryonic

deletion of *Dicer* or *DGCR8*, critical components of the miRNA biogenesis pathway,

does not appear to affect early stages of hair follicle development. However,

downgrowth is reduced by PD1, and by PD7 most *Dicer* or *DGCR8* mutant hair follicles

have either evaginated or begun to degrade, suggesting that miRNAs are necessary for

the completion of hair follicle morphogenesis and maintenance of follicle structures (Yi

et al., 2009).

Once hair follicle morphogenesis is completed and a hair shaft has formed (anagen) the

hair follicle undergoes a controlled degradative phase and regresses back toward the

epidermis (catagen), before entering a resting phase (telogen). The first catagen phase

occurs at around PD17 in most mouse strains. Hair follicles typically enter telogen by

PD20, and quickly enter a first postnatal anagen growth phase by PD21. These events

from PD1 to PD20 are referred to as the embryonic hair follicle growth cycle. Hair

follicles continue to undergo successive cycles of growth, regression and rest throughout

adult life; this is referred to as the adult hair follicle growth cycle.

Here, I show that when *Dicer* or *Drosha* is depleted, at or just before birth, a normal

embryonic anagen phase is sustained up until PD12, when dorsal hair on the top of the

head becomes wavy. Histological analysis reveals hair shaft defects in skin from the lower back by PD14. Hair follicles fail to regress and remain in an abnormal anagen until approximately PD24 and then rapidly and permanently degrade. At early time points following deletion, levels of FGF5, EGFR and Notch1 proteins are decreased in mutant skin and are dramatically depleted by PD17. Because these phenotypes are similar in both *Dicer* and *Drosha* depleted skin, I conclude that these effects are likely due to miRNA loss; my data further suggest that loss of miRNAs indirectly disrupts FGF, EGF and Notch signaling.

2.3 Materials and Methods

Generation and breeding of mouse strains, doxycycline induction and genotyping

The *Dicer* conditional allele consists of a floxed cassette replacing the RNaseIII Domain with one flanked by loxP sites (Murchison et al., 2005). Two different mouse lines containing a *Drosha* floxed allele were utilized. One line (denoted Drosha^{GI}) was created by Regeneron Pharmaceuticals Inc (Tarrytown, New York, USA) and contains a floxed gene inactivation cassette flanked by mutant loxP sites (Xin et al., 2005) and inserted between *Drosha* exons 3 and 4. The second Drosha line contains a floxed cassette replacing exon 9 (Chong et al., 2008). *Drosha*$^{fl/fl}$, or *Dicer*$^{fl/fl}$ mice were crossed to bitransgenic mice carrying KRT5-rtTA (a gift from Adam Glick) and tetO-Cre (Gossen et al., 1995) transgenes. The recombination of floxed-alleles was induced by feeding mice doxycycline chow (6g/kg, Bio-serv, Laurel, MD, USA) at E18, PD1, PD38 or PD45.

For analysis of Cre-recombinase activity, mice homozygous for the *Dicer*^{fl/fl} allele and double transgenic for KRT5-rtTA and tetO-Cre were bred to mice containing the Rosa26R Cre reporter allele (Jackson Labs, Bar Harbor, Maine, USA). Recombination was induced by feeding mice doxycycline chow (6g/kg, Bio-Serv, Laurel, MD, USA). Mice were bred and housed at the laboratory animal facility by the University of Pennsylvania and all experimental procedures involving mice were performed according to the guidelines of the IACUC committee of the of the University of Pennsylvania.

Wild-type, floxed and recombined alleles were detected by PCR of tail biopsy DNA or epidermal preparations. *Dicer* alleles were detected by combining the primer ATTGTTACCAGCGCTTAGAATTCC, with CATAGACAATTGTAGACGTAC for the wild type (560nts) and floxed (767nts) alleles or with the reverse primer GTACGTCTACAATTGTCTATG for the recombined allele (429nts). Drosha alleles were detected by combining the forward primer, GATGTGTTGGCAGAAGCTGA, with the reverse primer, CCGGAGCACAACACTAATCA, for detection of the wild type allele (606nts), or the reverse primer, ACATCATGAAGCCCCTTGAG, for detection of the folloxed allele (545nts), or the reverse primer TGCTCAGGTAGTGGTTGTCG for the recombined allele (759nts). The Drosha Exon9 allele was identified using the primer pair GCAGAAAGTCTCCCACTCCTAACCTTC and CCAGGGGAAATTAAACGAGACTCC to detect the wild type (251nts) or floxed (351nts) alleles. The Rosa26R allele was detected using the primers from the "The Jackson Laboratory's Genotyping Protocols Database", available online

Hair Follicle Isolation and RNA extraction

Backskins dissected from three plucked *Dicer* control and three plucked *Dicer* mutant mice were minced with scissors and digested in 1% Collagenase I (Sigma-Aldrich Corp., St. Louis, MO, USA) in HBSS (Invitrogen, Carlsbad, Ca., USA.) for 3 hours at 32°C. Cells were sedimented at 300xg for 5min, washed twice with HBSS and layered on 25ml of 10% Percoll (Sigma-Aldrich Corp., St. Louis, MO, USA), which was layered on top of 5ml of 100% Percoll. Intact follicles were obtained in the fraction between the 10% and100% Percoll layers after 15 min at 20xg. Total RNA was isolated using the miRVana miRNA isolation Kit (Ambion, Austin, TX., USA), and cDNA was generated using the High Compacity Reverse Transcription Kit (Applied Biosystems, Foster City, CA., USA).

Histology, Immunofluorescence, proliferation and TUNEL assay analysis

Skin biopsies from the lower dorsal region were fixed in 4% paraformaldehyde or 10% neutral buffered formalin, dehydrated, paraffin embedded and sectioned at 5μm. For histological analysis, sections were stained with Hematoxylin and Eosin. For Cre-recombinase reporter assays tissue was fixed and stained with X-gal, photographed and/or paraffin-embedded, sectioned and counterstained with Nuclear Fast Red (Sigma-Aldrich Corp., St. Louis, MO, USA). For immunofluorescence staining, sections were rehydrated, microwave pretreated and incubated with primary antibodies against type I

hair keratin (mouse monoclonal antibody clone AE13, Abcam, Cambridge, MA, USA, 1:40); cytokeratin15 (mouse monoclonal antibody, Vector Labs., Burlingame, CA, USA, 1:50); GATA3 (mouse monoclonal antibody HCG3-31, Sigma-Aldrich Corp., St. Louis, MO, USA, 1:100); phospho-SMAD1, phospho-SMAD5 and phospho-SMAD8 (polyclonal rabbit serum, Cell Signaling Technology, Danvers, MA, USA, 1:50); KI67 (mouse monoclonal antibody, Covance, Princeton, New Jersey, USA, 1:40); or phospho-H2A.X (polyclonal rabbit serum, Cell Signaling Technology, Danvers, MA, USA, 1:50). Biotinylated mouse or rabbit and Fluorescein- or Texas Red-conjugated streptavidin secondary antibodies were utilized (all from Vector Laboratories, Burlingame, CA, USA). For immunohistochemistry, sections were microwave pretreated in 10 mM sodium citrate, pH 6.0 and endogenous peroxidase activity was quenched by incubation in 3% hydrogen peroxide for 10 min. All incubations were performed at room temperature unless otherwise stated. FGF5 primary antibody was applied (Santa Cruz Biotechnology Inc., Santa Cruz, CA, USA, 1:50), sections were incubated overnight at 4°C, and then incubated with biotinylated secondary antibodies (Vector Laboratories, Burlingame, CA, USA) for 30 min. Visualization of the bound biotin was performed using Vectastain Elite ABC kit (Vector Laboratories, Burlingame, CA, USA) followed by DAB substrate kit according to manufacture's protocol. For apoptosis assays, the In Situ Cell Death Detection Kit (Roche Diagnostics) was used. Sections were viewed under a Leica DM4000B microscope (Leica Microsystems). Images were captured by using a Leica DC500 digital camera and Leica FireCam software version 1.4 (Leica Microsystems).

miRNA in situ hybridization

All digoxigenin-labeled LNA probes specific to the indicated miRNA were purchased

from Exiqon (Vedbaek, Denmark). Tissue was processed, paraffin embedded and

sectioned as described above and prepared for in situ hybridization according to the

maufacturer's protocol.

Drosha in situ hybridization

Skin sections were baked at 55°C, deparaffinized, and microwaved in 10mM sodium

citrate, pH 6.0 for 10 min. Endogenous peroxidase activity was quenched by incubating

the sections in 3% hydrogen peroxide for 10 min. Sections were incubated in Drosha

primary antibody at 1:100 (Bethyl Laboratories, Montgomery, TX) overnight at 4°C,

washed and incubated in a biotinylated secondary antibody (Vector Laboratories) for 30

min. Visualization of the bound biotin was performed using tge Vectastain Elite ABC kit

(Vector Laboratories), with the DAB substrate kit according to the manufactures protocol

(Vector Laboratories).

Detection of Beta-galactosidase expression in whole tissue

Skin was fixed in 2% PFA for 15min, cut into 1cm strips and stained with 1mg/ml of X-

gal in X-gal staining buffer (5mM Potassium Ferricyanide, 5mM Potassium

Ferrocyanide, 100mM Sodium Phosphate, 0.01% Sodium deoxycholate, 0.02% NP40,

$2.0mMMgCl_2$) at 37C overnight. Tissue was rinsed in Rinse Buffer (100mM Sodium

Phosphate, 0.01% Sodium deoxycholate, 0.02% NP40, $2.0mMMgCl_2$) twice, post-fixed

in 4%PFA for 1hr, and dehydrated, paraffin embedded using Xylene Substitute and

sectioned and rehydrated. Sections were counterstained with Eosin before photography.

Immunoblot analysis

Skin was biopsied from *Dicer* mutant mice induced from PD1-PD12, or PD1-PD15 and,

Dicer and *Drosha* control and mutant mice induced from PD1-PD17. 100mg of skin

tissue was homogenized in 600ul of cold RIPA buffer (150 mM NaCl, 1.0% IGEPAL,

0.5% sodium deoxycholate, 0.1% SDS, and 50 mM Tris, pH 8.0) supplemented with $1\times$

protease inhibitor cocktail for tissues and cells (Sigma-Aldrich, St. Louis, MO), $1\times$

phosphatase inhibitor cocktail I (Sigma-Aldrich, St. Louis, MO), incubated on ice for

1min, and spun at 10,000xg for 15min at 4°C. Equal amounts of lysate were loaded in

Laemelli sample buffer and electrophoresed on 4-to-15% gradient polyacrylamide-

sodium dodecyl sulfate gels (Bio-Rad, Hercules, CA) and then transferred to Hybond

ECL membranes (GE Healthcare, Buckinghamshire, England) using the Bio-Rad

Transblot semidry transfer system. Membranes were blocked for 1 h at room temperature

in Chemicon blocking solution (Millipore, Billerica, MS) and diluted 1:4 in Tris-buffered

saline plus 0.1% Tween 20 (TBST). Incubation in primary antibodies was carried out

overnight at 4°C. Antibodies were diluted into Chemicon blocking solution at the

following dilutions: EGFR, 1:500 (Santa Cruz, Santa Cruz, CA); Notch1, 1: 1000 (Cell

Signaling Technolgies, Beverly, MA); GAPDH, 1:500 (Cell Signaling Technologies,

Beverly, MA). Membranes were washed three times for 5 min in TBST with agitation

and incubated with horseradish peroxidase-conjugated secondary antibodies (Cell

Signaling Technologies, Beverly, MA) diluted 1:1,000 in Chemicon blocking solution

and incubated with the blots for 1 h at room temperature with gentle agitation.

Membranes were washed three times for 5 min in TBST with agitation and

immunoreactive bands were visualized by chemiluminescent detection with the ECL kit

(GE Healthcare, Buckinghamshire, England), exposure to Hyperfilm ECL (GE

Healthcare, Buckinghamshire, England) and development on a Kodak processor.

2.4 Results

Inducible Adult epidermal depletion of Dicer and Drosha

A conditional *Dicer* allele and two independent conditional *Drosha* alleles were used to

disrupt gene expression in adult mice. In the conditional *Dicer* allele, the RNaseIII

domain-encoding exons 22 and 23 are flanked by two loxP sites; in the presence of Cre-

recombinase (Cre) recombination occurs resulting in excision of the majority of both

RNaseIII domains, creating a non-functional allele (Murchison et al., 2005) (Figure

2.1A). The first *Drosha* allele (*Drosha^{GI}*; Regeneron Pharmaceuticals Inc.) contains a

floxed gene inactivation cassette inserted between exon 3 and exon 4. In this system, in

the presence of Cre the gene inactivation cassette is inverted from a transcriptionally-

silent to transcriptionally-active mode (Xin et al., 2005) (Figure 2.1B). In the second

conditional *Drosha* allele (*Drosha^{flEx9}*), exon9 is floxed by loxP sites and in the presence

of Cre, excision results in a nonfunctional allele (Chong et al. 2005; Figure 2.1C). Local

and temporal specificity of *Dicer* or *Drosha* deletion was obtained by utilizing the KRT5-

rtTA, tetO-Cre system. In this system the tet transactivator, rtTA, is expressed under the

control of a KRT5 promoter, which drives expression in the basal layer of the epidermis

and the outer root sheath of the hair follicle, importantly including the hair follicle bulge.

In the presence of the drug doxycyline, rtTA binds to the tetO promoter resulting in Cre expression. Therefore by breeding mice that are bi-transgenic for KRT5-rtTA and tetO-Cre to one of the three conditional alleles described above, and administering oral doxycyline, we are able to achieve temporal control of epidermal specific deletion of *Drosha* or *Dicer*. The results that follow were obtained using the conventional *Drosha* allele, except where noted otherwise.

To analyze the pattern and efficiency of Cre activity, we analyzed the activity of the Cre-reporter, beta-galactosidase, in *Dicer^{fl/fl}, KRT5-rtTA, tetO-Cre* mice carrying the *Rosa26R* Cre-reporter allele. X-gal staining was performed on whole skin biopsied at PD56, following induction from PD38-PD56 and stimulation of hair follicle growth at PD48 by hair plucking. Although Cre-mediated beta-galactosidase expression was slightly mosaic, recombination occurred in the majority of hair follicle epithelial cells and in the epidermis (Figure 2.1D,E). PCR primers that amplify the deleted-floxed *Dicer* locus (see Figure 2.1A) were used to confirm excision in genomic DNA extracted from isolated hair follicles of *Dicer* mutant mice induced from PD38, plucked on PD48 and biopsied on PD56 compared with similarly treated controls (Figure 2.1F). *Drosha* deletion was validated by immunohistochemistry on tissue sections from *Drosha^{GI}* mice induced from PD1-PD24. Immunostaining for Drosha was reduced in *Drosha^{GI}* mutant hair follicles, as well was epidermis, in comparison to the hair follicles and epidermis of control littermates (Figure 2.1G,H).

To determine the effects of *Dicer* and *Drosha* deletion on miRNA production in mutant

hair follicles, we analyzed expression of miR-34c, a miRNA highly expressed in mid

anagen hair follicles, and miR-205, a miRNA strongly expressed in both the epidermis

and hair follicle by in situ hybridization. Expression of both of these miRNAs was

reduced in Dicer mutant hair follicles induced at PD1 and biopsied at PD24, and in

Drosha^{GI} mutant hair follicles induced at E18 and biopsied at PD17 compared to

respective control hair follicles (Figure 2.2 A-H). Seven other miRNAs were also

reduced in *Dicer* mutant hair follicles induced at PD1 and biopsied at PD31 (Figure 2.3).

Drosha or Dicer deletion during the embryonic hair cycle results in alopecia

To determine whether Dicer or Drosha is required during for postnatal hair follicle

growth and cycling we initiated *Dicer* or *Drosha* depletion at, or just before birth and

analyzed skin at successive time points when control hair follicles are in mid-anagen,

catagen or telogen. Twelve days after birth, we observed wavy external hairs on the head

and dorsal neck region of both *Drosha*^{flEx9} and *Dicer* mutants. The growth of wavy hair

progressed posteriorly down to the lower back by PD14 (Figure 2.4A,E). Subsequently,

hair thinning and loss was observed, again progressing in anteroposterior direction

(Figure 2.4B,F). In addition mutants showed a temporary increase in dorsal pigmentation

and dry scaly skin occurring on the lower back (Figure 2.4C,G), before becoming

completely bald (Figure 2.4 D,H). Hair thinning and loss was delayed slightly in

Drosha^{flEx9} mutant compared with *Dicer* mutant mice. This relative delay in onset of hair

loss may be due to more efficient Cre-mediated excision of the *Dicer* allele, and/or to the

more downstream placement of Dicer relative to Drosha in the miRNA biogenesis

pathway. Although the phenotypes appeared slightly earlier in *Dicer* mutants, the progression of wavy hair followed by hair thinning and loss was nearly identical to that observed in *Drosha* mutants, suggesting that Dicer and Drosha play similar roles in postnatal hair shaft production.

Histological analysis reveals failed entry into catagen and hair follicle degradation in *Dicer* and *Drosha*^{flEx9} mutants

To determine the basis for the observed phenotypes, hemotoxylin and eosin staining was performed on sections of dorsal skin from *Dicer* and *Drosha*^{flEx9} mutant and control littermates. At the late anagen time point, when lower dorsal hair was wavy, histology revealed abnormal hair shaft structures in *Dicer* and *Drosha*^{flEx9} mutant hair follicles (Figure 2.5A-D). At later time points, *Dicer* and *Drosha*^{flEx9} mutant hair follicles failed to regress, instead remaining in an abnormal growth phase (Figure 2.5E-G), possibly accounting for the gross observation of increased skin pigmentation relative to control skin that contained regressing and resting hair follicles at this stage. Histologically, keratinized material was seen associated with degrading hair follicles at PD32 in *Drosha*^{flEx9} mutants and PD23 in *Dicer* mutants, accounting for the gross appearance of epidermal scales (also see Figure 3.3 A-D). By PD35 both *Dicer* and *Drosha*^{flEx9} mutant follicles continued to show signs of degradation (Figure 2.5I-J), and by PD50 hair follicles were completely degraded with only remnants persisting (Figure 2.5M-P). Histology revealed that inflammatory cells were closely associated with hair follicle cysts in both *Dicer* and *Drosha*^{flex9} mutants at PD32, and immunological staining for CD11b, a surface antigen present on macrophages, monocytes, granulocytes and natural killer cells,

revealed many more Cd11b positive cells in *Dicer* and *Drosha*^flEx9 mutants compared

with controls (see also Figure 3.4). However, at PD17, when hair follicles displayed hair

shaft defects, an inflammatory response was absent. These observations indicate that

inflammation occurred secondary to hair follicle defects, rather than causing them.

Since mutant hair follicles failed to produce a normal hair shaft we asked whether IRS

and hair shaft differentiation occurred appropriately. To assess this we stained skin

sections from *Dicer* mutant and control mice induced from PD1 until PD17 for GATA3

and AE13, markers of the IRS and hair shaft, respectively. Both GATA3 and AE13 were

expressed in appropriate locations in control and mutant hair follicles, although these

structures appeared slightly irregular in the mutant (Figure 2.6 A-D). We then asked

whether BMP signaling, which is necessary for matrix cell differentiation, occurred

appropriately. To address this we stained *Dicer* mutant and control skin induced from

PD1-PD17 for phospho-smads 1, 5, and 8. Expression of phospho-SMADs 1, 5, and 8

was also not affected (Figure 2.6 E,F). To test for cell death we performed a TUNEL

assay on skin sections from Dicer control and mutant mice. TUNEL positive cells were

observed in the bulb of hair follicles as early at PD14 (Figure 2.6G,H). These results

suggest that matrix, IRS and hair shaft differentiation occurs appropriately in *Dicer*

mutant hair follicles, and suggested that increased matrix cell death, rather then

differentiation defects, are responsible for the observed malformation of the hair shaft in

Dicer and *Drosha*^flEx9 mutants. I will explore this further in Chapter Four.

34

EGF and Notch1 signaling have both been shown to be necessary for normal hair shaft production. EGF signaling is also required for entry into catagen, and Notch1 is required for hair shaft and IRS cell maintenance (Kulessa et al., 2000; Murillas et al., 1995)Vauclair et al. 2005). As these phenotypes were observed in *Dicer* and *Drosha*^{flEx9} mutants, I assayed for expression of EGFR and Notch by immunoblot analysis of *Dicer* and *Drosha*^{flEx9} mutant and control skin lysates from mice induced from E18 until PD17, when mutant hair follicles are still present but hair shafts are defective. These experiments revealed that EGFR and the Notch1 receptor were reduced in *Dicer* and *Drosha*^{flEx9} mutant skin compared to control skin (Figure 2.7A.B). Immunoblots of *Dicer* control and mutant skin lysate taken from mice induced from E18 until PD12 and PD14 showed that the cleaved domain of Notch1 was reduced in the mutant skin as early as PD14 (Figure 2.7A).

To assess whether other signaling molecules involved in the anagen to catagen transition were altered in *Dicer* and *Drosha*^{flEx9} mutants, we examined protein expression of FGF5, a major regulator of the anagen-catagen transition. Immunostaining for FGF5 was performed on sections from *Dicer* control mutant mice induced from PD1 to PD17 and *Drosha*^{flEx9} control and mutant mice induced from E18 to PD17. Both *Dicer* and *Drosha*^{flEx9} mutant hair follicles showed reduced FGF5 expression in the outer root sheath, consistent with failure to enter catagen (Figure 2.7C-F). Since direct miRNA targets are expected to be upregulated in *Dicer* and *Drosha*^{flEx9} mutants, the effects of *Drosha* or *Dicer* depletion on FGF5, EGFR and Notch1 expression are likely to be indirect.

35

2.5 Discussion

Here I show that both Dicer and Drosha are required in late anagen for hair shaft formation. Dicer and Drosha are also required for the transition from anagen into catagen, and for normal FGF5, EGFR and Notch1 expression. Finally Dicer and Drosha are necessary for hair follicle maintenance as mutant hair follicles rapidly degrade at late time points following deletion. These results suggest specific functions for miRNAs in hair shaft production, catagen entry and hair follicle maintenance.

Hair shaft differentiation was not defective in *Dicer* and *Drosha^{flEx9}* mutants, as hair keratins and the IRS marker GATA3 were expressed appropriately. Similarly BMP signaling, observed by phospho-SMAD 1, 5, and 8 expression in the hair follicle bulb, was unaltered in *Dicer* and *Drosha^{flEx9}* mutant mice. However, hair shaft formation was not maintained as external hairs became wavy beginning at PD12 in *Dicer* and *Drosha^{flEx9}* mutant mice, and hair keratin structures observed in skin sections at PD14 in *Dicer* mutants were abnormal. Immunoblot analysis for Notch signaling at PD14 revealed reduced levels of the cleaved domain in *Dicer* mutant skin, indicating reduced Notch activity. BMP signaling promotes matrix cell differentiation (Kulessa et al., 2000), but Notch signaling is required for hair shaft and IRS cell maintenance (Pan et al., 2004). Therefore, the observation of unaltered BMP signaling and reduced Notch activity in late anagen *Dicer* and *Drosha^{flEx9}* mutant skin compared to control skin, correlated with the observed phenotypes of failed IRS and hair shaft maintenance despite normal differentiation.

36

FGF5 expression was attenuated in the ORS of *Dicer* and *Drosha^{flEx9}* mutant hair follicle at PD17. FGF5 is normally upregulated late in anagen, and is implicated in catagen initiation (Rosenquist and Martin, 1996), providing a partial mechanism for the sustained anagen phase observed in *Dicer* and *Drosha^{flEx9}* mutant skin at PD20. Similarily EGFR protein expression was reduced in *Dicer* and *Drosha^{flEx9}* mutant skin by PD17. EGF activity is also likely involved in catagen induction, as mice expressing a skin specific, dominant negative EGFR mutation fail to enter catagen and remain in an aberrant anagen stage (Murillas et al., 1995). These data indicate that the effects of *Dicer* and *Drosha* depletion effect FGF5, EGFR and Notch1 signaling disrupting normal progression through anagen and into catagen. Since Dicer and Drosha both process miRNAs, it is that components or regulatory molecules of these pathways may be direct miRNA targets.

2.6 Figures and Legends

Figure 2.1. Conditional *Drosha* and *Dicer* knockout alleles, and validation of *Dicer* and *Drosha* deletion and Cre expression in the hair follicle (A) Schematic representation of the wild-type and floxed *Dicer* allele. Arrows denote primer positions used for detection of wild type (wt), floxed (fl), and knockout (ko) alleles. WT-F, wild type- forward primer, WT-R, wild type-reverse primer, KO-F, knockout forward primer. (B) Schematic representation of the wild-type and floxed gene inversion *Drosha* alleles. Arrows denote primer positions used for detection of wild type (wt), floxed (fl), and knockout (ko) alleles. GI, gene inactivation; SA, splice acceptor; PA, polyadenylation signal; mLoxP, mutant LoxP sequence; LE, left LoxP element; RE right LoxP element; WT-F, wild type- forward primer, WT-R, wild type-reverse primer; FI-R, -reverse primer; KO-R, knockout-reverse primer. (C) Schematic representation of the wild-type and floxed exon9 *Drosha* alleles. (D,E) X-gal staining (blue) of skin sections from *Dicer^{fl/fl}, KRT5-rtTA, tetO-Cre Rosa26R* mice without doxycycline treatment (D) or doxycycline treated for 18 days (E). X-gal staining (arrows) was absent in the untreated control, and was present in the majority of epidermal and hair follicle epithelial cells in doxycycline treated mutants. (F). PCR analysis using primer pairs flanking the excised locus verifies *Dicer* exons 22 and 23 excision in genomic DNA extracted from isolated epidermis and hair follicles of *Dicer* mutant mice induced from PD38, depilated at PD49, and harvested at PD55, and absence of the recombined allele in identically treated control littermates. (G,H) Immunohistochemistry for Drosha protein in skin sections of PD24 control littermate and *Drosha^{flGI/flGI}, KRT5-rtTA, tetO-Cre* mutant skin following doxycycline treatment from PD1. Nuclear localized Drosha is detected in hair follicles (black arrows) and epidermis (blue arrow) in control skin (G) and is reduced in *Drosha^{flGI}* mutant skin.

Figure 2.1

A *Dicer* Construct

B *Drosha* Floxed-Gene Inversion Construct

C *Drosha* Floxed-exon9 Construct

D *Dicer^{fl/fl}, KRT5-rtTA, tetO-Cre, Rosa26R*

E *Dicer^{fl/fl}, KRT5-rtTA, tetO-Cre, Rosa26R*

Not Induced

Induced (18 days)   50 μm

F Doxycycline-induced hair follicles

Dicer^{fl/fl}, tetO-Cre

Dicer^{fl/fl}, KRT5-rtTA, tetO-Cre

Dicer

Tubulin

G *Drosha^{flGI/flGI}, KRT5-rtTA, tetO-Cre*

H *Drosha^{flGI/flGII}, KRT5-rtTA, tetO-Cre*

Not Induced

Induced (24 days)   50 μm

39

Figure 2.2 Validation of miRNA loss in *Dicer* and *Drosha*^{flGI} control and mutant skin. (A-H) In situ hybridization for *miR-34c* (A-D) and *miR-205* (E-H) in skin from *Dicer* mutant and control littermate mice doxycycline treated from PD1 and assayed at PD12 (A,B,E,F), and *Drosha*^{flGI} mutant and control littermate mice doxycycline treated from PD1 and assayed at PD24 (C,D,G,H). Arrows indicate positive signals (purple or blue). Dark brown/black coloration is due to hair pigmentation. Mutant and control pairs were photographed at the same magnification.

Figure 2.2
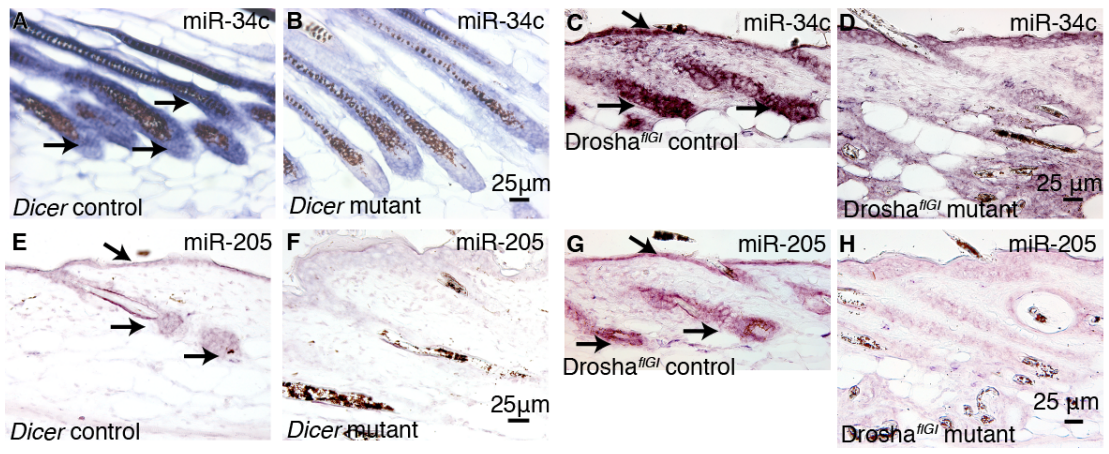
Figure 2.3. ISH shows reduction of multiple miRNAs in *Dicer* mutant hair follicles, in comparison to controls. In situ hybridization using digoxigenin-labeled probes for the indicated miRNAs in PD31 *Dicer$^{fl/fl}$, KRT5-rtTA, tetO-Cre* mutant and control *Dicer$^{fl/fl}$, tetO-Cre* littermate skin following doxycycline treatment from E18. Arrows indicate positive signals (purple). All sections were photographed at the same magnification.

Figure 2.3

25μm

43
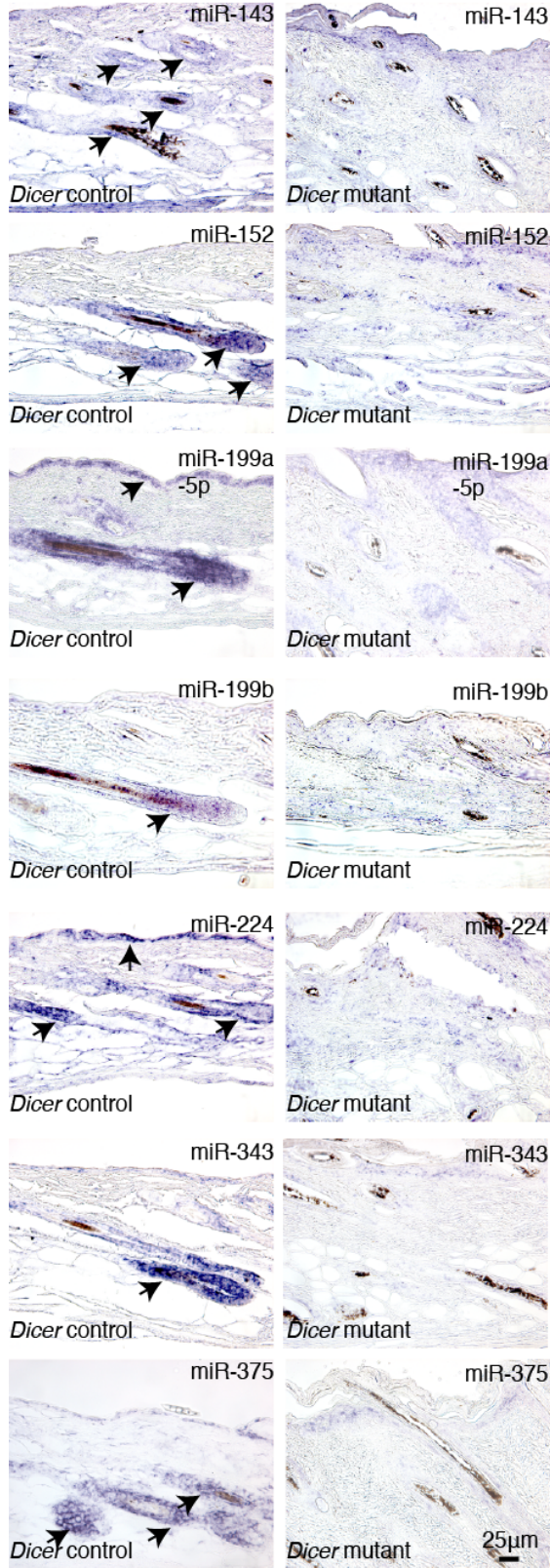
Figure 2.4. Anterior to posterior progression of wavy hair and alopecia in *Dicer* and *Drosha*^{flEx9} mutant mice. (A-D) *Dicer* (E-H) and *Drosha*^{flEx9} control (top) and mutant (bottom) mice, doxycycline treated from PD1 and photographed at the time points indicated. Wavy hair was noted in both mutants by PD14 (A,E, white arrows). Hair loss was observed by PD17 (B,F) and progressed in an anterior-posterior direction (C,G). Scaly skin was observed transiently (D,G, blue arrows), and resolved in an anterior-posterior direction, leaving smooth, permanently hairless skin (D,H).

Figure 2.4
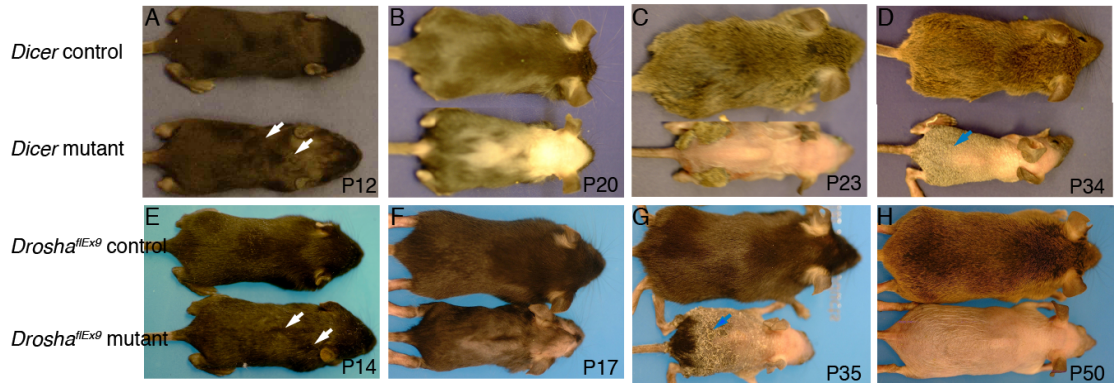
Figure 2.5. Hair shaft defects and failure of catagen in *Dicer* and *Drosha*^{flEx9} mutant skin.   Histology of dorsal skin from *Dicer* and *Drosha*^{flEx9} mutant mice and their control littermates at successive postnatal stages following doxycycline treatment from PD1. Control hair follicles are in anagen at PD14-PD17, telogen at PD20, anagen at PD32-PD35, and have re-entered telogen by PD50. Irregular hair shafts are apparent in mutants by PD14-PD17 (arrows in (B,D). By PD20, mutant follicles fail to regress and begin to show signs of degradation. At PD35, mutant HF show increasing signs of degradation (I,S) and by PD50-PD59 only follicle remnants persist (J,T). Scale bars apply to their respective columns.

Figure 2.5
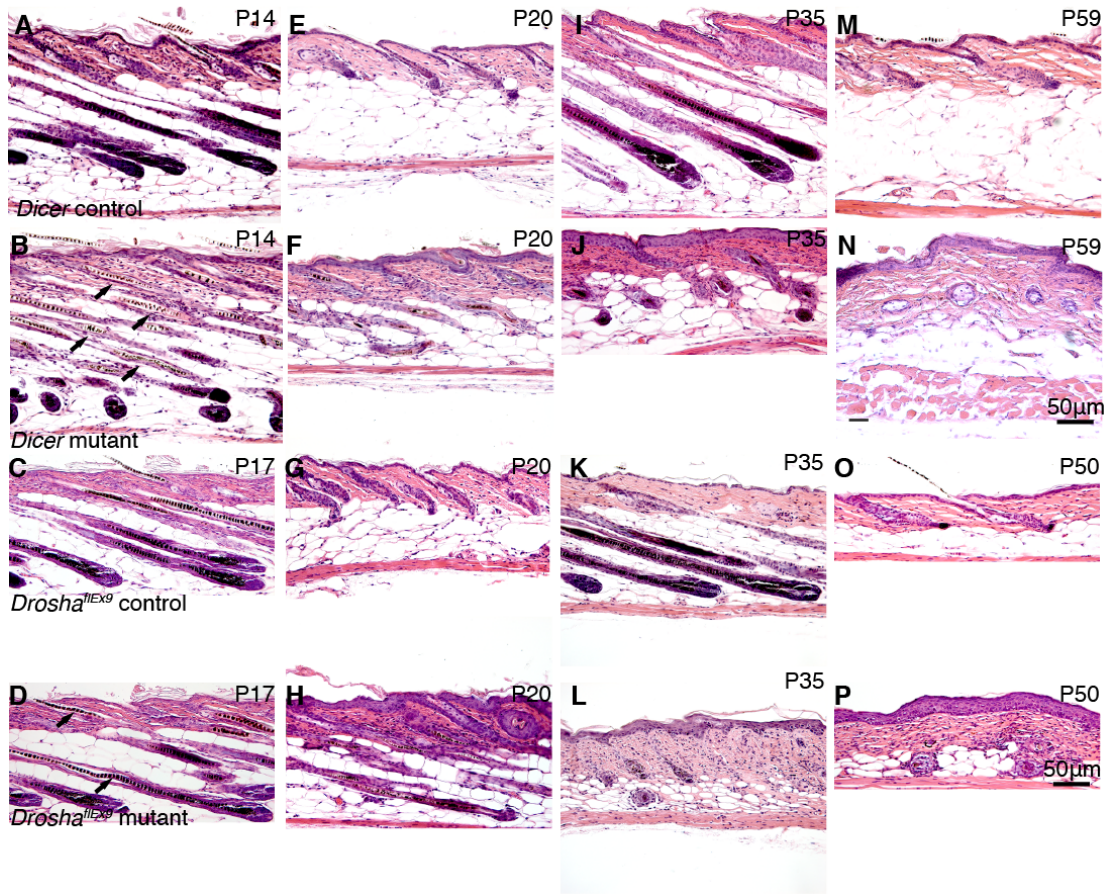
Figure 2.6. IRS and Hair shaft differentiation are unaltered but cell death occurs in the bulb of Dicer mutant hair follicles. Immunostaining of sections from *Dicer* mutant mice induced from birth and biopsied at PD17 or PD14. (A,B). Staining for AE13 (red) in *Dicer* control and mutant skin at PD17. Note hair shafts are abnormal but still AE13 positive in the mutant. (C,D). Staining for GATA3 (green) in *Dicer* control and mutant skin at PD17. (E,F). Staining for phospho-SMADs 1,5, and 8 (red) in *Dicer* control and mutant skin at PD17. (G,H). TUNEL assay for cell death was performed on *Dicer* control and mutant skin biopsied at PD14. TUNEL positive nuclei (green) were found in hair bulbs of *Dicer* mutant skin.

Figure 2.6
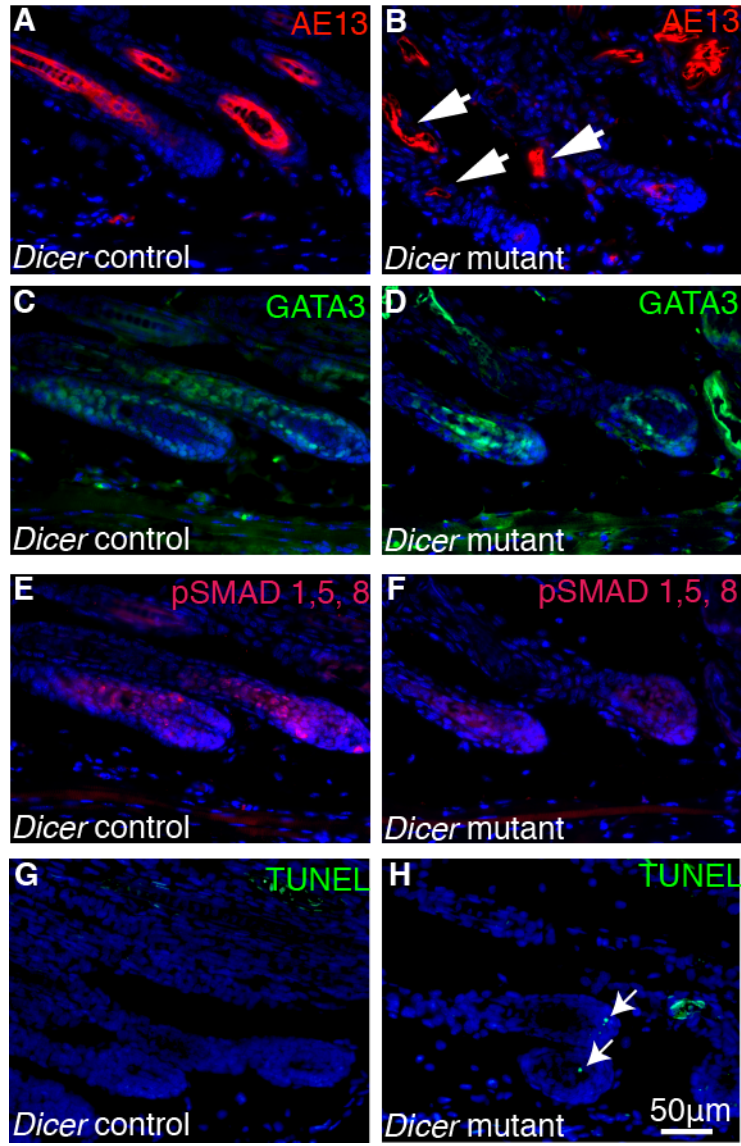
**Figure 2.7. EGFR, Notch1 and FGF5 are downregulated in Dicer and *Drosha^{flEx9}*
mutant skin.** (A,B) Immunoblotting for full length (FL) Notch1, Notch1 NICD,
GAPDH or beta-actin using *Dicer^{flEx22-23}* (A) and *Drosha^{flEx9}* (B) mutant and littermate
control skin extracts at the time points indicated, following doxycycline treatment from
E18. (C-F) Immunohistochemistry for FGF5 (brown) in PD17 dorsal skin sections from
Dicer mutant (D) and control littermate (C) and *Drosha^{flEx9}* mutant (F) and control
littermate (E) following doxycycline treatment from PD1. Black arrows in (C,E) indicate
expression of FGF5 in the ORS of control hair follicles. Dark brown-black cells are
pigmented.

Figure 2.7

A

| | *Dicer* Control | *Dicer* Mutant | *Dicer* Control | *Dicer* Mutant | *Dicer* Control | *Dicer* Mutant |

EGFR

FL Notch

CL Notch

GAPDH

PD12   PD14   PD17

B

Drosha^flEx9 Control   *Drosha^flEx9* Mutant

EGFR

FL Notch

CL Notch

Beta-Actin

PD17

Dicer control   *Dicer* mutant

C   P17   D   P17

FGF5   FGF5   100μm

Drosha^flEx9 control   *Drosha^flEx9* mutant

E   P17   F   P17

FGF5   FGF5   100μm

51
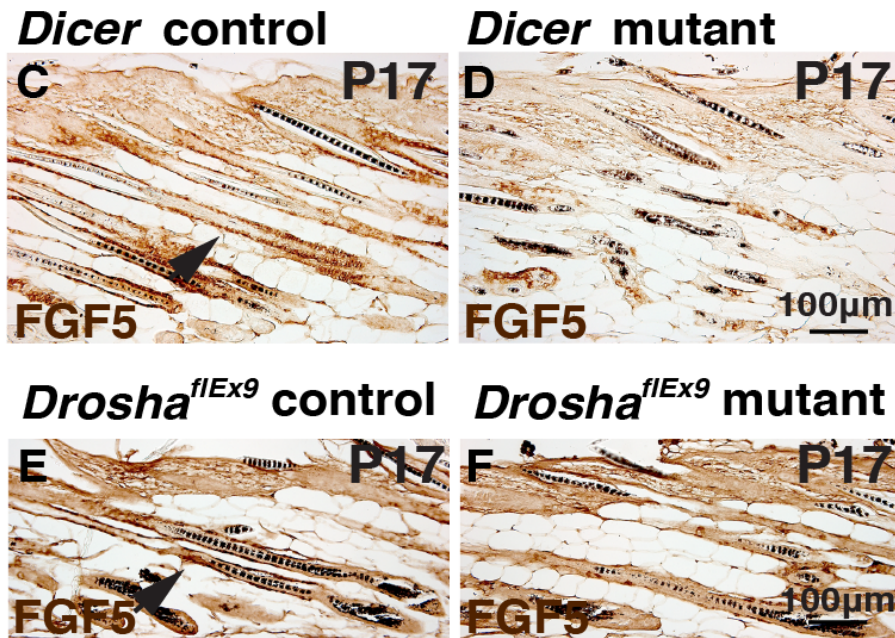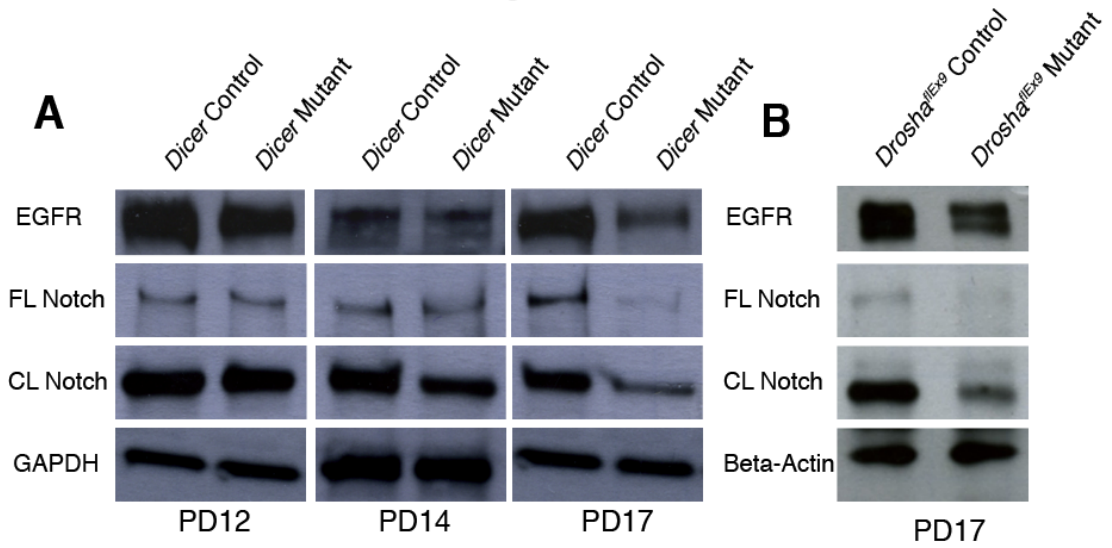
CHAPTER THREE.

Dicer and Drosha are required for adult epidermal homeostasis

3.1 Abstract

Previous studies have shown that hyperproliferation and expansion of the proliferative

p63-positive compartment occur when epidermal *Dicer* and *DGCR8* are depleted early in

embryogenesis. Although miR-203 directly targets p63 in the non-proliferative,

suprabasal layer, and p63 is known to promote proliferation partly by suppressing miR-

34 family members, the involvement of other miRNAs in adult epidermal homeostasis

has not been evaluated. Here we use two independent approaches to disrupt miRNA

biogenesis, by inducibly depleting either *Dicer* or *Drosha* specifically in the epidermis of

adult mice. We find that depletion of either *Dicer* or *Drosha* in adult life results in

epidermal hyperproliferation and expansion of the p63-expression domain. We also

observe that, in both epidermal-specific *Dicer* and *Drosha* mutant skin, dermal

inflammation occurs concomitantly with epidermal hyperproliferation. Inflammation is a

novel finding in *Dicer* and *Drosha* mutant skin; however, a variety of other skin-specific

mutations have been reported to cause both epidermal hyperproliferative and hair follicle

degradation, suggesting that these processes may be related. In addition, the

inflammatory cytokine TSLP was elevated in mutant skin and is a sensitive assay for

mild barrier defects, suggesting this is a possible mechanism contributing to

inflammation. Interestingly, the inflammatory response to acute wounding was similar in

Drosha or Dicer mutants and controls. This observation suggests that miRNA-depleted

cells are not intrinsically more sensitive to inflammatory insults then controls, but that

degrading hair follicles and/or mild barrier defects elicit an inflammatory response in unwounded mutant skin.

3.2 Introduction

MiRNA production has been disrupted in many systems by obstructing the function of

one of two enzymes necessary for miRNA biogensis, Drosha or Dicer. Global loss of

Dicer function results in early embryonic lethality, and inducible deletion of *Dicer* in

mouse embryonic stem cells causes defects in proliferation, suggesting that Dicer may be

necessary for stem cell maintenance in certain systems. When *Dicer* or *DGCR8*, a

cofactor of Drosha, are specifically depleted in the KRT14 compartment during

embryogenesis, the epidermis stratifies normally but becomes hyperproliferative

(Antonini et al., 2010; Lena et al., 2008; Yi et al., 2008). Depletion of either protein also

results in increased expression of the progenitor cell-associated protein p63 (Antonini et

al., 2010; Lena et al., 2008; Yi et al., 2008). The p63 protein is a member of the p53

tumor suppressor family, and in the skin is required for normal epidermal homeostasis.

There are numerous p63 isoforms, but the main isoform expressed in the basal layer of

the epidermis is ΔNp63α, which has been shown to be a direct target of miR-203 (Lena et

al. 2008). MiR-203 is predominantly expressed in the suprabasal layer, and by

suppressing p63 expression is thought to promote suprabasal differentiation (Lena et al.

2008; Yi et al. 2008). In myloid cells miR-92 regulates the p63-isoform, ΔNp63β,

(Manni et al., 2009) but the miRNA regulation of other p63-isoforms in the skin has not

been evaluated. However, the miR-34 family is directly regulated by p63, and miR-34a

and miR34c have been shown to directly suppress Cyclin D1 and cyclin dependent kinase

4 in keratinocyes. In vivo, the miR34 family is presumed to function in the suprabasal

layers of the epidermis, where cell cycle progression is undesirable (Antonini et al.,

2010). Although miR-203 and the miR-34 family are involved in adult epidermal

homeostasis, many additional miRNAs are expressed in embronic and adult skin, suggesting that other miRNAs may play regulatory roles in the epidermis. Because either epidermal *Dicer* and *DGCR8* have only been depleted constitutively, it is not known whether these phenotypes arise from defects in epidermal development and/or comitment, or whether more factors are also actively required in adult life. Since DGCR, which is specifically necessary for miRNA and not pre-ribosomal processsing, was depleted it is not known if Drosha has major non-miRNA roles in adult epidermal maintenance. Therefore a direct comparison between the loss of *Dicer* and the loss of *Drosha* in adult skin is warranted to elucidate both miRNA and non-miRNA functions in established skin. Here I will show that inducible deletion of either *Dicer* or *Drosha* in adult skin causes epidermal hyperproliferation. Phenotypes were identical in the two mutants, indicating non-miRNA functions of either enzyme are minimal in adult epidermis. However, we found that these phenotypes coincide with hair follicle degradation, and since dermal inflammation was associated with follicular degradation these processes may be related to the epidermal phenotypes. Healing of acute wounds was only slightly impaired in Drosha and Dicer mutants. Levels of inflammation and the rate of wound closure following acute wounds occurred normally; however, the healing epidermis appeared disorganized in both Dicer and Drosha mutants. These data suggest in addition to intrinsic depletion of epidermal miRNAs, dermal inflammation may contribute to epidermal hyperproliferation in *Dicer* or *Drosha* mutant skin. Dicer and Drosha are also required for proper formation of the healing epidermis during wound healing.

3.3 Materials and Methods

Generation and breeding of mouse strains, doxycycline induction and genotyping

As described in Chapter Two, mice carrying either a *Dicer* conditional allele (Murchison et al., 2005), or a *Drosha^{flEx9}* conditional allele (Chong et al., 2008) were bred to bitransgenic mice carrying the *KRT5-rtTA* (gifted from Adam Glick) and *tetO-Cre* (Gossen et al., 1995) transgenes. For analysis of Cre-recombinase activity, mice homozygous for the *Dicer* floxed allele (*Dicer$^{fl/fl}$*) and double transgenic for *KRT5-rtTA* and *tetO-Cre* were bred to mice carrying the Rosa26R Cre reporter allele (Jackson Labs, Bar Harbor, Maine, USA). Recombination was induced by feeding mice doxycycline chow (6g/kg, Bio-Serv, Laurel, MD, USA). For specific depletion in hair follicles stem cells mice homozygous for the Dicer$^{fl/fl}$ allele were bred to mice carrying a KRT15-CrePR1 transgene (Morris et al. 2004) and the Rosa26R allele (Jackson Labs, Bar Harbor, Main, USA). All mice were bred and housed at the laboratory animal facility by the University of Pennsylvania and all experimental procedures involving mice were performed according to the guidelines of the IACUC committee of the University of Pennsylvania. Wildtype and the *Dicer* transgenic alleles were detected by combining the primer ATTGTTACCAGCGCTTAGAATTCC, with TCGGAATAGGAACTTCGTTTAAAC for the wild type (560nts) and floxed (767nts) alleles or with GTACGTCTACAATTGTCTATG for the recombined allele (429nts). The wildtype and *Drosha* alleles were identified using the primer pair GCAGAAAGTCTCCCACTCCTAACCTTC and CCAGGGGAAATTAAACGAGACTCC to detect the wild type (251nts) or floxed (351nts) alleles. The Rosa26R allele was detected using the primers from the "The

Jackson Laboratory's Genotyping Protocols Database", available online

(http://jaxmice.jax.org/protocolsdb/f?p=116:2:3075908288454288::NO:2:P2_MASTER_
PROTOCOL_ID,P2_JRS_CODE:4615,012695).

Epidermal isolation and quantitative RT-PCR for miRNAs

The underside of backskin from *Dicer* control or mutant mice, induced from PD1-PD15,

was scraped with a razor blade to remove subcutaneous fat, and was treated with 2.4U/ml

of dispase II (Roche Diagnostics, Indianapolis, Ind., USA) at 35°C for 2hrs to separate

epidermis from dermis. Quantitative real-time RT-PCR was performed on total RNA

samples extracted from the epidermis (miRVana miRNA isolation Kit, Ambion, Austin,

TX., USA). cDNA for individual miRNAs was generated using the TaqMan miRNA

Reverse Transcription Kit (Applied Biosystems, Foster City, CA., USA). Samples were

amplified by using the TaqMan Universal PCR Master Mix, No AmpErase UNG

(Applied Biosystems, Foster City, CA., USA) and analyzed on an AB Step One Plus Real

Time PCR System (Applied Biosystems, Foster City, CA., USA). Both real time and RT

primers were purchased from Applied Biosystems (TaqMan miRNA assays, Applied

Biosystems, Foster City, CA., USA).

Histology, Immunofluorescence, and X-gal staining

Skin biopsies from the lower dorsal region were fixed in 4% paraformaldehyde or 10%

neutral buffered formalin, dehydrated, paraffin embedded and sectioned at 5μm. For

histological analysis, sections were stained with Hemotoxylin and Eosin. For Cre-

recombinase reporter assays tissue was fixed in 2%PFA for 15min. Skin was cut into

1cm strips and stained with 1mg/ml of X-gal in X-gal staining buffer (5mM Potassium Ferricyanide, 5mM Potassium Ferrocyanide, 100mM Sodium Phosphate, 0.01% Sodium deoxycholate, 0.02% NP40, $2.0mMMgCl_2$) at $37°C$ overnight. Tissue was rinsed in Rinse Buffer (100mM Sodium Phosphate, 0.01% Sodium deoxycholate, 0.02% NP40, $2.0mMMgCl_2$) twice, photographed or post-fixed in 4%PFA for 1hr, dehydrated, paraffin embedded, and sectioned and rehydrated as usual with the exception of using Xylene Substitute in place of Xylene. Sections were counterstained with Eosin (Sigma-Aldrich Corp., St. Louis, MO, USA) before photography.   For immunofluorescence staining, sections were rehydrated, microwave pretreated and incubated with primary antibodies against CD34 (polyclonal rabbit, Abcam, Cambridge, UK); CD11b (rat monoclonal antibody, Millipore, Billerica, MA1:50); cytokeratin10 (mouse monoclonal antibody, Covance, Princeton, New Jersey, USA, 1:500); Ki67 (mouse monoclonal antibody, Covance, Princeton, New Jersey, USA, 1:40); p63 (mouse monoclonal, Neomarkers, Fremont, USA, 1:100); or phospho-H2A.X (polyclonal rabbit serum, Cell Signaling Technology, Danvers, MA, USA, 1:50).

Toluidine Blue Staining for Mast Cells

For the detection of mast cells, paraffin embedded skin sections were deparaffinized and rehydrated. The sections were stained in toluidine blue solution for 3 minutes and then washed with distilled water three times. The stained sections were dehydrated quickly with ethanol at graded concentrations, cleared in xylene substitute, and mounted.

Wound healing

Dicer and *Drosha* control and mutant mice were fed doxycycline chow (6 mg/kg, Bio-Serv, Laurel, MD, USA) at PD48, ten days prior to wounding. At PD58 1cm^2 full thickness skin was excised from the upper back an anesthetized mouse. Wounds were allowed to heal uncovered for eight days before the wounded region was biopsied. Wounding and all other experiments involving mice were performed in accordance with guidelines of the IACUC committee of the University of Pennsylvania. The numbers of CD11b+ and TBO+ cells in each sample were counted in at least six fields of view at the wound edge. 1.42 square millimeters of field area was used for each view. The number of mast cells obtained from each field was divided by 1.42 and expressed as the number of mast cells per mm^2. The results were presented as mean ± SEM for two control and two mutant mice.

3.4 Results

Generation of *Dicer* and *Drosha* mutant mice and validation of miRNA loss

To elucidate the role of Dicer and Drosha in postnatal hair development, it was necessary to generate inducible conditional *Dicer* and *Drosha* mutant mice. As discussed in Chapter Two, we utilized a conditional *Dicer* allele or one of two conditional *Drosha* alleles: either a gene inversion allele (Drosha^{GI}) or the conventional, conditional *Drosha* allele (*Drosha^{flEx9}*). Mice carrying either conditional allele were bred to mice bitransgenic for *KRT5-rtTA, tetO-Cre*. This system allows for the spatial and temporal excision of a portion of the conditional allele creating a non-functional gene, but only when the drug doxycycline is administered orally. Mice homozygous for a conditional

allele and bitransgenic for *KRT5-rtTA, tetO-Cre* allow for doxycycline-inducible deletion of *Dicer* or *Drosha* in the KRT5 progenitor expressing compartment of the skin and descendants of KRT5 promoter active cells, which include the entire epidermis and hair follicle epithelia.

Validation of Dicer, Drosha and miRNA loss in the epidermis

Efficiency of Cre expression was analyze by breeding in the Cre-reporter allele, Rosa26R, to the *Dicer*^{fl/fl}, KRT5-rtTA, tetO-Cre mouse line. Following induction from PD38-PD56, skin was biopsied and beta-galactosidase expression was analyzed by X-gal staining. Although Cre-mediated beta-galactosidase expression was slightly mosaic, recombination occurred in the majority of epidermal cells (Figure 3.1A). Epidermal *Dicer* and *Drosha* depletion was then validated by semi-quantitative PCR analysis. PCR primers, amplifying the deleted-floxed *Dicer* locus (Figure 2.1A) were used to confirm excision in genomic DNA isolated from the epidermis of *Dicer* mutant mice induced from PD38-PD55 (Figure 3.1B). RT-PCR analysis of RNA extracted from the epidermis of *Drosha*^{GI} mutant mice treated with oral doxycyline from PD1-PD26 showed reduced *Drosha* mRNA expression (Figure 3.1C).

To determine the effects of *Drosha* and *Dicer* deletion on miRNA production we analyzed the expression of several miRNAs by quantitative-real time PCR.   Mice were induced from birth and skin was biopsied at PD15. The epidermis was isolated from total skin and total RNA was extracted. We found miR-16, miR-205, miR-27b, miR-100 and

miR-140 were all reduced in both *Dicer* and *Drosha*^{flEx9} mutant mice compared with controls (Figure 3.1D).

Dicer and Drosha are necessary to repress progenitor cell proliferation in adult epidermis

We first validated the role of Dicer as a suppressor of epidermal progenitor cell proliferation (Antonini et al., 2010; Lena et al., 2008; Yi et al., 2008), during telogen. *Dicer* mutants induced for fifty-four days (PD38-PD92) began to show epidermal thickening (Figure 3.2A,B), and assays for proliferation carried out after ninety days of induction in *Dicer* mutant mice (PD38-PD128) revealed increased numbers of Ki67 positive cells compared with littermate controls (Figure 3.2C,D). Expression of p63 was also expanded, and increased number of KRT10-expressing cells resided in the KRT10 layer in mutant epidermis (Figure 3.2E,F).

Mutant skin was next evaluated during the growth stage of the hair follicle growth cycle. *Dicer* mice were induced at birth and assayed at PD7, PD17, and PD32, and *Drosha*^{flEx9} mice were induced at birth and assayed at PD8, PD17, and PD32. The epidermis became thicker by PD32 in *Dicer* and *Drosha*^{flEx9} mutant mice, and cornified material was observed to be closely associated with the epidermis, forming a scab like structure above the skin (Figure 3.3M-P). Immunological staining revealed an increased number of ki67-expressing cells (Figure 3.3 Q-T), as well as expansion of p63-expressing cells into the KRT10-expressing layer (Figure 3.3U-V). These data indicate that both *Dicer* and *Drosha* have shared roles in the skin, and their absence in the KRT5-positive

compartment leads to hyperproliferation of the basal layer of the epidermis. In contrast, Ki67 and p63 expressing cells were not over-represented in mutant epidermis at the PD17 time point, indicating that the epidermis was not hyperproliferative at this time point (Figure 2.5A-L).

Dicer and _Drosha_ loss in the KRT5 compartment leads to dermal inflammation

Because the deregulation of epidermal homeostasis is not evident until late time points, we asked if other aspects of _Dicer_ or _Drosha_ loss in the skin could contribute to epidermal expansion. Since hair follicles degrade in late anagen time point and following long time periods in older mice, in which hair follicles cycle spontaneously but asynchronously, we asked if inflammation was present. Hemotoxylin and Eosin stained sections revealed that inflammatory cells were closely associated with hair follicle cysts in both _Dicer_ and _Drosha_^{flEx9} mutants at PD32 (data not shown). Immunological staining for CD3, a T-cell marker, and CD11b, a leukocyte marker, was performed on skin from _Dicer_ and _Drosha_^{flEx9} control and mutant mice biopsied at early and late, anagen time points following deletion in telogen. The number of CD3-expressing cells was unaltered in _Dicer_ and _Drosha_^{flEx9} mutant skin from mice induced at birth and assayed at PD32 (Figure 3.4G-J). However, the number of CD11b-expressing cells was greatly increased in both _Dicer_ and _Drosha_^{flEx9} mutant skin at PD32 (Figure 3.4 K-N). To determine if the number of mast cells was also increased, PD32 _Dicer_ control and mutant skin sections were stained for toluidine blue O (TBO), a stain used to identify mast cells by reacting with heparin. TBO staining of _Dicer_ mutant skin sections showed an increased presence of mast cells, compared to control sections (Figure 3.4O,P). By contrast, CD11b-

62

expressing cells were not increased at PD17 in *Dicer* and *Drosha*^{flEx9} mutant skin, a timepoint when hair follicles were already defective, but had not yet degraded (Figure 3.4A-D). Similar to CD11b staining, TBO staining of PD17 *Dicer* control and mutant skin sections did not reveal increased mast cell production in mutant skin (Figure 3.4E,F). The similar timing of epidermal hyperproliferation and onset of inflammation suggest that dermal inflammation may contribute indirectly to epidermal hyperproliferation in *Dicer* and *Drosha*^{flEx9} mutant skin.

Dicer and Drosha function are necessary for organization of the healing epidermis

To address the role of Dicer and Drosha in the epidermis under stress conditions, we surgically wounded *Dicer* and *Drosha*^{flEx9} control and mutant mice. A full thickness $1cm^2$ excision was made on the lower dorsum of anesthetized control and mutant mice and allowed to heal over eight days. Wound healing appeared grossly normal in both *Dicer* and *Drosha*^{flEx9} control and mutant mice. However, histology revealed disorganization of the healing epidermis in *Dicer* and *Drosha*^{flEx9} mutants compared to control skin (Figure 3.5A-H). To determine if the number of monocytes, macrophages, natural killer cells and granulocytes was changed between *Dicer* and *Drosha*^{flEx9} mutant and control mice, sections of wounded skin were stained for CD11b (Figure 3.6A-H). Mast cells were also examined using TBO staining (Figure 3.6I-P). The average density of CD11b+ cells/mm^2 or TBO+ cells/mm^2 at the edge of the wound, immediately past the myofibroblast-populated region, was not significantly different between control and mutant dermis (Figure 3.6Q,R), indicating that both *Dicer* and *Drosha*^{flEx9} mutants are capable of a normal inflammatory response to acute wounding. Inflammation is a novel

finding in *Dicer* and *Drosha*^flEx9 mutant skin; however, a variety of other skin-specific

mutations have been reported to cause both epidermal hyperproliferative and hair follicle

degradation, suggesting that these processes may be related. In Chapter Five, I will show

that the inflammatory cytokine TSLP was elevated in mutant skin. TSLP levels are a

sensitive assay for mild for mild barrier defects, suggesting this is a possible mechanism

contributing to inflammation. Interestingly, the inflammatory response to acute

wounding was similar in *Dicer* and *Drosha*^flEx9 mutants and controls. This observation

suggests that miRNA-depleted cells are not intrinsically more sensitive to inflammatory

insults than controls, but that degrading hair follicles and/or mild barrier defects elicit an

inflammatory response in unwounded mutant skin.

2.5 Discussion

We show that deletion of *Dicer* or *Drosha* in the epidermis leads to epidermal thickening,

the transient production of keratinized material above the cornifed layer of the skin,

hyperproliferation and expansion of the p63-expresssing basal compartment. We also

observe disorganization of the healing epidermis following acute wounding, but we did

not observe a heightened immune response in this situation. Since these phenotypes were

nearly identical in both *Dicer* and *Drosha*^flEx9 mutant mice, we conclude that they result

from the loss of Dicer- or Drosha-dependent miRNAs.

Loss of miR-203 in the basal layer of the epidermis results in upregulation of suprabasal

p63 (Yi et al., 2008). Furthermore miR34a and miR34c, also expressed in the suprabasal

compartment, have been shown to target cyclin D1 and cyclin dependent kinase 4, which

likely hampers cell cycle progression (Antonini et al. 2010). These studies are consistent with our data and suggest that miRNAs have roles in maintaining the basal and suprabasal layers of the epidermis. Interestingly, epidermal effects of *Dicer* and *Drosha* loss were not observed until relatively late time points and occurred concomitantly with inflammation. The delayed appearance of these phenotypes could be due in part to the relatively slow turnover of epidermis compared with hair follicle cells. However, it is also likely that inflammation resulting from hair follicle degradation and/or mild defects in the epidermal barrier contributed to epidermal hyperproliferation.

3.6 Figures and Legends

Figure 3.1. Validation of allele and miRNA depletion in the epidermis. (A) Sections from X-gal stained (blue) paraffin embedded skin from *Dicer*$^{fl/fl}$, *tetO-Cre*, *Rosa*$^{+/-}$ (left), and *Dicer*$^{fl/fl}$, *rtTA*, *tetO-Cre*, *Rosa*$^{+/-}$ (middle), and whole mount of X-gal stained skin from a *Dicer*$^{fl/fl}$, *rtTA*, *tetO-Cre*, *Rosa*$^{+/-}$ mouse (right).   Mice were induced from PD38 until PD56. (B) Semi-quantitative PCR analysis verifying *Dicer* gene excision in genomic DNA isolated from the epidermis of *Dicer* mutant and control mice induced from PD38-55. (C) Semi-quantitative PCR analysis verifying loss of *Drosha* gene expression in *Drosha*^{GI} mutant and control epidermis induced from E18-PD17. (D) *Dicer* and *Drosha* depletion was initiated at birth and skin was biopsied at PD15. The epidermal fraction was isolated and quantitative PCR was performed for the indicated miRNAs. Control expression levels were set at one after normalization to GAPDH. *Dicer*: n=2 mutants, 2 controls; *Drosha*: n= 1 mutant, 1 control. A two tailed Students t-test was performed on *Dicer* control and mutant epidermal samples. P-values are as follows: miR-16, p=0.0250; miR-205, p=0.0208; miR-27b, p=0.1635; miR-100, p=0.0.0385; miR-140-3p, p=0.1688.

Figure 3.1

A. Cre activity in the KRT5-rtTA, teto-Cre system

Dicer^fl/fl, tetO-Cre, Rosa26R

Dicer^fl/fl, KRT5-rtTA, tetO-Cre, Rosa26R

Dicer^fl/fl, rtTA, tetO-Cre, Rosa26R

25µm

B Doxycycline-induced epidermis

Dicer

Tubulin

C Doxycycline-induced epidermis

K5-rtTA, tetO-Cre

Drosha^+/+ Drosha^fl/+ Drosha^fl/fl

+   -   +   -   +   -

Drosha

GAPDH
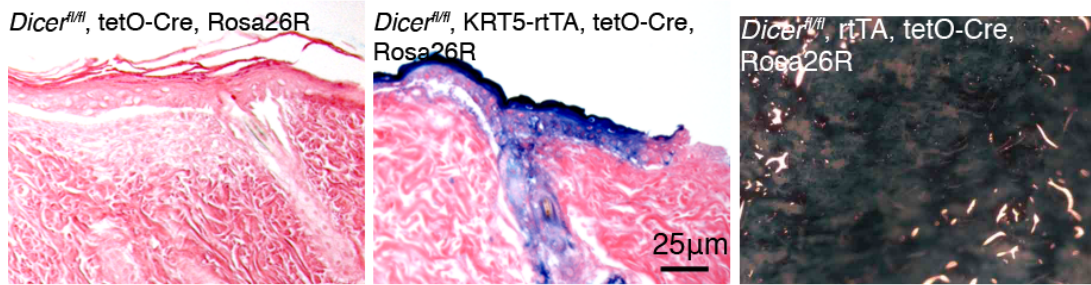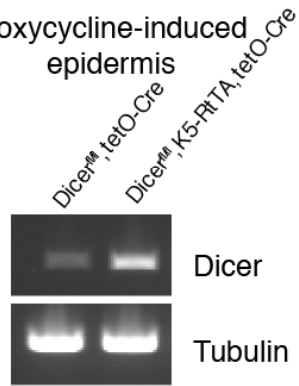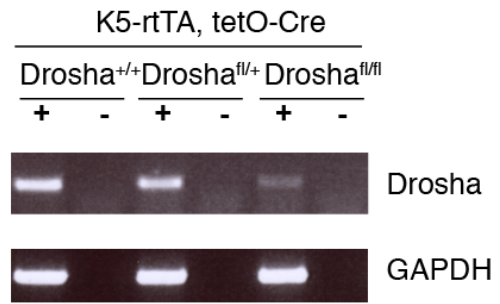
D miRNA expression in *Dicer* and *Drosha^flEx9* control and mutant mice

- ■ Dicer control
- ■ Dicer mutant
- □ Drosha control
- ■ Drosha mutant

miR-16 miR-205 miR-27b miR-100 miR-140-3p
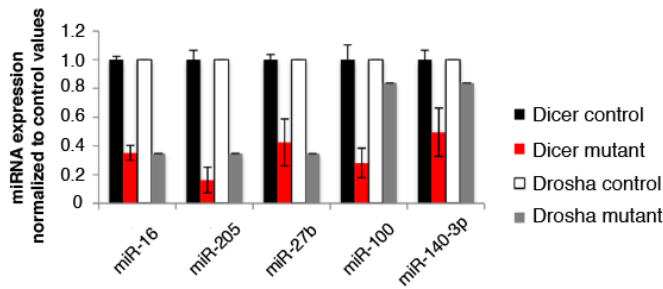
Figure 3.2. Epidermal hyperproliferation expansion of the stem cell-like p63 compartment in *Dicer* mutant skin during telogen. Histology of dorsal skin from *Dicer* (A,B) control and mutant littermates. *Dicer* control and mutant mice were induced at PD38 and skin was biopsied at PD92. (C,D) Immunofluorescence of the proliferation marker Ki67 (green) in paraffin sectioned dorsal skin from *Dicer* control and mutant mice induced at PD38 and biopsied at PD128. (E-F) Immunofluorescence for p63 (green) and KRT10 (red) in paraffin sectioned dorsal skin from *Dicer* control and mutant mice induced at PD38 and biopsied at PD128. Arrows denote p63 and KRT10 co-expressing cells.

Figure 3.2

A — P92 — *Dicer* control
B — P92 — *Dicer* mutant — 50μm

C — P128 — Ki67
D — P128 — 25μm

E — p63 K10
F — 25μm
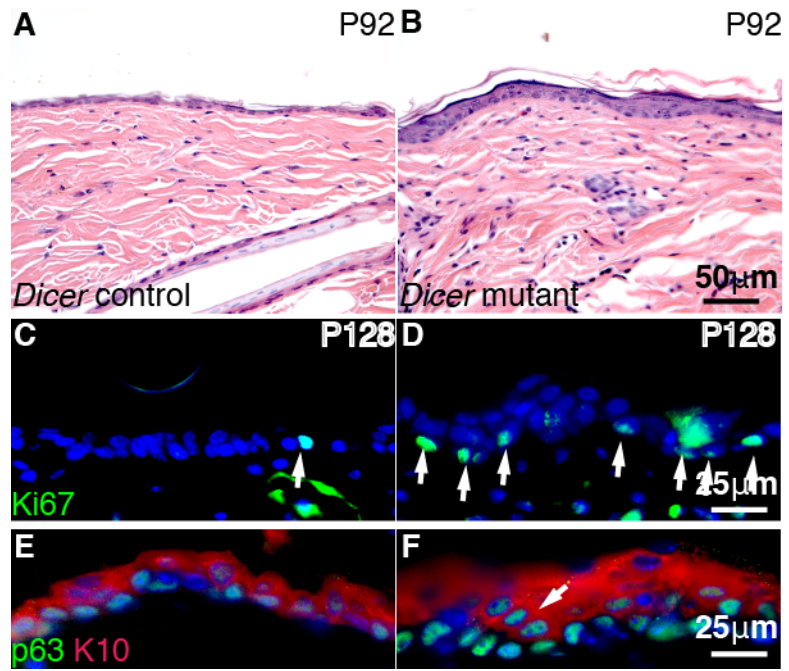
Figure 3.3. Epidermal hyperproliferation expansion of the stem cell-like p63 compartment in *Drosha^{flEx9}* and *Dicer* mutant skin during anagen. Skin sections from *Dicer* and *Drosha^{flEx9}* a control and mutant littermates after 17 and 32 days of induction. (A-D). Histology of dorsal skin from *Dicer* (A,B) and *Drosha^{flEx9}* (C,D) control and mutant littermates at PD17. (E-H) Immunofluorescence for proliferation marker Ki67 (green) in PD17 paraffin sectioned dorsal skin in *Dicer* control (I) and mutant (J) skin and *Drosha^{flEx9}* control (K) and mutant (L) skin. Arrows indicate Ki67-positive basal keratinocytes in controls. (I-L) Immunofluorescence for p63 (red) and KRT10 (green) in *Dicer* control (I) and mutant (J) epidermis, and *Drosha^{flEx9}* control (K) and mutant (L) mutant epidermis at PD17. (M-P) Histology of dorsal skin from *Dicer* (M,N) and *Drosha^{flEx9}* (O,P) control and mutant littermates at PD32. (N) *Dicer* mutant hair follicles have mostly degraded, but small remaining keratin cysts can still be observed. A large keratin containing scab and hair shafts are also observed above the epidermis. (P) *Drosha^{flEx9}* mutant hair follicles display keratin cysts as they degrade. The epidermis is thicker with keratinized material above it. (Q-T) Immunofluorescence for proliferation marker Ki67 (green) in paraffin sectioned dorsal skin in *Dicer* control (Q) and mutant (R) skin and *Drosha^{flEx9}* control (S) and mutant (T) skin. Arrows denote Ki67-positive basal keratinocytes in controls. Note nearly all basal keratinocyes and hair follicle cyst cells are Ki67-positive in *Dicer* and *Drosha^{flEx9}* mutant skin. (U-X) Immunofluorescence for p63 (red) and KRT10 (green) in *Dicer* control (U) and mutant (V) epidermis, and *Drosha^{flEx9}* control (W) and mutant (X) mutant epidermis. Note expansion of the p63-layer in *Dicer* and *Drosha^{flEx}* mutants (V, X).

Figure 3.3
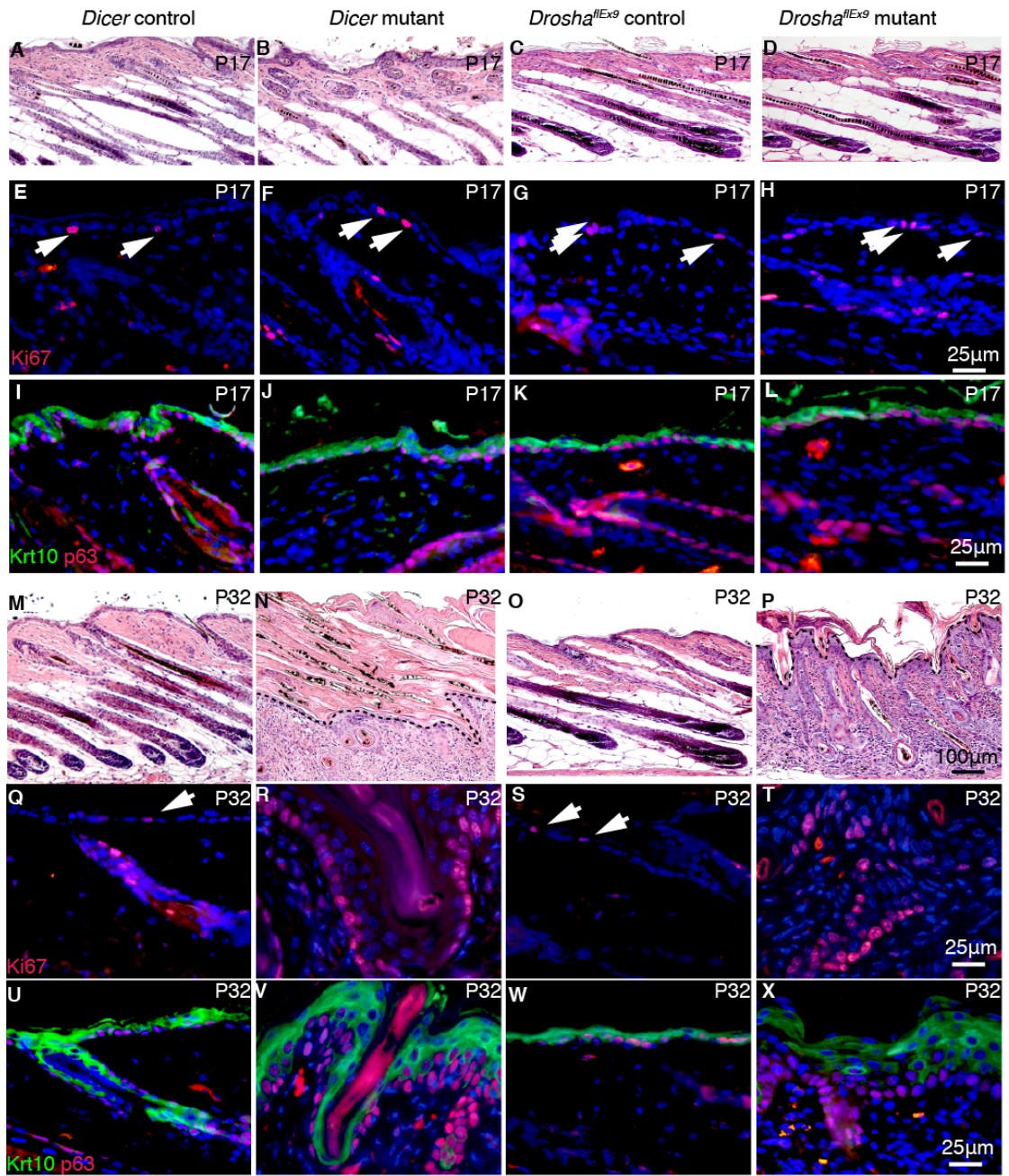
Figure 3.4. I**nflammation in *Dicer* and *Drosha*^{flEx9} mutant skin following hair follicle degradation.** Paraffin sectioned dorsal skin from PD17 and PD32 *Dicer* and/or *Drosha*^{flEx9} control and mutant mice, induced at PD1, were analyzed for the immune cell or epidermal markers indicated. (A-D) Immunofluorescence for CD11b (red) in *Dicer* control (A) and mutant (B) and *Drosha*^{flEx9} control (C) and mutant (D) skin. (E-F) Toluidine blue O staining of paraffin sectioned dorsal skin sections *Dicer* control (E) and mutant (F) skin. (G-J) Immunofluorescence for CD3 (green), in *Dicer* (G,H) and *Drosha*^{flEx9} (I,J) control and mutant skin. (K-N) Immunofluorescence for CD11b (red) in *Dicer* (K,L) and *Drosha*^{flEx9} (M,N) control and mutant skin. (O-P) Toluidine blue O staining (purple) for mast cells in *Dicer* control (O) and mutant (P) skin. Arrows indicate CD4, CD11b, or Toluidine blue O positive cells in the dermis of *Dicer or Drosha*^{flEx9} control or mutant skin sections. Note there are many more CD11b-expressing and toluidine blue O-positive cells in mutant than in control sections at PD32.

Figure 3.4
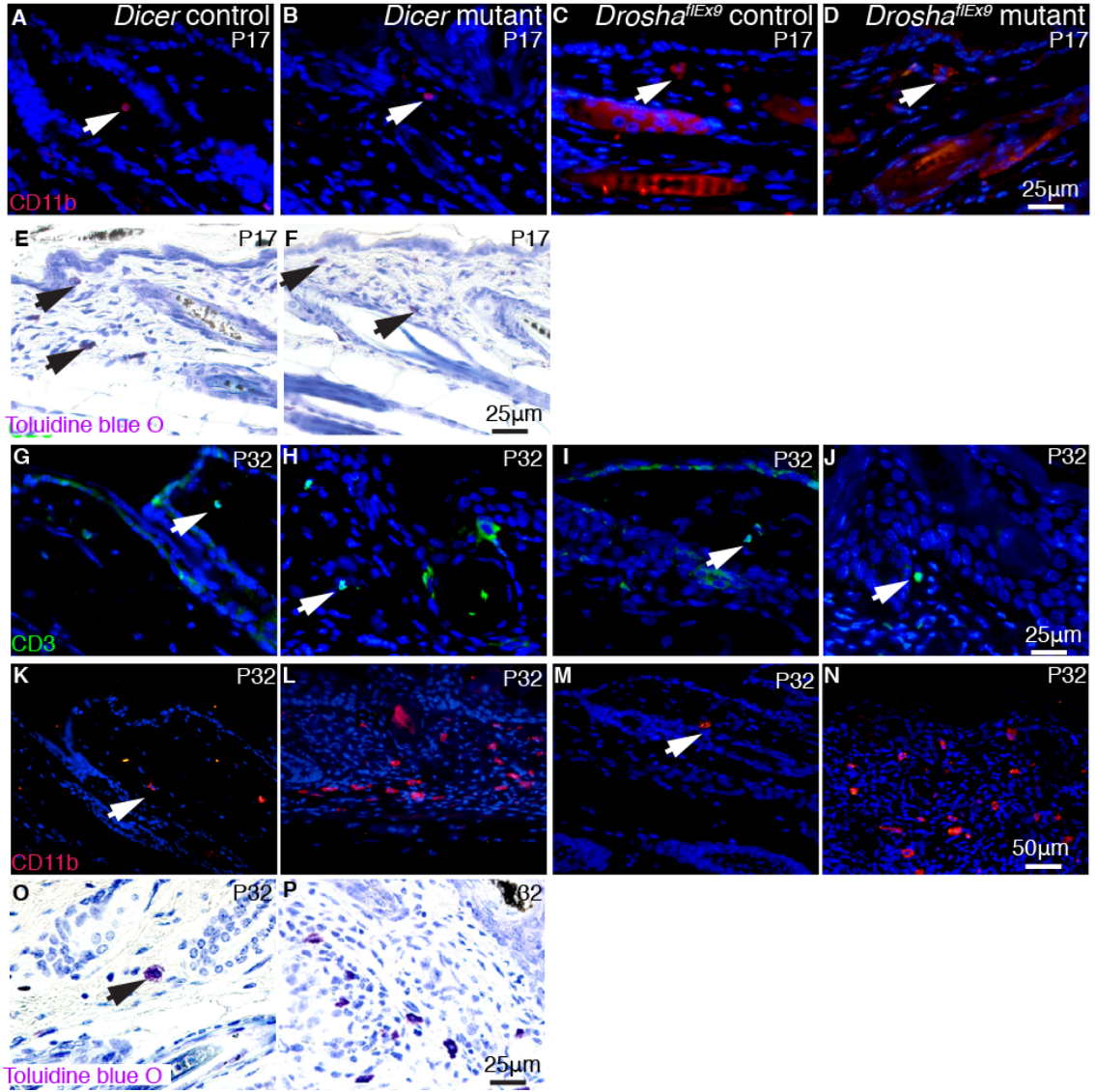
Figure 3.5. The healing epidermis is disorganized in Dicer and Drosha control and mutant wounded skin sections. *Dicer* and *Drosha^{flEx9}* control and mutant littermates were placed on oral doxycycline at PD38. Mice were anesthetized at PD48 and a full thickness 1cm^2 skin excision was made on the lower dorsum of each animal. Each wound site was biopsied eight days later. (A-H) H&E stained sections showing wound margins, marked by dashed lines in (A-D). (E-H) show higher magnification photographs of the boxed areas in (A-D). (E,G) Dotted lines represent the boundary between the granular and spinous layer, and dashed lines represent the boundary between the basal and spinous layer in the healing epidermis of *Dicer* and *Drosha^{flEx9}* control wounded skin sections. (F,H) Both the granular-spinous, and the spinous-basal boundaries are difficult to identify in the disorganized healing epidermis in *Dicer* and *Drosha^{flEx9}* mutant wounded skin sections.

Figure 3.5

Dicer control	*Dicer* mutant	*Drosha*^{flEx9} control	*Drosha*^{flEx9} mutant

A   B   C   D

100μm

E   F   G   H

25μm
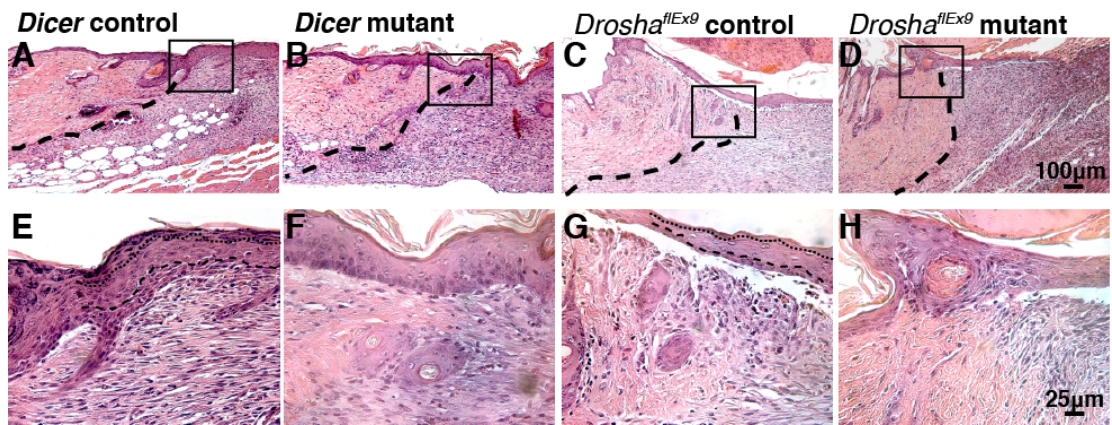
Figure 3.6. Numbers of inflammatory cells following acute wounding are similar in *Dicer* and *Drosha^flEx9* mutants compared with littermate controls.
Immunofluorescence for CD11b and staining for toluidine blue O was performed on sections of wounded skin in Dicer and Drosha^flEx9 control and mutant mice, and the density of positive cells were quantified. (A-H) Immunofluorescence for CD11b (red) at the wound margin photographed at low (A-D) and high (E-H) magnification. (I-N) Toluidine blue O staining for mast cells (purple) at the wound margin photographed at low (I-L) and high (M-N) magnification. (Q) Quantification of the numbers of CD11b-positive cells per mm^2 in the dermis at the wound margin in *Dicer* and *Drosha^flEx9* control and mutant littermates. (R) Quantification of the numbers of mast cells per mm^2 in the dermis at the wound margin in *Dicer* and *Drosha^flEx9* control and mutant littermates (n=2 *Drosha^flEx9* mutants and 2 controls; n=2 *Dicer* mutants and 2 controls; cells were counted in 7 fields at 40x magnification for each sample). N.S., not statistically significant.

Figure 3.6
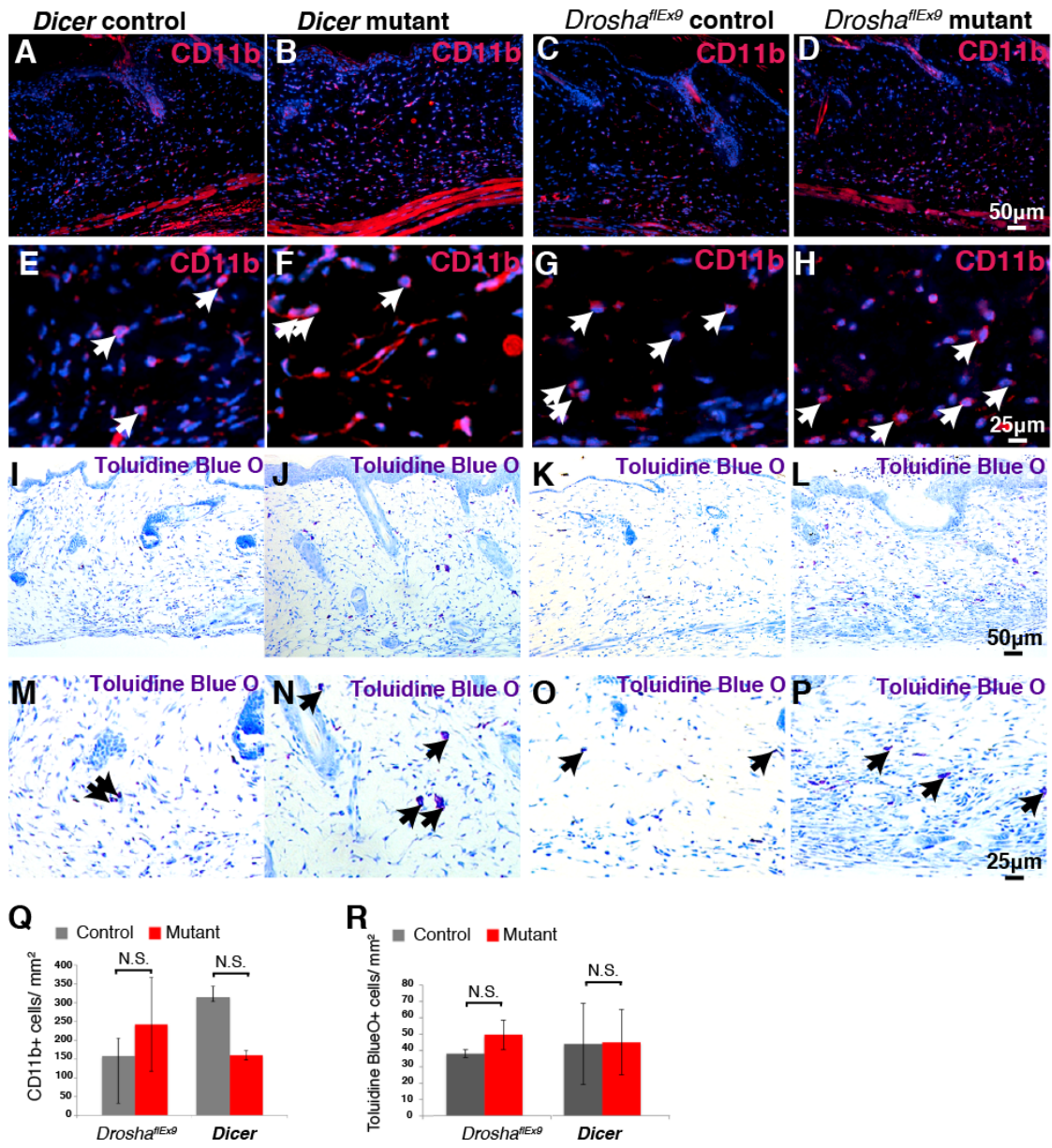
CHAPTER FOUR.

Dicer and Drosha are required in depilation-induced anagen

for matrix cell viability and maintenance of hair follicle structures.

4.1 Abstract

Hair follicles, like other skin appendages, are independently maintained as mini-organs containing their own stem cell population. Unlike other skin appendages, hair follicles undergo cycles of growth (anagen), regression (catagen) and rest (telogen). During each cycle a hair follicle must stimulate its stem cell population to divide and rapidly produce a transient amplifying compartment (the matrix), and all the structures necessary to produce a new hair shaft. However, the mechanims that enables matrix cells to sustain rapid proliferation rates without succumbing to telomere shortening, oxidative damage or errors accumulated during DNA synthesis remain undefined. To address whether miRNAs are required for initiation of hair follicle growth we generated skin-specific, inducible *Dicer* and *Drosha* mutant mice. Here we show that *Dicer* and *Drosha* mutant hair follicles are able to enter anagen, but fail to sustain a viable matrix, as cell death and DNA damage occurs in the hair follicle bulb. Since Dicer and Drosha both are required to process miRNAs, we conclude that miRNAs act to protect the matrix from cell death and DNA damage during early anagen.

4.2 Introduction

Once hair follicle morphogenesis is completed and a hair shaft has been produced, the lower region of the hair follicle degrades, and the dermal papilla, which is a condensate of dermal cells closely associated with the hair follicle, regresses with it to rejoin the uppermost portion of the hair follicle. The hair follicle then undergoes a resting phase, during which time the hair follicle stem cells remain quiescent. After the resting phase is complete, the stem cells again become active and the hair follicle enters a new growth phase. This is known as the hair follicle growth cycle, and consists of three main phases: anagen (the growth phase); catagen (the regression phase); and telogen (the resting phase). Hair follicle growth is synchronous in young mice, and the first postnatal anagen phase occurs shortly after PD20 in most mouse strains. At this time, hair follicle stem cells are stimulated to divide, most likely by dermal signals (Cotsarelis et al., 1990; Oliver and Jahoda, 1988; Plikus et al., 2008; Reynolds and Jahoda, 1992), and stem cell progeny migrate downward to form a rapidly dividing matrix population that surrounds the dermal papilla and differentiates to produce a new IRS and hair shaft (Fuchs, 2007; Millar, 2002; Oshima et al., 2001). Differentiation of matrix cells into hair shaft and IRS occurs as a result of BMP signaling (Kulessa et al., 2000), and Notch signaling is necessary for the maintenance of these structures (Pan et al., 2004).

As described in earlier Chapters, disruption of the miRNA biogenesis pathway causes defects in later stages of follicle morphogenesis and prevents entry into catagen of the embryonic hair follicle growth cycle. To address whether miRNAs are also required in the adult hair follicle growth cycle, we asked if Dicer or Drosha are necessary to maintain

resting, telogen hair follicles or for onset of a new anagen growth phase. Here I show

that *Dicer* and *Drosha* deletion of either of the miRNA biogenesis endonucleases does

not immediately affect hair follicle integrity during telogn. In contrast, while Dicer and

Drosha are not required for anagen onset, they are essential for viability of the matrix and

subsequent maintenance of the follicle. Although matrix cell proliferation was not

affected, *Dicer* or *Drosha* loss resulted in increased cell death and DNA damage in the

hair follicle bulb, suggesting that miRNAs play a protective role in the matrix population.

4.3 Materials and Methods

Generation, breeding, genotyping and induction of mouse strains

As described in Chapter Two, either a *Dicer* conditional allele (Murchison et al., 2005),

or the conventional *Drosha* conditional allele (*Drosha*^{flEx9}) (Chong et al., 2008) were

breed to bi-transgenic mice containing the *KRT5-rtTA* (gifted from Adam Glic) and *tetO-

Cre* (Gossen et al., 1995) alleles. Recombination was induced by feeding mice

doxycycline chow (6g/kg, Bio-Serv, Laurel, MD, USA). For analysis of Cre-

recombinase activity, mice homozygous for the *Dicer*-floxed allele (*Dicer*$^{fl/fl}$) and double

transgenic for *KRT5-rtTA* and *tetO-Cre* were bred to mice containing the *Rosa26R* allele

(Jackson Labs, Bar Harbor, Maine, USA). For depletion in the *KRT15-Cre* compartment,

Dicer$^{fl/fl}$ mice were bred to mice containing the *K15-CrePR1* allele (Morris et al. 2004)

and the *Rosa26R* allele (Jackson Labs, Bar Harbor, Maine, USA). Recombination was

induced by applying 0.1g Mifepristone (Sigma-Aldrich corp., St. Louis, MO) in ethanol

to dorsal skin after hair trimming. All mice were bred and housed at the laboratory

animal facility by the University of Pennsylvania and all experimental procedures

involving mice were performed according to the guidelines of the IACUC committee of the University of Pennsylvania.

Wildtype and the *Dicer* transgenic alleles were detected by combining the primer ATTGTTACCAGCGCTTAGAATTCC, with TCGGAATAGGAACTTCGTTTAAAC for the wild type (560nts) and floxed (767nts) alleles or with GTACGTCTACAATTGTCTATG for the recombined allele (429nts).   The wildtype and *Drosha* alleles were identified using the primer pair GCAGAAAGTCTCCCACTCCTAACCTTC and CCAGGGGAAATTAAACGAGACTCC to detect the wild type (251nts) or floxed (351nts) alleles.

Histology, immunofluorescence, proliferation and TUNEL assay analysis

Skin biopsies from the lower dorsal region were fixed in 4% paraformaldehyde or 10% neutral buffered formalin, dehydrated, paraffin embedded and sectioned at 5μm. For histological analysis, sections were stained with Hematoxylin and Eosin. For immunofluorescence staining, sections were rehydrated, microwave pretreated and incubated with primary antibodies against type I hair keratin (mouse monoclonal antibody clone AE13, Abcam, Cambridge, MA, USA, 1:40); cytokeratin15 (mouse monoclonal antibody, Vector Labs., Burlingame, CA, USA, 1:50); GATA3 (mouse monoclonal antibody HCG3-31, Sigma-Aldrich Corp., St. Louis, MO, USA, 1:100); phospho-SMAD1, phospho-SMAD5 and phospho-SMAD8 (polyclonal rabbit serum, Cell Signaling Technology, Danvers, MA, USA, 1:50); Ki67 (mouse monoclonal antibody, Covance, Princeton, New Jersey, USA, 1:40); or phospho-H2A.X (polyclonal

81

rabbit serum, Cell Signaling Technology, Danvers, MA, USA, 1:50). Biotinylated mouse or rabbit and Fluorescein- or Texas Red-conjugated streptavidin secondary antibodies were utilized (all from Vector Laboratories, Burlingame, CA, USA). For apoptosis assays, the In Situ Cell Death Detection Kit (Roche Diagnostics) was used. Sections were viewed under a Leica DM4000B microscope (Leica Microsystems). Images were captured by using a Leica DC500 digital camera and Leica FireCam software version 1.4 (Leica Microsystems). For proliferation, cell death and DNA damage analyses, 8-30 consecutive fields were analyzed at 40X.

CldU and IdU sequential labeling, and BrdU labeling

Dicer control and mutant littermates were labeled with CldU at PD1, PD2, and PD3, induced on PD38, plucked on PD48 and labeled for 2 hours with IdU on PD55 before skin was biopsied. CldU and IdU labeling, tissue preparation and staining were performed according to published protocols (Teta et al., 2007; Tuttle et al., 2010). For BrdU incorporation assays, *Dicer* control and mutant mice were injected with 10mg/ml of BrdU (Sigma-Aldrich corp., St. Louis, MO) two hours before biopsy.

4.4 Results

Generation and Validation of *Dicer* and *Drosha*, epidermal-specific, inducible mice

In order to deplete *Dicer* and *Drosha* specifically in either the resting phase or at the onset of anagen, it was necessary to create skin-specific *Dicer* and *Drosha* inducible mutant mice. To accomplish this we took advantage of the KRT5-*rtTA, tetO-Cre* induction system, described in Chapter Two. Briefly, this system allows for the temporal

expression of Cre with administration of the drug doxycycline, as the transactivator rtTA can only bind to the *tetO* promoter under this condition. To achieve Cre expression, specifically in skin epithelial cells, rtTA is expressed under the KRT5 promoter. To generate *Dicer* and *Drosha* inducible mutant mice, we bred mice containing a conditional *Dicer* allele or one of two conditional *Drosha* alleles, *Drosha*[flGI] or *Drosha*[flEx9] (see Figure 2.1), also described in Chapter Two, with mice that were bitransgenic for the *KRT5-rtTA* and *tetO-Cre* transgenes. All three conditional alleles used loxp-site technology allowing for the spatial and temporal disruption of the *Dicer* and *Drosha* alleles.

As described in Chapter Two and Chapter Three, we confirmed that Dicer and Drosha were depleted, and miRNA levels were substantially reduced, following inducible deletion of either *Dicer* or *Drosha.* (see Figure 2.1, Figure 2.2, Figure 2.3 and Figure 3.1).

Drosha and Dicer are required for short-term maintenance of telogen hair follicles
To begin to determine whether Drosha or Dicer are required for adult hair follicle cycling we first asked whether deletion of these genes affects telogen hair follicles. The first telogen stage occurs around PD20 and is very short; however the second telogen stage begins around PD50 and lasts minimally for 28 days (Plikus et al., 2008). After this time point, hair follicle cycling is no longer completely synchronous in the mouse, and hair follicles spontaneously enter anagen at varying time points. *Dicer* control and mutant mice were placed on oral doxycycline at PD38, ten days prior to the onset of telogen, and

skin was biopsied at PD68, or PD128. *Drosha*[GI] littermates were placed on oral

doxycycline at PD38 and biopsied at PD56. Histology from *Dicer* control and mutant

skin revealed that hair follicle integrity was sustained in the majority of hair follicles at

PD68. However, by PD128, once most hair follicles have spontaneously reentered

anagen, hair follicle degradation was observed. Staining for the stem cell marker KRT15,

revealed the stem cell compartment was maintained in Dicer mutant mice at PD68, but

was lost by PD128 (Figure 4.1 A-D, C-D). In *Drosha*[flGI] mutant mice hair follicles were

intact at PD56, and staining for the hair follicle stem cell marker, KRT15, showed that

the stem cell compartment was maintained at this stage (Figure 4.1E,F). These data

indicate that telogen follicles are not immediately affected by the loss of *Dicer* or

Drosha. However, once hair follicles spontaneously re-enter anagen, degradation

including the loss of stem cells is observed.

Drosha or Dicer are required to sustain anagen following hair plucking

Although hair follicle growth becomes asynchronous after the first postnatal hair growth

cycle, hair plucking can be used to re-synchronize hair follicle growth. To examine Dicer

and Drosha function at the onset of anagen, we induced *Dicer* deletion prior to telogen at

PD38 and *Drosha* deletion in telogen at PD51 and then initiated hair growth by plucking

telogen hair from the lower dorsal region. In *Dicer* littermate controls external hair re-

growth was observed by fourteen days post plucking; however re-growth was absent in

plucked regions of Dicer mutant skin (Figure 4.2). Immunostaining for P-cadherin, a

marker for early anagen, at three days after hair plucking showed that in both control and

Dicer mutant mice hair follicles entered early anagen (Figure 4.3A-D). At six days after

plucking both *Dicer* mutant and control littermate hair follicles showed signs of further

downgrowth; however unlike controls, *Dicer* mutant hair keratinocytes failed to

completely surround the dermal papilla (Figure 4.3E-H). By eight days after plucking

Dicer mutant follicles were smaller than controls (Figure 4.4A,D), and cell numbers in

the expanding matrix region were 61±6% lower than in control hair follicles, estimated

by counting DAPI positive nuclei (600-1700 DAPI positive cells counted per mouse; n=

four controls and four mutants; p-value= 0.0006). By contrast with controls, *Dicer*

mutant hair follicles at this stage failed to penetrate the subdermal fat layer, and the

medulla of the emerging hair shaft failed to form. By ten days after hair plucking *Dicer*

mutant hair follicles began to degrade (Figure 4.4B,E), and were atrophic when assayed

fourteen days after hair plucking (Figure 4.4C,F).

The phenotype of *Drosha^{flEx9}* mutants examined eight and twelve days after hair plucking

was slightly milder then that of *Dicer* mutants and took longer to develop. However,

similar to *Dicer* mutant hair follicles, *Drosha^{flEx9}* mutant follicles were observed to be

smaller than control littermate follicles and failed to penetrate deep into the dermis

(Figure 4.4G,H,J,K). By twenty-five days after hair plucking *Drosha^{flEx9}* mutant hair

follicles were mostly degraded (Figure 4.4I,L). Time points for subsequent analysis were

chosen based on the timing of onset of defects in the two mutants. These histological

observations indicate that Dicer and Drosha are dispensable for anagen onset, but are

necessary for the production of external hair, and for the maintenance of anagen follicles.

The similar phenotypes in Dicer and Drosha mutants suggest that miRNAs play key roles

in controlling these processes.

Drosha and _Dicer_ mutant hair follicles retain stem cells in early anagen

To determine whether loss of bulge stem cells could account for the decreased size of the early anagen matrix in _Dicer_ and _Drosha_^{flEx9} mutants, we assayed for expression of the stem cell markers KRT15 and CD34 eight or twelve days after plucking, respectively, when mutant follicles showed severe histological defects (Figure 4.4A,D,H,K). Interestingly, similar levels of KRT15 and CD34 staining were observed in mutant follicles and littermate controls (Figure 4.5A-D, E-H). Bulge cells are slow cycling and retain labeled deoxyribonucleotides (Cotsarelis et al., 1990). To determine whether label-retaining cells are affected by _Dicer_ deletion, _Dicer_ mutant and littermate control mice were injected with chloro-deoxyuridine (CldU) for the first three days after birth, and were doxycycline treated from PD38, followed by hair plucking at PD48. Mice were injected with iodo-deoxyuridine (IdU) to label proliferating cells, two hours before skin biopsy at eight days after plucking. The numbers of CldU-positive label-retaining cells, IdU-positive proliferating cells, and double positive proliferating label-retaining cells, assayed by immunofluorescence, were not significantly different in _Dicer_ mutant and control hair follicles (Figure 4.5I-K). Similarly, significant differences were not observed in the numbers or proliferation of Sox9-positive ORS cells that are necessary for maintenance of the matrix (Nowak et al., 2008) in _Dicer_ mutant and control hair follicles at three days after plucking (Figure 4.5L-N). Taken together, these data indicate that loss or failure of proliferation of bulge stem cells and Sox9-positive ORS cells are unlikely to account for matrix defects in early anagen.

86

Specific deletion of *Dicer* in bulge stem cells does not prevent their contribution to the matrix population

To assay more directly for the requirements for miRNAs in early anagen stem cells, we generated *Dicer^{f/fl}, KRT15-CrePR1, ROSA26R* mice in which deletion of *Dicer* is specifically induced in stem cells by application of topical RU486, and X-gal staining can be used to track the fates of Cre-active cells and their progeny. Experimental mice, and control littermate *Dicer^{+/+}, KRT15-CrePR1, ROSA26R* mice, were treated daily with topical RU486 for 4 days starting at PD46. Hair was plucked at PD50 and dorsal skin was biopsied 7 days later. In both mutant and control hair follicles, mosaic X-gal staining was observed in the ORS, matrix, precortex and IRS (Figure 4.5O,P). These results are consistent with my observation that stem cells were not depleted immediately following *KRT5-rtTA, tetO-Cre*-mediated inactivation of *Drosha* or *Drosha^{flEx9}*, and suggest that *Dicer*-deleted stem cells can contribute to the matrix and differentiate into hair shaft and IRS.

Drosha and _Dicer_ mutant hair follicles matrix cells differentiate appropriately

It was possible that mosaic Cre reporter activity did not correlate perfectly with *Dicer* deletion in *Dicer^{fl/fl}, KRT15-CrePR1, ROSA26R* mice. To determine whether Cre-active cells and their progeny could also contribute to hair follicle lineages in the more completely deleted *KRT5-rtTA, tetO-Cre* system we analyzed X-gal expression in induced *Dicer^{fl/fl}, Krt5-rtTA, tetO-Cre, ROSA26R* dorsal skin at eight days after plucking. X-gal staining was present in the ORS, IRS, and precortex of mutant hair follicles (Figure. 4.6). Consistent with this, immunofluorescence of *Dicer* and *Drosha^{flEx9}* mutant

87

skin at eight or twelve days after plucking, respectively, revealed appropriately

compartmentalized expression of the matrix marker LEF1, the IRS marker GATA3

(Figure 4.7A-D) (Kaufman et al., 2003), the hair shaft marker AE13 (Lynch et al., 1986)

(Figure 4.7E-H), and AE15, which marks IRS and hair shaft medulla cells (O'Guin et al.,

1992) (Figure 4.8), in mutant follicles. Immunofluorescence of plucked *Dicer* and

Drosha[flEx9] mutant skin for phospho-Smads 1, 5 revealed that BMP signaling, necessary

for IRS and hair shaft differentiation, was active in mutant hair follicles (Figure 4.7I-L).

These data indicate that IRS and hair shaft differentiation occurred appropriately.

However mutant hair follicles were smaller than controls, contained fewer matrix and

differentiating cells, and these did not assemble into normal differentiating structures

(Figure 4.8).

Dicer and Drosha mutant hair follicle matrix cells display normal rates of proliferation

As defective differentiation did not appear to account for *Dicer* and *Drosha*[flEx9] mutant

hair follicle phenotypes, we asked whether *Dicer* or *Drosha* deletion affected

proliferation rates. *Dicer* and *Drosha*[flEx9] mutant hair bulbs contained lower numbers of

Ki67 positive cells than littermate controls at eight and twelve days after plucking,

respectively; however mutant hair bulbs also contained fewer cells than controls (Figure

4.9A-D). Proliferation rates, estimated by calculating the percent of Ki67-positive DAPI-

stained cells in at least eight hair bulbs from control and mutant mice, were not

significantly altered by *Dicer* or *Drosha* deletion (*Dicer*[flEx22-23] control: 50±12%;

Dicer[flEx22-23] mutant: 47 ±5%; *Drosha*[flEx9] control, 42±4% Ki67-positive cells; *Drosha*[flEx9]

mutant 37±6%; not statistically significant), indicating that *Dicer* and *Drosha* are not required for normal rates of matrix proliferation (Figure 4.9E,F).

Deletion of *Drosha* or *Dicer* causes matrix cell apoptosis and a DNA damage response

We next asked whether the diminished size of *Dicer* and *Drosha*^flEx9 mutant hair bulbs following hair plucking was due to increased cell death. TUNEL positive cells were rarely observed in the bulge or matrix of control hair follicles at eight or twelve days after plucking (Figure 4.9G,I). By contrast at eight or twelve days after plucking, respectively, *Dicer* and *Drosha*^flEx9 mutant follicles displayed increased apoptosis, particularly in the matrix (Figure 4.9H,I), consistent with elevated *Dicer* mutant matrix cell death in embryonic anagen (Figure 2.6G,H). At eight days after plucking, 1.1±0.3% of cells were TUNEL positive in *Dicer* mutant follicles compared to 0.020±0.007% in control follicles (p= 0.005). Likewise at twelve days after plucking, 2.8±0.7% of *Drosha*^flEx9 mutant matrix cells were TUNEL positive compared to 0.2±0.1% of control matrix cells (p=0.0003). (Figure 4.9K,L). Interestingly, mutant matrix compartments also displayed elevated expression of the DNA damage response marker pH2A.X at eight and twelve days after plucking, respectively (Figure 4.9M-P). Quantification of pH2A.X positive cells as a percentage of the bulb population revealed that these increases were statistically significant (*Dicer* control: 0.02±0.01%; *Dicer*^flEx22-23 mutant: 1.2±0.3%, p=0.032; *Drosha*^flEx9 control: 0.0±0.0%; *Drosha*^flEx9 mutant: 1.7±0.2%, p=4.4×10^{-12}) (Figure 4.9Q,R). These data indicate that *Dicer* and Drosha play essential roles in preventing cell death and DNA damage in rapidly proliferating matrix cells during early anagen.

89

4.5 Discussion

In this Chapter I showed that Dicer and Drosha are not required for the short-term

maintenance of hair follicle and bulge stem cells in telogen, for activation of bulge cells

and matrix cell proliferation, anagen onset, or differentiation. However, Dicer and

Drosha are required to sustain anagen, by protecting the matrix cell compartment from

cell death and DNA damage. Because these phenotypes are shared in both *Dicer* and

Drosha^{flEx9} mutant mice, these effects are likely due to miRNA loss.

Previous findings showed that when *Dicer* is deleted in the epidermis constitutively,

starting at E14 (Andl et al., 2006), the KRT15 bulge stem cell compartment is not

established. However, when *Dicer* and *Drosha^{flEx9}* mutation is induced during adult

telogen the KRT15-expressing stem cell compartment is initially maintained before the

hair follicle itself degrades. Similarly, the stem cell compartment is present in *Dicer* and

Drosha^{flEx9} mutant hair follicles at early stages after plucking when histological defects

were already apparent. These results suggest that miRNAs do not play specific roles in

the hair follicle stem cell population and support miRNA profiling results that indicate

that the same profile of miRNAs is present in both progenitor cells for epidermal and hair

follicle populations (Zhang et al., 2011). However, based on *Dicer* and *Drosha^{flEx9}*

mutant phenotypes, miRNAs do have specific functions in the hair follicle matrix during

early anagen in adult mice. Matrix cells must undergo numerous rounds of replication

during this period, and these results suggest that miRNAs could play a protective role

during this process.

4.6 Figures and Legends

Figure 4.1. **The hair follicle stem cell compartment is sustained in *Dicer* and *Drosha^flGI* mutant telogen hair follicles.** *Dicer* and *Drosha* depletion was initiated at PD38 and skin was biopsied during telogen from the lower dorsal region at the time points indicated. Arrows indicate either KRT15 or S100A4 immunostaining in the hair follicle bulge. (A,B). KRT15 staining (red) is unaltered in *Dicer* mutant mice at PD68. (C,D) *Dicer* mutant hair follicles degrade and remain absent for KRT15 at PD128. (E,F) KRT15 staining is unaltered in *Drosha^flGI* mutant hair follicles at PD56 compared to control hair follicles. All images were taken at the same magnification.

Figure 4.1
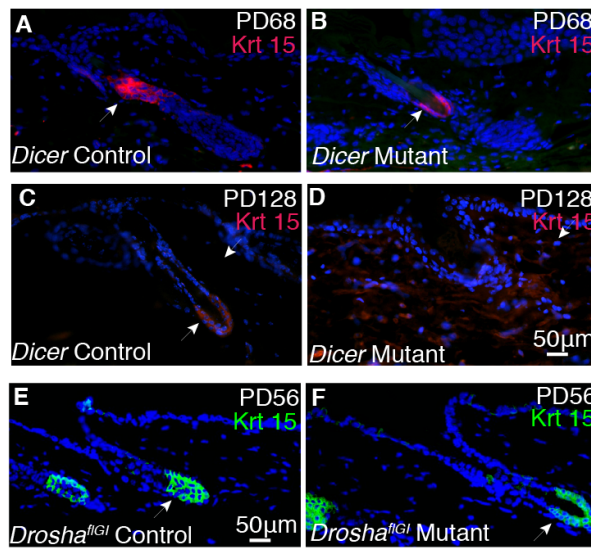
Figure 4.2. **Hair fails to re-grow in *Dicer* mutant mice after hair plucking.**   Side-view of a *Dicer* control and *Dicer* mutant mouse, fourteen days after hair plucking. Note hair fails to re-grow in the plucked region of the Dicer mutant compared to the plucked region of its littermate control.

Figure 4.2

14 Days post plucking

Dicer control   *Dicer* mutant
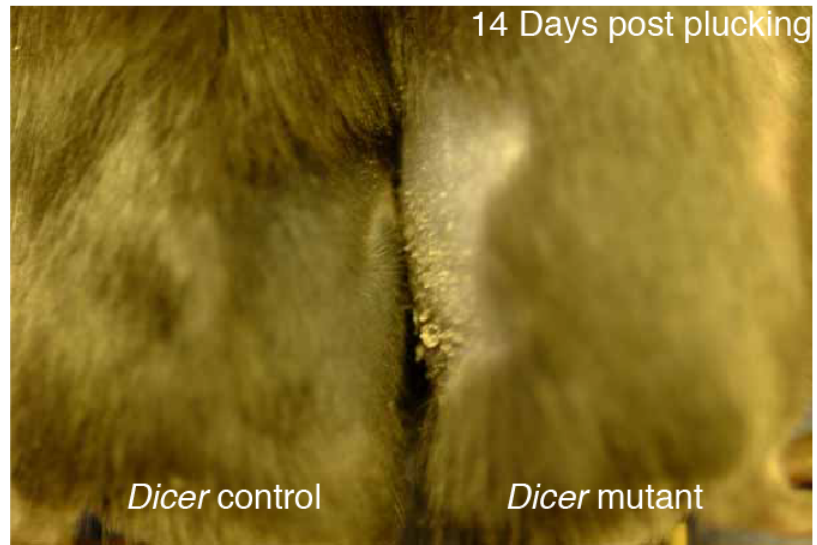
Figure 4.3. ***Dicer* mutant hair follicles enter anagen, but are not able to sustain downgrowth.** *Dicer* depletion was initiated ten days prior to hair-plucking and skin was biopsied either three or six days later from the lower dorsal region. (A,B). Immunostaining for PCAD (green) in *Dicer* control and mutant skin three days after hair plucking. (C,D). Histology from *Dicer* control and mutant skin reveals *Dicer* mutant hair keratinocytes are not able to surround the dermal papilla at six days after hair plucking (E,F) Alkaline phosphotase staining (blue-purple) on skin biopsied six days after hair plucking.

Figure 4.3
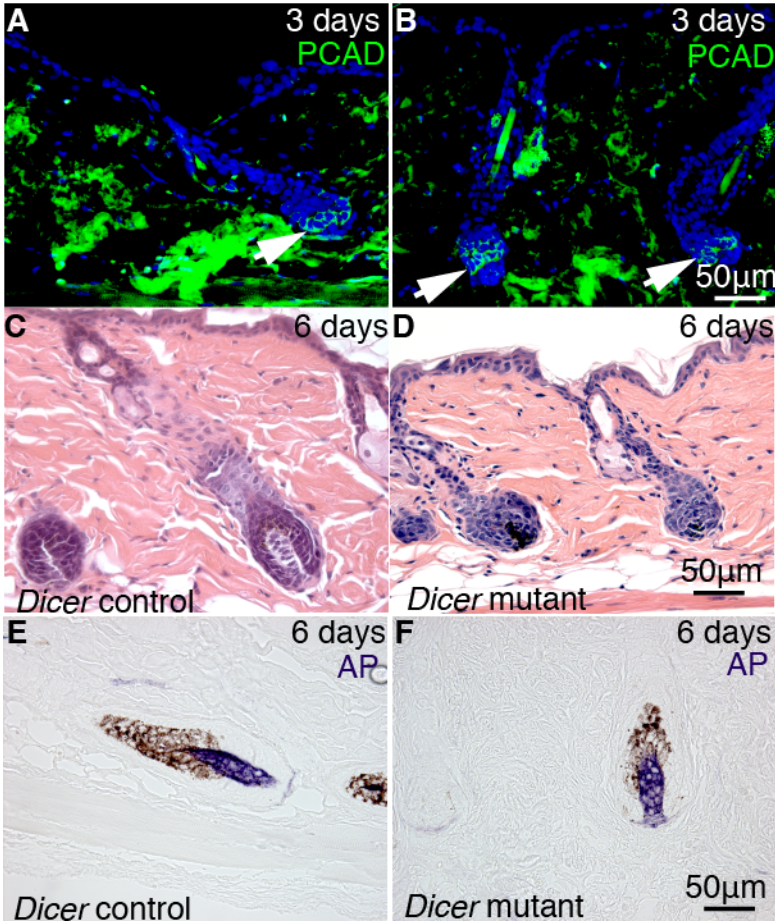
Figure 4.4. **Hair follicle growth begins but is not sustained in *Dicer* and *Drosha* mice after plucking-induced anagen.** *Dicer* and *Drosha*^{flEx9} mutants and littermate controls were placed on doxycycline at PD38, ten days prior to hair plucking. Skin was biopsied from the lower dorsal region at successive days post-plucking as indicated and analyzed by H&E staining. Defects in hair follicle downgrowth were observed in *Dicer* mutants by eight days after plucking and in *Drosha*^{flEx9} mutants by twelve days, and hair follicles subsequently started to degrade in both mutants. Scale bar in (L) applies to (A-L).

Figure 4.4
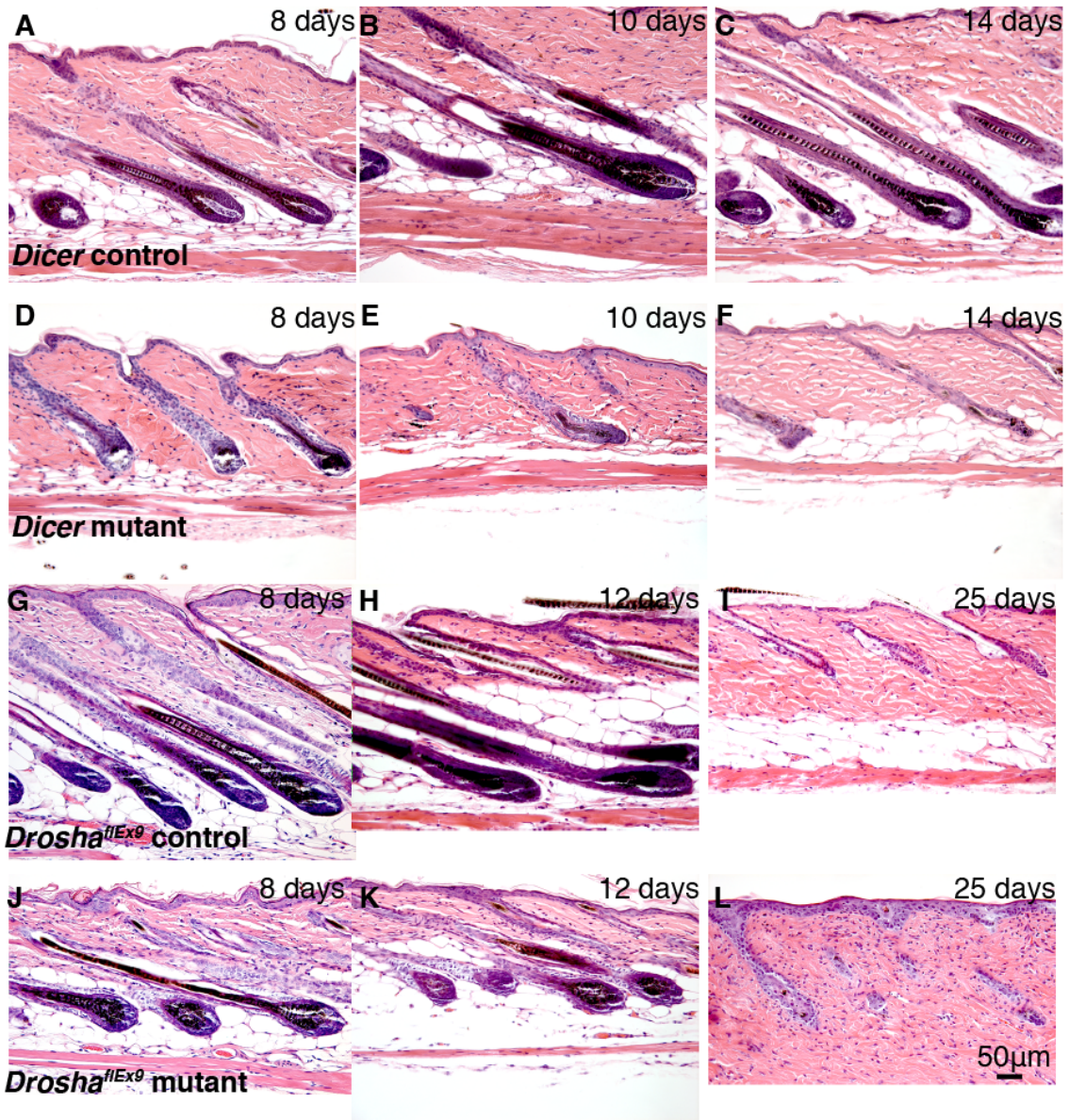
Figure 4.5. **Maintenance and proliferation of *Dicer* and *Drosha*^{flEx9} mutant hair follicle progenitors in early anagen and contribution of *Dicer* mutant bulge cell progeny to the matrix and its derivatives.** (A-D) Immunofluorescence for KRT15 (red) in induced *Dicer* (A,B) and *Drosha*^{flEx9} (C,D) control (A,C) and mutant (B,D) skin, twelve (A,B) or eight (C,D) days after hair plucking. (E-H) Immunohistochemistry for CD34 (brown) in induced *Dicer* (E,F) and *Drosha*^{flEx9} (G,H) control (E,G) and mutant (F,H) skin, twelve (E,F) or eight (G,H) days after hair plucking. (I,J) Immunofluorescence for CldU-labeled (red) LRCs and IdU-labeled (green) proliferating cells in induced *Dicer* mutant (J) and control littermate (I) skin five days after. (K) Quantification of the numbers of CldU, IdU and double labeled cells per *Dicer* mutant (J) and control (I) hair follicle section at five days after plucking (n=2 controls and 3 mutants; $\geq$ 6 hair follicles analyzed per sample). (L,M) Immunofluorescence for Sox9 (green) and BrdU (red) in *Dicer* mutant and control skin at three days after plucking. (N) Quantification of the numbers of BrdU, Sox9 and co-labeled cells per *Dicer* mutant and control hair follicle section at three days after plucking (n=2 controls and 2 mutants; $\geq$ 6 hair follicles analyzed per sample). (O,P) X-gal stained dorsal skin from *Dicer*^{fl/fl}*, KRT15-CrePR1, ROSA26R* (P) and control littermate *Dicer*^{+/+}*, KRT15-CrePR1, ROSA26R* (O) mice induced from PD46-PD49, and analyzed seven days after hair plucking at PD50. Arrows indicate Cre-active cells and their progeny in the bulge, matrix, precortex and IRS. Scale bars apply also to littermate controls. N.S., not statistically significant.

Figure 4.5

100
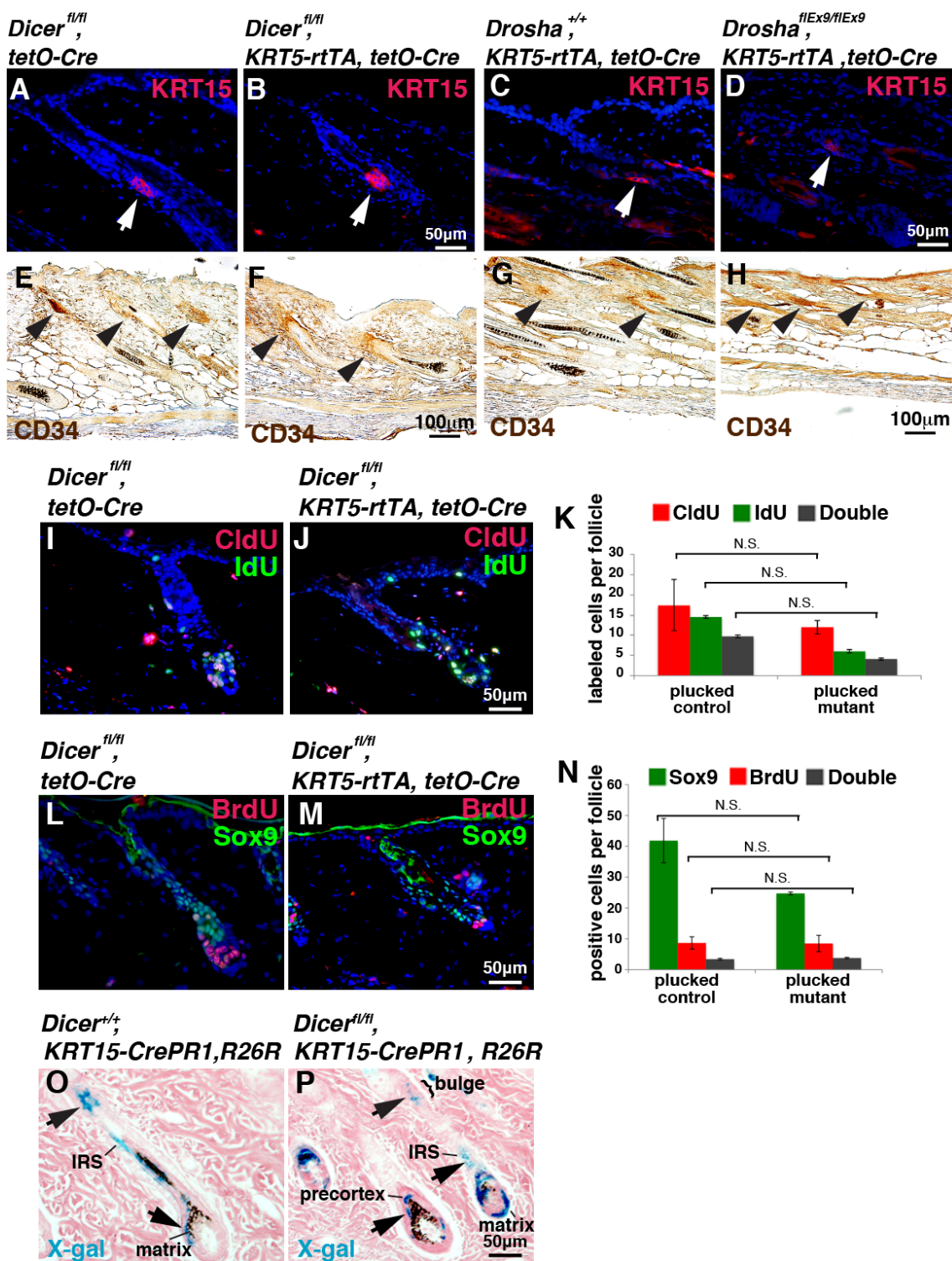
Figure 4.6. **Cre-active cells contribute to all layers of the hair follicle.** (A,B) *Dicer^{f/fl}*, *KRT5-rtTA, tetO-Cre, ROSA26R* mutants (B) and *Dicer^{f/fl}, tetO-Cre, ROSA26R* control littermates (A) were placed on doxycycline at PD38, depilated to induce anagen at PD48, and biopsied after eight days. X-gal staining (blue) revealed contribution of Cre-active cells to the matrix, precortex, ORS and IRS in *Dicer* mutant hair follicles.

Figure 4.6

Dicer^fl/fl, tetO-Cre, Rosa26R

Dicer^fl/fl, KRT5-rtTA, tetO-Cre, Rosa26R

A X-gal

eight days

B X-gal

ORS

precortex
matrix

50µm
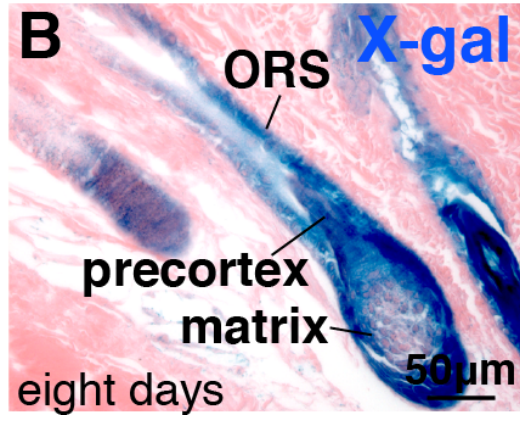
eight days

Figure 4.7. ***Dicer* and *Drosha*^{flEx9} mutant matrix cells differentiate appropriately**
(A-L) Control littermate and *Dicer* and *Drosha*^{flEx9} mutant mice were placed on
doxycycline ten days prior to hair plucking. Dorsal skin was biopsied eight (*Dicer*
mutants and controls) or twelve days (*Dicer* mutants and controls) after depilation and
assayed by immunofluorescence for GATA3, AE13, or phospho-SMAD 1, 5, 8 (green)
and LEF1 (red). Scale bar in (L) applies to (A-L).

Figure 4.7
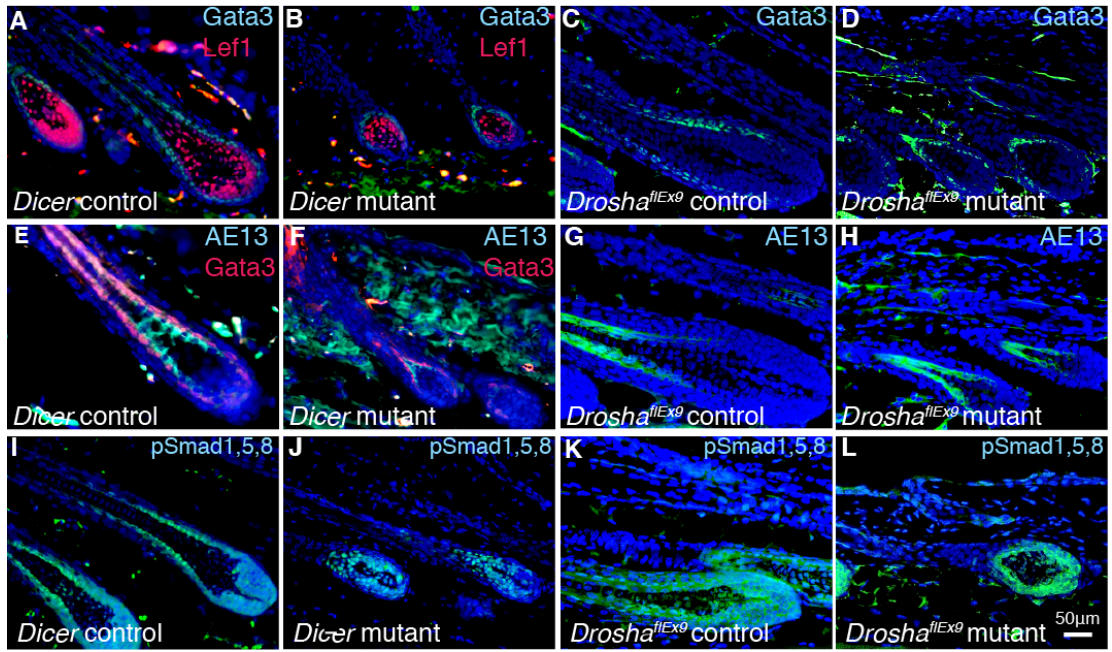
Figure 4.8. **Following plucking induced anagen initiation, *Dicer* mutant hair follicles are smaller than littermate controls and contain fewer differentiating IRS cells.** *Dicer* mutant and littermate control mice were placed on doxycycline at PD38, hair was plucked at PD48, and hair follicles were analyzed at seven (A,B) or eight (C,D) days after plucking. (A,B) Light micrographs of isolated hair follicles from *Dicer* mutant skin seven days after plucking reveal the smaller sizes of mutant compared with control hair follicles. (C,D) Immunoflourescence for the IRS and hair shaft medulla marker AE15 (red) in serial sections of *Dicer* mutant (D) and littermate control (C) skin eight days after plucking reveals formation of a smaller IRS compartment and medulla in mutant hair follicles compared with controls. Sections in (C,D) were counterstained with DAPI (blue). Scale bar in D applies to (C,D).

Figure 4.8

Dicer control   *Dicer* mutant
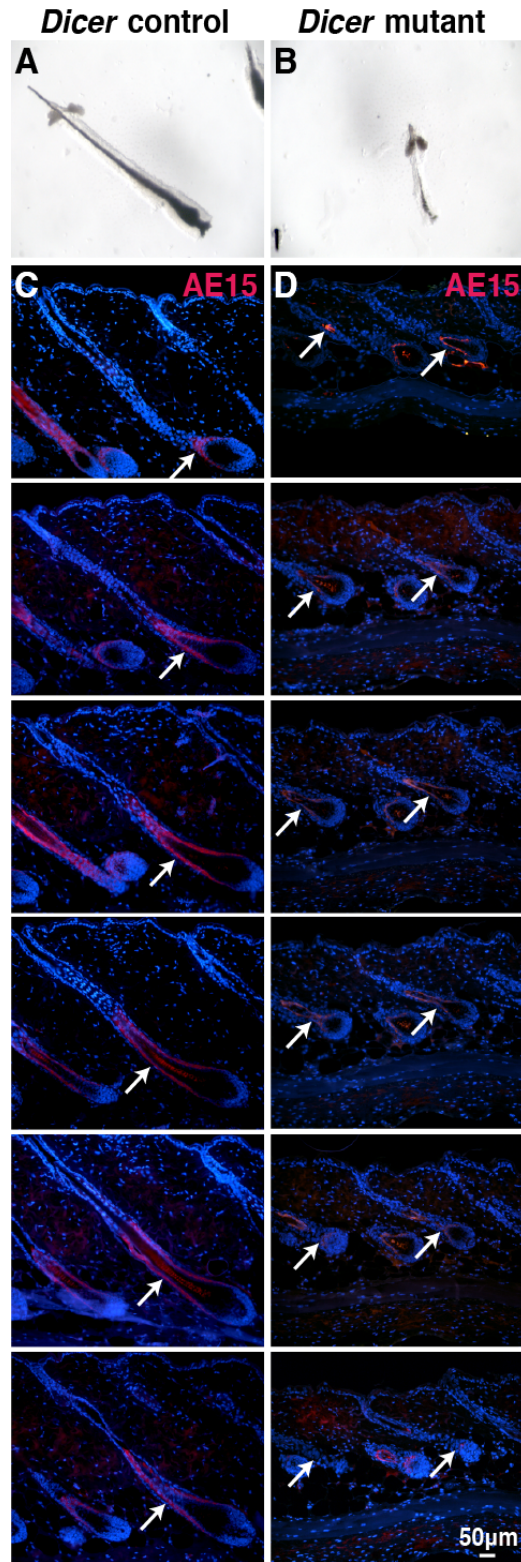
Figure 4.9. ***Dicer* and *Drosha*^{flEx9} mutant matrix cells display increased rates of apoptosis and DNA damage.** Control littermate and *Dicer* and *Drosha*^{flEx9} mutant mice were placed on doxycycline ten days prior to hair plucking. Dorsal skin was biopsied eight (*Dicer* mutants and controls) or twelve days (*Dicer* mutants and controls) after depilation and assayed by immunofluorescence for Ki67 (green) (A-D) and pH2A.X (red) (M-P) , or subjected to TUNEL staining (green) (G-I), as indicated. White arrows indicate positive signals. Scale bars apply also to control littermate images. (E-F, K-L, Q-R) Percentages of positively staining hair bulb cells, expressed as mean ± SEM for at least 8 control and 8 mutant follicles for Ki67 staining (E,F) or at least 30 control and 30 mutant follicles for TUNEL staining (K-L) and pH2A.X expression (Q,R). Both mutants showed statistically significant increases (*) in apoptosis and DNA damage relative to controls, but unchanged proliferation rates. NS, not statistically significant.

Figure 4.9
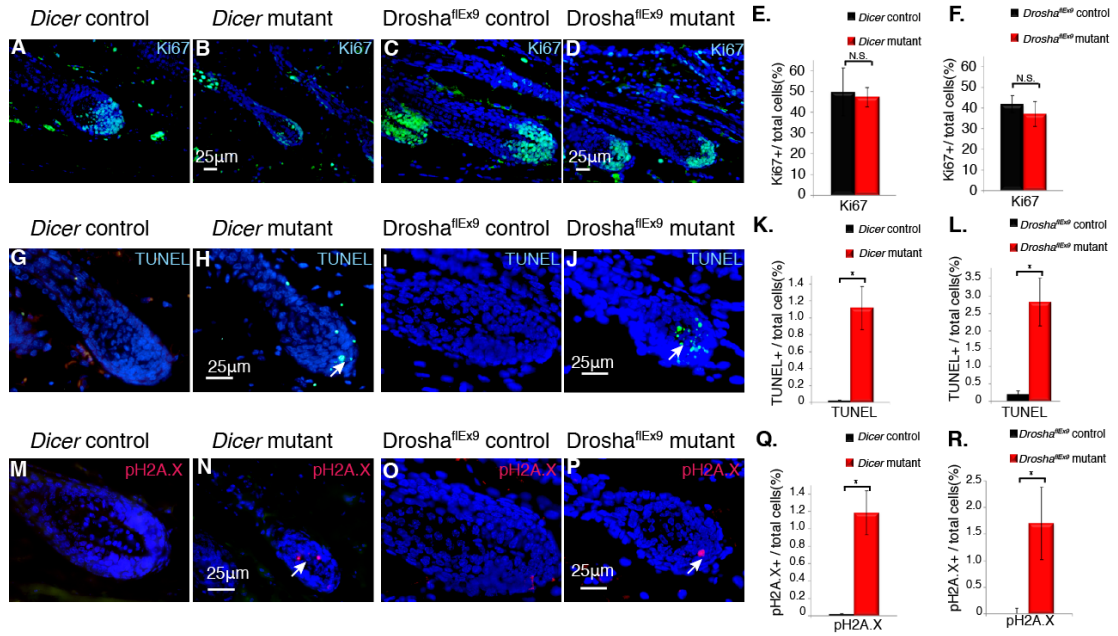
CHAPTER FIVE

Analysis of Notch signaling and selected miR-205 targets
in *Dicer* control and mutant skin

5.1 Abstract

Dicer or *Drosha* loss does not affect maintenance of resting hair follicles, but produces dramatic defects in cell survival in the rapidly proliferating matrix population during early anagen, blocks transition to a normal regression phase, and prevents long-term maintenance of follicular structures and their associated stem cells. An inflammatory response is observed concomitant with follicular degradation and epidermal hyperplasia, but is preceded by initial hair follicle defects including matrix cell apoptosis and DNA damage. Levels of EGFR and Notch1 are reduced at early time points following *Dicer* and *Drosha* deletion and may contribute to observed hair shaft phenotypes and failed hair follicle maintenance. These data demonstrate specific requirements for *Dicer* and *Drosha* in maintaining the ability of adult hair follicles to undergo normal cycles of growth and regression. The similar phenotypes observed in induced *Dicer* and *Drosha* epidermal mutants suggest that these functions are largely associated with miRNA processing. Consistent with this, *Dicer* deletion resulted in upregulation of multiple direct targets of the highly expressed epithelial miRNA, *miR-205*, which is depleted in *Dicer* and *Drosha-*deficient skin.

5.2 Introduction

As described in earlier Chapters, disruption of miRNA biogenesis during early anagen

does not affect anagen onset, but results in failed viability and DNA damage in the

transiently amplifying matrix region and subsequent loss of hair follicles. *Dicer* and

Drosha loss during later stages of follicle morphogenesis prevents entry into the catagen

phase of the embryonic hair follicle growth cycle. Epidermal loss of Notch signaling

produces phenotypes similar to those observed following miRNA depletion, including

severe abnormalities in later stages of hair shaft morphogenesis; the ability of

Dicer/Drosha and *Notch*-depleted bulge stem cells to contribute to the matrix, IRS and

ORS; failure of hair follicle maintenance; interfollicular epidermal hyperproliferation;

and inflammation (Demehri and Kopan, 2009; Demehri et al., 2008; Lee et al., 2007; Pan

et al., 2004; Vauclair et al., 2005). Consistent with this, levels of FL-Notch1 and NICD

were reduced by PD17 in *Dicer* and *Drosha*^{flEx9} mutant compared with control skin

following induction from E18 (Figure 2.7A,B).

Expression of skin-specific dominant negative EGFR also results in phenotypes similar to

those observed in *Dicer* and *Drosha*^{flEx9} mutant mice, including wavy ectopic hair and

failed transition into telogen (Murillas et al. 1995). Analysis of EGFR protein levels

revealed a deficiency in *Dicer* and *Drosha*^{flEx9} skin during anagen (Figure2.7). Although

loss of EGF and Notch signaling provides insight into the mechanisms of failed catagen

entry and hair shaft and IRS maintenance, respectively, it is not known whether miRNAs

directly regulate these phenotypes in the skin. In this Chapter, I test the hypothesis that

EGF and Notch ligands are be deregulated by loss of miRNAs. I show that HBEGF is

highly upregulated in Dicer mutant skin at a time point just before external hairs become

wavy, suggesting HBEGF as a possible direct target of miRNAs. I also explore

downstream effects of loss of Notch signaling in the epidermis, which has been shown to

result in mild barrier defects and inflammation (Demehri et al., 2008). I show that the

cytokine TSLP, a sensitive readout for epidermal barrier defects such as those that occur

by loss of Notch signaling, is highly upregulated in *Dicer* mutant skin at PD15, a time

point before inflammation is observed. These data suggest that Notch loss in the

epidermis of *Dicer* and *Drosha^{flEx9}* mutants may contribute to a mild barrier defect

resulting in inflammation and epidermal hyperproliferation.

The function of a few miRNAs, such as miR-125b and miR-203, has been tested in the

skin (reviewed in Chapter 1.7). Although many miRNAs are present in the skin, the

function of the vast majority has not been explored. In Chapter Two and Three, I showed

by QPCR and ISH that miR-205 is highly expressed in both the hair follicle and

epidermis and is significantly reduced in *Dicer* and *Drosha* deficient skin (Figure 2.2,

and Figure 3.1). MiR-205 is also highly expressed in other epithelial tissues (Gregory et

al., 2008; Ryan et al., 2006), and has been shown in renal cells to directly target Zeb2 and

Src (Gregory et al., 2008; Majid et al. 2011). To date, little is known about miR-205

function in the skin, except that in melanoma cancer cells E2F1 is a direct miR-205 target

(Dar et al. 2011). In this Chapter, I show that E2F1, Zeb2 and Src mRNA are

upregulated in Dicer mutant skin at PD15, suggesting that these proteins are direct targets

of miR-205 in skin epithelial cells.

5.3 Materials and Methods

Generation, breeding, genotyping and induction of mouse strains

As described in Chapter Two, either a *Dicer* conditional allele (Murchison et al., 2005), or the conventional *Drosha* conditional allele (Chong et al., 2008) were breed to bitransgenic mice containing the *KRT5-rtTA* (gifted from Adam Glick) and *tetO-Cre* (Gossen et al., 1995) alleles. Recombination was induced by feeding mice doxycycline chow (6g/kg, Bio-Serv, Laurel, MD, USA). All mice were bred and housed at the laboratory animal facility by the University of Pennsylvania and all experimental procedures involving mice were performed according to the guidelines of the IACUC committee of the University of Pennsylvania.

Wildtype and the *Dicer* transgenic alleles were detected by combining the primer ATTGTTACCAGCGCTTAGAATTCC, with TCGGAATAGGAACTTCGTTTAAAC for the wild type (560nts) and floxed (767nts) alleles or with GTACGTCTACAATTGTCTATG for the recombined allele (429nts).   The wildtype and *Drosha* alleles were identified using the primer pair GCAGAAAGTCTCCCACTCCTAACCTTC and CCAGGGGAAATTAAACGAGACTCC to detect the wild type (251nts) or floxed (351nts) alleles.

Quantitative real-time RT-PCR for miRNAs

Quantitative real-time RT-PCR was performed on total RNA samples extracted from the full thickness skin (miRVana miRNA isolation Kit, Ambion, Austin, TX., USA). cDNA for individual mRNAs was generated using the High Capacity cDNA Reverse

Transcription Kits (Applied Biosystems, Foster City, CA., USA). Samples were

amplified by using the TaqMan Universal PCR Master Mix (Applied Biosystems, Foster

City, CA., USA) and analyzed on an AB Step One Plus Real Time PCR System (Applied

Biosystems, Foster City, CA., USA). Real time taqman primers were purchased from

Applied Biosystems (Applied Biosystems, Foster City, CA., USA).

5.4 Results

The EGFR ligand HBEGF is upregulated in Dicer mutant skin during anagen.

Because miRNA targets are expected to be upregualted in *Dicer* and *Drosha*^flEx9^ mutants,

the effects of *Dicer* or *Drosha* depletion on EGFR and Notch1 expression are likely to be

indirect. Therefore I examined the expression of potential negative regulators of the EGF

and Notch pathways. Both of these receptors have the potential to be negatively

regulated by overexpression of their ligands, in a negative feedback response. To

determine if EGF or Notch family ligands were upregulated in *Dicer* mutant skin, we

isolated RNA from *Dicer* control and mutant mice induced at E18 and biopsied at PD12,

a time point just before external hair became wavy. QPCR analysis revealed that the

EGF ligand family member, HBEGF was highly upregulated in *Dicer* mutant skin,

compared to control skin at PD12 (Figure 5.1A). Interestingly EGFR mRNA levels were

not changed; however Notch2 mRNA was significantly reduced. Altered Jag1 or Jag2

mRNA levels did not reach statistical significance, although Jag2 mRNA showed a trend

towards upregulation in mutant skin (p=0.120) (Figure 5.1B).

***TSLP* levels are elevated in *Dicer* mutant skin**

Similar to phenotypes observed in *Dicer* and *Drosha*^{flEx9} mutant mice, epidermal Notch

deficiency resulted in inflammation, which is believed to occur as a result of defective

barrier formation, and is associated with elevated levels of the keratinocyte-derived

cytokine TSLP (Demehri et al., 2008). To determine if TSLP was upregulated in *Dicer*

mutant skin we assayed for TSLP mRNA levels at PD15, a time point prior to observed

inflammation, in control and mutant skin following doxycycline treatment from E18. We

observed a more than 10-fold elevation in TSLP mRNA levels in *Dicer* mutant compared

with control skin (Figure 5.2A). Another keratinocyte-derived cytokine, IL18 was also

significantly upregulated at this time point (Figure 5.2B). Consistent with the observed

inflammation, these data suggest that mildly impaired barrier function may contribute to

elevated levels of TSLP and inflammation.

Direct targets of *miR-205* are upregulated in *Dicer* mutant skin

To identify direct effects of miRNA depletion on epidermal target mRNAs, we focused

on *miR-205*, as it is one of the most abundant epithelial miRNAs (Andl et al., 2006; Yi et

al., 2006), and is dramatically depleted in epidermal *Dicer* and *Drosha* mutants (Figure

2.2, and Figure 3.1). Of particular interest was the direct *miR-205* target *E2f1* (Dar et al.,

2011), a key regulator of the G1/S transition and p53-mediated apoptosis (DeGregori,

2002). *KRT5* promoter-driven over-expression of *E2f1* in transgenic mouse skin epithelial

cells results in apoptosis of early anagen hair follicle matrix cells and interfollicular

epidermis hyperproliferation (Pierce et al., 1998), replicating phenotypes observed in

114

epidermal *Dicer* and *Drosha* mutants. QPCR analysis of dorsal skin samples from PD15

Dicer mutants and control littermates induced from E18 revealed a statistically

significant increase in the levels of *E2f1* mRNA in mutants relative to controls (n=2

mutants and 2 controls; p=0.038) (Figure 5.3). These data suggest that *miR-205*-mediated

E2f1 mRNA degradation may be important in preventing matrix cell apoptosis in early

anagen and interfollicular epidermal hyperproliferation.

The transcriptional repressor Zeb2 is another direct target of *miR-205* (Paterson et al.,

2008) that is elevated in *Dicer* mutant compared with control skin at PD15 in a

statistically significant manner (n=2 mutants and 2 controls; p=0.022) (Figure 5.3).

Among other roles, Zeb2 regulates epithelial-mesenchymal transition (EMT) (Gregory et

al., 2008). *Dicer* deletion in embryonic epidermis results in an unusual phenotype of hair

follicle evagination (Andl et al., 2006; Yi et al., 2006), and we observed apparent

extrusion of keratinized hair follicle cells in induced postnatal epidermal *Drosha* and

Dicer mutants (Figure 3.3). These phenotypes that may be related to abnormal control of

intercellular adhesion and cell movements by dysregulated *Zeb2*.

A third direct *miR-205* target, the non-receptor intracellular tyrosine kinase Src (Majid et

al., 2011), was also upregulated in *Dicer* mutant skin, although this did not reach

statistical significance (n=2 mutants and 2 controls; p=0.073) (Figure 5.3). Elevated

levels of epidermal Src cause hyperproliferation, hair follicle defects, and chronic

inflammation (Matsumoto et al., 2003; Yagi et al., 2007), and could contribute to these

abnormalities in miRNA-depleted skin. Taken together, these results suggest that

upregulation of multiple miRNA target genes contributes to the complex phenotypes of epidermal *Dicer* and *Drosha*[flEx9] mutants.

5.5 Discussion

Here I show that mRNA expression of HBEGF, a ligand of the EGFR signaling family, was significantly upregulated in early anagen skin biopsied from *Dicer* mutant and control mice induced from E18 to PD12. This suggests that regulation is likely complex and the observed affects may possibly be due to a negative feedback regulatory loop. Jag1 mRNA levels were unaltered, and Jag2 mRNA levels trended upward in *Dicer* mutant skin although this did not reach statistical significance. Since some miRNAs regulate translation rather then degradation of mRNA targets, assaying for levels of Jag2 protein in *Dicer* mutants may be helpful in determining if its expression level is affected in *Dicer* mutant mice. Consistent with the downregulation of Notch activity, I found more than 10-fold elevation in *TSLP* mRNA levels in *Dicer* mutant compared with control epidermis from mice induced from E18 and biopsied at PD15. This observation suggests that barrier function may be impaired as a result of intrinsic defects in the interfollicular epidermis including impaired Notch signaling (Yi et al., 2008) and/or loss of hair follicle integrity. A recent study showed that treatment of epidermal *Dicer*-depleted mice with MC903, a vitamin D3 analog, triggers increased levels of TSLP production relative to those observed in MC903-treated control mice (Hener et al., 2011). In this latter study, however, epidermal *Dicer*-depleted mice had a normal phenotype in the absence of MC903 treatment, suggesting that *Dicer* deletion was incomplete. While TSLP levels are directly and positively controlled by *miR-375* in intestinal cells (Biton et

al., 2011), decreased *miR-375* levels in *Dicer*-deficient epidermis and hair follicles (Figure 2.3) suggest that epidermal *TSLP* is regulated by other, less direct, mechanisms. Whether depletion of miRNAs contributes directly or indirectly to decreased levels of Notch1 and Notch1 NICD in *Drosha*^flEx9^ and *Dicer* mutants, will be important areas for future investigation.

The most immediate and striking phenotypes in *Drosha*^flEx9^ or *Dicer* mutants were observed in the early anagen HF matrix, one of the most rapidly proliferating adult cell populations, which displayed increased apoptosis and DNA damage. The extremely rapid proliferation of matrix cells may render them particularly susceptible to double stranded breaks, resulting in increased requirements for genomic repair. We observed increased expression of the direct *miR-205* target *E2f1*, a key regulator of the G1/S transition and p53-mediated apoptosis, in *Dicer* mutant skin (Dar et al., 2011). Interestingly, forced expression of *E2f1* in transgenic mouse skin epithelial cells causes a similar phenotype of HF matrix cell apoptosis and IFE hyperproliferation (Pierce et al., 1998), suggesting that *miR-205*-mediated *E2f1* mRNA degradation may be important in preventing matrix cell apoptosis in early anagen and IFE hyperplasia. E2F1 is post-translationally modified in response to DNA damage, localizes to DNA strand breaks, recruits repair factors, and promotes DNA repair (Degregori, 2011), and thus may also contribute to the abnormal DNA damage response observed in miRNA-depleted matrix cells.

5.6 Figure legends

Figure 5.1. **Transcriptional upregulation of HBEGF and downregulation of Notch2 in Dicer mutant skin during early anagen.** (A,B) Quantitative PCR analyses of *HBEGF* and *Notch2* mRNAs extracted from PD15 *Dicer* mutant and control skin following doxycycline treatment from E18 (n=2 control and 2 mutant samples for each experiment; qPCR replicated 3x for each sample). Control expression levels were normalized to 1.0. Relative expression levels are graphed (arbitrary units). P-values were calculated using a 2-tailed Students t-test. (*) indicates statistically significant differences.

Figure 5.1
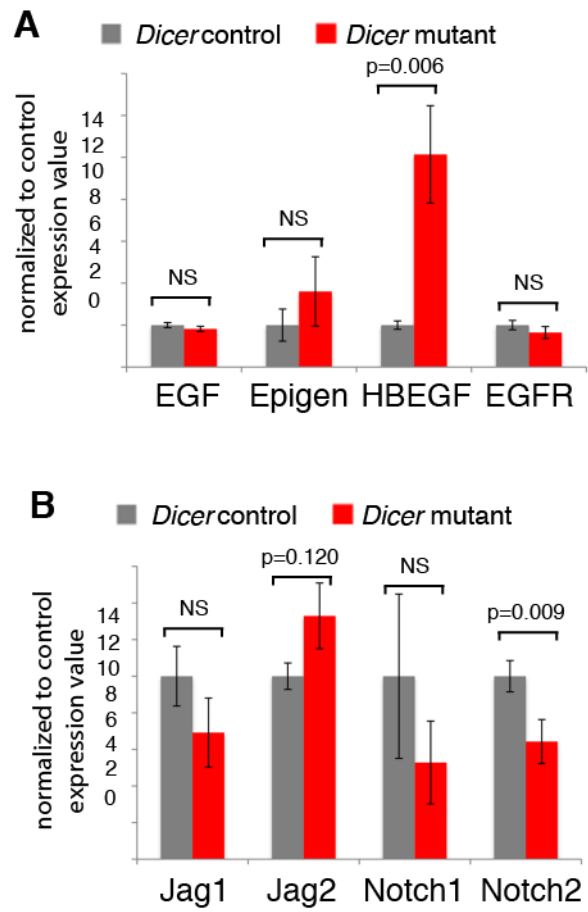
Figure 5.2. **Tslp and IL18 mRNA levels are increased in Dicer mutant skin prior to inflammation** (A,B) Quantitative PCR analyses of *Tslp* and *IL18* mRNAs extracted from PD15 *Dicer* mutant and control skin following doxycycline treatment fro E18 (n=2 control and 2 mutant samples for each experiment; qPCR replicated 3x for each sample). Control expression levels were normalized to 1.0. Relative expression levels are graphed (arbitrary units). P-values were calculated using a 2-tailed Students t-test. (*) indicates statistically significant differences.

Figure 5.2
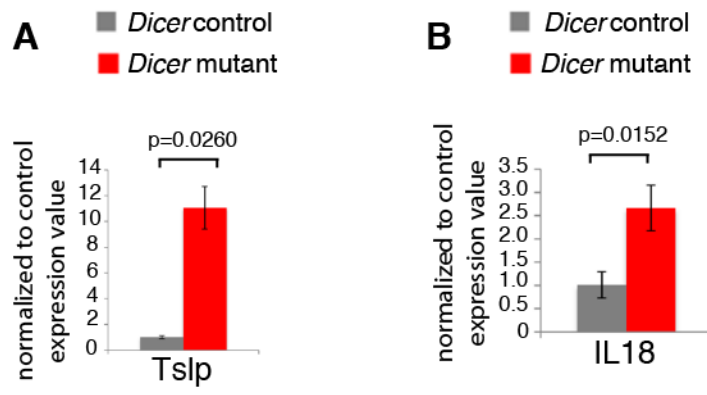
Figure 5.3 **Direct miR-205 targets *E2f1*, *Zeb2* and *Src* are upregulated in miRNA-depleted skin.** (C,D) Quantitative PCR analyses of *E2f1*, *Zeb2* and *Src* mRNAs extracted from *P15 Dicer* mutant and control skin following doxycycline treatment from E18 (n=2 control and 2 mutant samples for each experiment; qPCR replicated 3x for each sample). Control expression levels were normalized to 1.0. Relative expression levels are graphed (arbitrary units). P-values were calculated using a 2-tailed Students t-test. (*) indicates statistically significant differences.

Figure 5.3
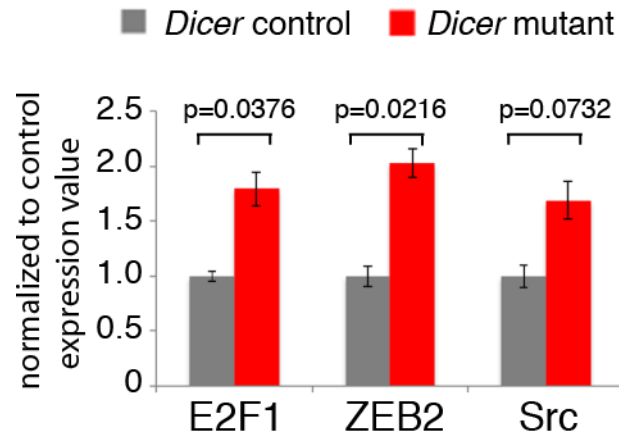
CHAPTER SIX
Conclusion

6.1 Summary of Findings

The function of Dicer and a few specific miRNAs have been studied in other constantly regenerating systems such as the stomach and colon. *Dicer* function is required in the embryonic mesenchyme and mesogastrium for stomach, intestine and spleen development. During stomach morphogenesis miR-7a and miR-203 target the mesenchymal transcription factor Barx1, which is required for stomach specification but must be quickly repressed in the epithelium for late-gestational stomach development to occur (Kim et al., 2011). Embryonic *Dicer* ablation in the villi and crypt cells of the small and large intestines causes disorganization of the intestinal epithelium, with cell death occurring in intestinal crypts and accelerated jejunal cell migration. Similar to our observation of dermal inflammation in *Dicer* and *Drosha* mutants, intestinal inflammation was observed following impaired intestinal barrier function (McKenna et al., 2010). TNF-alpha mediates intestinal permeability in response to inflammation, and recently has been show to upregulate miR-122, which directly targets the tight junction protein occludin (Ye et al., 2011), suggesting that miRNAs may regulate intestinal permeability in adult intestine.

However, to date *Dicer* and *Drosha/DGCR8* loss have not been carefully evaluated at distinct time points during normal adult tissue regeneration. Because of the regenerative properties of the hair follicle growth cycle and epidermis, the skin provides a dynamic system to study miRNA function, allowing us to determine the effect of miRNA loss

124

during specific cellular processes including proliferation, differentiation, programmed cell death, and progenitor cell maintenance. Here I show that Dicer and Drosha play similar roles in postnatal skin epithelial cells. In the interfollicular epidermis, Dicer and Drosha are necessary to suppress epidermal proliferation and restrict the size of the basal and suprabasal layers. In contrast, the effect of *Dicer* and *Drosha* deletion in the hair follicle is dependent on the timing of excision. Hair follicle defects resulting from loss of *Dicer* and *Drosha* were observed during early and late anagen, and at the transition into catagen.

Previous findings demonstrated that when *Dicer* is deleted during embryogenesis, the KRT15 bulge stem cell compartment was never established (Andl et al., 2006). Following short term depletion, after the establishment of the KRT15 compartment, *Dicer* or *Drosha* are not required for stem cell maintenance in telogen stage hair follicles. However, after long term depletion or when hair keratinocytes are activated, either during the natural hair cycle or after hair plucking, dramatic defects in hair follicle growth are observed. This suggests that miRNAs do not have specific functions in maintaining resting hair follicles or in hair follicle stem cells.

During early anagen, hair follicle stem cells are activated in both *Dicer* and *Drosha*^{flEx9} mutant hair follicles, and are able to produce matrix keratinocytes that proliferate at normal rates and differentiate appropriately, indicating that miRNAs are not necessary for anagen entry after hair plucking. However, miRNAs are necessary to sustain anagen and in particular to prevent cell death and DNA damage, as both TUNEL positive and

125

pH2A.X expressing cells were observed in rapidly proliferating mutant matrix cells but not in control matrix cells. Although the epidermis became hyperproliferative at late time points following deletion, pH2A.X recruitment was not observed in epidermal keratinocytes of *Dicer* and *Drosha*^{flEx9} mutant skin but occurred nearly exclusively in mutant early anagen hair follicle bulbs. Because the matrix undergoes heavy proliferation to generate the cells necessary for a new hair shaft and inner root sheath, some DNA damage may be common as a consequence of sustained replication. MiRNAs may play a protective role during this phase of the hair follicle growth cycle.

Dicer or *Drosha* deletion in an established anagen phase results in failed hair shaft formation as external hairs become wavy and the IRS compartment is smaller and malformed. Although we cannot rule out direct roles for miRNAs in hair shaft formation, differentiation markers and keratins were appropriately expressed. Taken together with evidence of cell death and DNA damage in the matrix, these data suggest that the defect was not due to a failure of inner root sheath and hair shaft development, but from a deficiency in the number of IRS and hair shaft progenitors arising from the matrix population.

After the anagen phase is complete, control hair follicles regressed, but *Dicer* and *Drosha*^{flEx9} mutant hair follicles failed to do so, instead maintaining an abnormal growth phase. The failure of *Dicer* and *Drosha*^{flEx9} mutant hair follicles to enter catagen suggests that miRNAs regulate the anagen-to-catagen transition. Future studies may explore the

roles of miRNAs in dampening the expression of signaling molecules that either promote

anagen, or inhibit catagen.

When *Dicer* and *DGCR8* are deleted in the epidermis constitutively starting at E14, the

epidermis becomes hyperproliferative, and the epidermal p63 compartment is expanded

(Antonini et al., 2010; Lena et al., 2008; Yi et al., 2008). Similarly, our data show

epidermal hyperproliferation and p63 expansion when *Dicer* and *Drosha* are deleted

individually in adult epidermis, suggesting that Drosha/DGCR8 and Dicer functions, or

the cofactors that regulate them, do not change substantially in the epidermis after birth.

Independent of the timing of initiation of *Dicer* and *Drosha* deletion, hair follicles

eventually degraded, forming utricles that merged with the hyperproliferative epidermis.

Interestingly, it has been reported that many mutants with hair follicle degradation also

show epidermal hyperproliferation, suggesting that these processes may be related. In

Dicer and *Drosha*^{flEx9} mutants dermal inflammation occurred concomitantly with

hyperproliferation. It is likely that this, together with intrinsic loss of interfollicular

miRNAs such as miR-203 (Yi et al., 2008), contributes to the hyperproliferation of the

epidermis in *Dicer* and *Drosha* mutant mice.

We observed that the hair follicle and epidermal phenotypes in *Dicer* and *Drosha* mutant

mice were similar to mice either lacking epidermal Notch1 or expressing a dominant

negative EGFR receptor in the epidermis (Murillas et al. 1995; (Vauclair et al., 2005).

Here I show that the EGFR, and Notch1 and Notch2 recptors were downregulated in

Dicer and *Drosha^{flEx9}* mutants. Loss of Notch signaling in the epidermis is thought to

result in defects barrier formation, resulting in increased production of the cytokine

thymic stromal lymphopoietin (TSLP) by epidermal keratinoctyes, which in turn

mediates an inflamatory response (Demehri et al., 2008). Interestingly, when we tested

for increased TSLP mRNA levels in *Dicer* mutant skin we found a ten fold increase in

compairson to controls. Decreased, Notch signaling could account at least in part for

increased levels of TSLP and inflammation in *Dicer* and *Drosha^{flEx9}* mutant skin.

Whether the Notch pathway is directly or indirectly regulated by miRNAs will be an

important area for future investigation.

MiR-205 directly targets E2F1, Zeb2 and Src in other biological systems (Dar et al.,

2011; Gregory et al., 2008; Majid et al., 2011) and we show upregulation of these

proteins in *Dicer* mutant compared to control skin. Future studies will determine whether

miR-205 expression is sufficient to rescue the increase in E2F1 and Zeb2 expression in

mutant skin, and will explore the function of E2F1, Zeb2 and Src in normal skin (see

section 6.3). As the field progresses it will be interesting to see if genomic integrity,

regulation of Notch activity, barrier function or tissue maintenance are common functions

of miRNAs in other adult regenerative systems, such as the stomach, intestine or colon.

6.2 Limitations of Approach

Because both the *Dicer* and *Drosha* global knock out mutations are embryonic lethal, it

was necessary to deplete *Dicer* and *Drosha* specifically in the skin. A limitation of this

approach is the skin specific promoters that are available. The KRT5 promoter is active

in both the basal layer of the epidermis and the ORS of the hair follicles. Although the

effects of *Dicer* or *Drosha* deletion are of interest in both skin compartments, this system

does not allow us to delineate between epidermal-autonomous loss of *Dicer* or *Drosha*,

and the effects of hair follicle degradation on epidermal proliferation. Further studies

using an epidermal specific promoter, such as involucrin, which has been used to

successfully drive other epidermal mutations, would be necessary to address this.

However, a caveat of this approach is that many of these epidermal specific promoters

are not active in the basal cell population.

Another limitation of using the KRT5-rtTA, tetO-Cre system, was that it did not delineate

whether inflammation was due to defects in the interfollicular epidermis, or from

degrading hair follicles, and whether inflammation directly contributes to epidermal

proliferation. Below, I outline possible experiments to address these concerns.

Are defects in the interfollicular epidermis the sole cause of inflammation?

Hair follicle specific Cre mouse lines are available, and may be a more practical approach

to determine whether hair follicle defects contribute to hyperproliferation of the inter

follicular epidermis. In Chapter Four, we use the *KRT15-CrePR1* mouse line to deplete

Dicer specifically in the hair follicle stem cell compartment. Unfortunately, Cre

expression in this system was mosaic so the full phenotypes associated with *Dicer* loss

were not observed. Future studies using the temoxifen inducible *Shh-CreER* (Harfe et al.,

2004), or the *KRT19CreER* (Means et al., 2008; Youssef et al.2012) mouse lines to delete

Dicer or *Drosha* specifically in the hair follicle may be necessary to address hair follicle

specific phenotypes, but spatial and temporal regulation of Cre activity should first be tested by breeding in the *Rosa26R* transgene. If Cre activity is limited to hair follicles within the skin, these inducible Cre mice would be crossed into the *Dicer* or *Drosha*^{flEx9} mutant strains, and induced at birth. Dermal inflammation would be addressed analyzing by skin histology at PD17, PD20, PD32 and PD35. If inflammatory cells were present, we would conclude that inflammation was associated with hair follicle degradation. However, if *Dicer* and *Drosha* were efficiently deleted in hair follicles but did not degrade or inflammation was not associated with their degradation, then we would conclude that *Dicer* or *Drosha* deficiency in the epidermis contributes to hair follicle phenotypes.

Does inflammation associated with follicular degradation cause epidermal hyperproliferation?

If *Dicer* depletion using a hair follicle specific Cre system, proposed above, results in the same hair follicle phenotypes as KRT-promoter driven deletion, including degradation of the hair follicle, epidermal keratinocytes could then be monitored at successive time points for signs of hyperproliferation. If the epidermis is not hyperproliferative in hair follicle specific, *Dicer* or *Drosha*^{flEx9} -depleted mice, then we would conclude that intrinsic loss of epidermal miRNAs causes epidermal hyperproliferation in *Dicer* or *Drosha*^{flEx9} *KRT5-rTTA, tetO-Cre* mutant mice. If the epidermis becomes hyperproliferative, then we would conclude that, inflammation caused by degrading hair follicles contributes contributing to epidermal hyperproliferation in *Dicer* and *Drosha*^{flEx9} mutants. To determine whether hair follicle degradation per se is sufficient to drive

130

epidermal hyperproliferation, mice expressing the inducible suicide gene HSVTK under the KRT15 promoter, in which bulge cells are ablated when a nucleoside analog ganciclovier is administered (Ito et al., 2005), could be used to determine whether epidermal hyperproliferation is non specific, or specific to *Dicer* or *Drosha* loss in the hair follicle. Since KRT15 is also expressed in the gut, and induced KRT15-HSVTK mice do not survive long, skin would be grafted on to nude mice, and we would ask if the epidermis becomes hyperproliferative after hair follicles degrade.

Does suppressing inflammation reduce epidermal hyperproliferation?

Temporal concurrence of epidermal hyperproliferation with inflammation suggested that hyperproliferation might occur in response to inflammation caused by hair follicle degradation. However, it is possible that inflammation arises due to both hair follicle and intrinsic epidermal defects. We could directly test if inflammation contributes to epidermal hyperproliferation by administering an anti-inflammatory drug, such as topical 1% hydrocortisone or subcutaneous injections of meloxicam, to $Dicer^{fl/fl}$, KRT5-rtTA, tetO-Cre, mutants and controls prior to hair follicle degradation, and the thickness of the epidermis could be quantified between treated and non-treated *Dicer* and $Drosha^{flEx9}$ mutant mice, in comparison with treated and non-treated control mice. If suppression of inflammation by drug treatment occurs, then the thickness of the epidermis would be monitored. If the thickness of the epidermis is suppressed with decreased inflammation, we can conclude that the inflammatory response in *Dicer* and $Drosha^{flEx9}$ mutant mice, irrespective of its origin, directly contributes to epidermal hyperproliferation.

131

6.3 Future Directions

Validation of miR-205 regulation and contributions of Ef21, Zeb2 and Src

overexpression to the phenotypes of *Dicer* and *Drosha*^{flEx9} mutant mice.

To address whether miR-205 is sufficient to reduce E2F1, Zeb2 or Src levels in *Dicer* or

Drosha skin, transgenic mice overexpressing miR-205 under an epidermal specific

promoter, (e.g. KRT5 or KRT14) would be generated and bred to *Dicer* or *Drosha*^{flEx9}

mutant mice. E2F2, Zeb2 and Src expression levels could be compared between *Dicer* or

Drosha^{flEx9}mutant mice with or without miR-205 overexpression. If E2F1, Zeb2 and Src

expression levels are reduced, *Dicer* and *Drosha*^{flEx9} mutant mice with and without the

miR-205 transgene would be analyzed during early anagen and catagen for rescue of

epidermal and follicular phenotypes related to E2F1, Zeb2 and Src protein function.

Does E2F1 overexpression cause matrix cell death in Dicer and Drosha^{flEx9} mutant skin?

E2F1 is a transcription factor that regulates transitions from G1 to S-phase as well as p53

mediated apoptosis. Consistent with this latter role, KRT5-promoter driven

overexpression of E2F1 results in cell death, specifically in the matrix region (Pierce et

al. 1998), similar to the phenotypes we observed in *Dicer* and *Drosha*^{flEx9} mutant mice in

early anagen (Figure 4.6 M-R). Mice globally deficient in E2F1 are viable and fertile,

but show thymocyte maturation defects, exocrine gland dysplasia, testicular atrophy,

decreased salivation and are prone to various cancers as they age (Field et al., 1996).

To determine whether elevated E2F1 contributes to matrix cell apoptosis in *Dicer* and *Drosha*^{flEx9} mutants, matrix cell viability could be analyzed in *Dicer* and *Drosha*^{flEx9} mutant mice homozygous for E2F1 deletion.

Does E2F1 overexpression result in disorganzation of the healing epidermis in wounded Dicer and Drosha^{flEx9} *mutant skin?*

Drosha and Dicer mutants exhibited disorganiztion of the epidermis during wound healing. Interestingly, examination of the skin of E2F1 deficient mice revealed decreased integrin expression and signaling in the epidermis. E2F1 deficient keratinocyes were shown to be defective in proliferation, adhesion, and migration, and consistent with these findings E2F1 deficient mice were defective in cutaneous wound repair (D'Souza et al., 2002). However, adhesion and migration of epidermal keratinocytes and wound healing have not been analysed in mice overexpressing E2F1. I would first ask whether transgenic E2F1 mice also show defective wound repair. Specifically I would wound transgenic E2F1 mice, and use histology to determine if the healing epidermis is disorganized. I would assay sections from wounded transgenic E2F1 mice for upregulation of integrin expression. If I found defects in the healing epidermis similar to those observed in *Dicer* or *Drosha*^{flEx9} mutant mice, I would ask whether deficiency of E2F1 in *Dicer* or *Drosha*^{flEx9} mutant mice rescues epidermal defects during wound healing. If E2F1 mRNA levels were reduced in *Dicer* or *Drosha*^{flEx9} mutant mice expressing a miR-205 transgene in the experiments proposed above, I would also ask whether forced expression of miR-205 is sufficient to rescue epidermal wound healing defects.

Does increased Zeb2 expression promote EMT in Dicer and Drosha^{flEx9} mutant mice?
Zeb2 is a transcription factor that regulates epithelial-mesenchymal transitions (EMT)
(Gregory et al., 2008). During EMT, epithelial cells lose apical-basolateral polarity,
dissolve cell-cell junctions, such as tight junctions, adherens junctions and desmosomes,
and take on mesenchymal phenotypes by forming stress fibers, and reorganizing actin to
increase migration or invasion. Zeb2 promotes EMT by repressing expression of E-
cadherin and cell-cell junction proteins such as the tight junction proteins claudin-4 and
ZO-3, and the desmosome protein Plakophilin-2, while activating expression of proteins
associated with a mesenchymal fate, such as Vimentin, N-cadherin, and matrix
metalloproteinase-2 (Bindels et al., 2006; Taki et al., 2006; Vandewalle et al., 2005). In
addition to roles in tissue formation during development, EMT is thought to be necessary
in postnatal skin for proper wound healing. Furthermore, analysis of expression of the
EMT positive-regulator Snail1 in human skin suggests that missregulated EMT in the
follicular epithelium may result in post menopausal alopecia (Nakamura and Tokura,
2010). Overexpression of Zeb2 in *Dicer* and *Drosha^{flEx9}* mutants may account for
phenotypes resulting from abnormal intercellular adhesion and cell migration. For
instance, *Dicer* deletion in embryonic epidermis causes an unusual phenotype of hair
follicle evagination (Andl et al., 2006; Yi et al., 2006), and we observed apparent
extrusion of keratinized hair follicle cells in induced postnatal epidermal *Dicer* and
Drosha^{flEx9} mutants (Figure 3.3M-P). Furthermore, the healing epidermis in wounded
Dicer and *Drosha^{flEx9}* mutant was disorganized (Figure 3.5).

To determine if the observed phenotypes are related to deregulation of Zeb2, I would first ask whether E-cadherin, claudin-4, ZO-3, and Plakophilin-2, are reduced and whether Vimentin, N-cadherin, and matrix metalloproteinase-2 are up regulated in *Dicer* or *Drosha*^{flEx9} mutant compared to control skin biopsied at PD30, just prior to apparent extrusion of keratinized material. I would assay for their expression by immunoblotting and/or IHC. If the expression levels of any of these proteins correlated with Zeb2 overexpression, I would then look more closely at cell-adhesion in the epidermis by examining the formation of tight junctions and desmosomes by electron microscopy. Expression levels of Zeb2 targets could also be compared between Dicer control and mutant wounded tissue. Lack of normal cell adhesion proteins in the Dicer mutant could account for disorganization of the healing epidermis.

Does EMT occur in Dicer mutant hair follicles?

To determine whether *Dicer* mutant follicular epithelium could be losing epithelial characteristics and taking on a mesenchymal fate, I would fate label hair follicle keratinocytes using the *Dicer*$^{fl/fl}$ *KRT5-rtTA tetO-Cre Rosa26R* mouse line. Mice would be induced at E18 and skin would be biopsied at PD32 and X-gal stained. The presence of blue cells interspersed in the dermis could indicate that follicular epithelial cells were taking on a mesenchymal fate. Confirmation of an epidermal to mesenchymal transformation could be further addressed by staining for co-expression of E-cadherin, X-gal staining and Fibronectin. If transgenic expression of miR-205, as outlined above, reduces Zeb2 expression to endogenous levels in *Dicer* or *Drosha*^{flEx9} deficient mice, I

135

would ask whether forced miR-205 expression could rescue any EMT defects observed in *Dicer^{fl/fl} KRT5-rtTA tetO-Cre Rosa26R* mice.

Does overexpression of Src contribute to hyperproliferation, hair shaft defects or inflammation in Dicer or Drosha^{flEx9} mice?

Similar to *Dicer* and *Drosha^{flEx9}* mutant phenotypes, overxpression of Src results in hyperproliferation, defective hair shaft formation, and chronic inflammation (Matsumoto et al., 2003; Yagi et al., 2007). Because upreguation of Src did not reach statistical significance, I would first confirm that Src protein levels and downstream signaling are upregulated in *Dicer* and *Drosha^{flEx9}* mutant skin. If Src is overexpressed in *Dicer* and *Drosha^{flEx9}* mutant mice, I would ask if hyperproliferation, defective hair shaft formation and inflammation is related to Src upregulation. Src deficient mice, available from Jackson Labs, are osteopetrotic and lack incisors; however mice heterozygous for Src are viable and healthy. To determine if Src depletion could rescue *Dicer* or *Drosha^{flEx9}* mutant phenotypes I would generate mice heterozygous for the Src mutation and deficient in *Dicer* and *Drosha*. I would test for rescue of epidermal hyperproliferation, hair follicle defects and inflammation. If these phenotypes were not rescued, then I would test whether homozygous loss of Src is capable of rescuing the phenotypes in *Dicer* or *Drosha^{flEx9}* mice. I would expect compound *Dicer/Drosha* and *Src* mice to survive up until weaning; however, because *Dicer* and *Drosha^{flEx9}* mutant mice may also have nutritional defects, grafting of mutant and control skin onto nude mice might be necessary to analyze the potential rescue of epidermal and hair follicle phenotypes. If transgenic expression of miR-205, outlined above, could reduce Src expression to

endogenous levels in *Dicer* or *Drosha*[flEx9] deficient mice, rescue of hair follicle defects

and epidermal proliferation would be tested using the same phenotypic analysis described

for *Dicer* and *Drosha*[flEx9] mutant mice. Rescue of *Dicer* or *Drosha*[flEx9] deficient

hyperproliferation, hair follicle defects, or inflammation in either the miR-205 transgenic

when Src is down regulated, or the Src deficient system, would support the hypothesis

that miRNAs regulate Src in the skin.

Identification of miRNAs and mRNAs associated with the RISC complex in the

epidermis and hair follicle subpopulations

To identify miRNAs that are active in the Ago2-containing RISC complex within

epidermal basal cells, our lab has employed a technique to isolate an Ago2 complex

containing either miRNA or mRNA species from postnatal day one epidermal basal cells.

We took advantage of mice expressing a nuclear GFP, H2B-GFP, under the KRT14

promoter (Rendl et al., 2005). KRT14-H2B-GFP mice produce basal cells that fluoresce

when excited with the proper wavelength of light, permitting FACS-isolation of GFP

high basal and ORS cells and GFP low suprabasal and matrix cells (Rendl et al., 2008).

Zhenquan Yu, a postdoc in the Millar Lab, FACS isolated GFP-expressing cells from

KRT14-H2B-GFP mice at PD1. The cells were lysed and the extract was UV-

crosslinked and an agarose-conjugated antibody, raised against Ago2, was used to isolate

the complex. The complexes were separated by size using electrophoresis into Ago2-

miRNA and Ago2-mRNA populations. RNA was extracted from these complexes, and

after mild digestion of long mRNAs and the addition of sequencing linkers and tags, the

miRNA and mRNA species associated with the Ago2 complex were sequenced and aligned to the mouse genome. Computer analysis searches for over-represented six nucleotide sequences in the mRNA Ago footprints, were conducted to identify miRNA seed regions. This approach identifies hundreds of putative miRNAs and mRNA targets in epidermal basal cells of the PD1 mouse and could be further refined analyse suprabasal and matrix cell populations in the adult. In particular HITS CLIP analyses will be performed on specific skin cell populations at stages just before phenotypes appear in Dicer and Drosha mutants, including during the anagen-catagen transition and at early anagen timepoints in K14-H2B-GFP mice. Below, I outline possible experimental strategies to achieve this goal.

Future experiments will also use *Dicer* and *Drosha^flEx9* mutant mice to validate putative miRNA targets. Since we expect miRNA targets to be overexpressed in the *Dicer* and *Drosha^flEx9* mutants, mRNAs found in the Ago2 complex can be prioritized based on their overexpression, and the overexpression of the corresponding protein, in *Dicer* and *Drosha^flEx9* mutant skin.

Identification of miRNAs and mRNAs associated with Ago2 in hair follicles during late anagen

In Chapter Two, I showed that *Dicer* and *Drosha^flEx9* mutant hair follicles fail to regress and remain in an abnormal anagen compaired to control hair follicles. This observation suggests that miRNAs play an active role in progression from anagen to catagen. Since the ORS and matrix cell populations can be readily FACS sorted from the skin, I would

first ask which miRNAs and mRNAs are present in the Ago2 complex during late anagen. I would isolate the total GFP+ populations, containing ORS and matrix, at the late anagen time point from *KRT14-H2B-GFP* mice. To first enrich for the follicular GFP population, I would separate the epidermis from the dermal portion of the skin from a PD18 day old mouse by digestion with 2.5% trypsin and mild mechanical removal of the epidermis. Once left with only the dermal portion, I would digest with 1% Collagenase I to produce a single cell suspension. GFP+ cells would then be isolated by FACS sort, and the Ago2 miRNA and mRNA populations would be further isolated and their respective RNAs would be sequenced as described above. I would validate putative miRNA targets by QPCR, Western and/or ISH and IHC in the skin from *Dicer* and *Drosha^{flEx9}* control and mutant littermates induced at E18 and biopsied at PD18.

Identification of miRNAs and mRNAs associated with Ago2 in the hair follicle matrix during early anagen.

In Chapter Four, I showed that significant DNA damage and apoptosis is present specifically in the matrix of *Dicer* and *Drosha^{flEx9}* mutant hair follicles following hair plucking. I hypothesize that specific miRNAs play a protective role in the matrix during periods of high rates of cell division. To identify miRNAs associated with the RISC complex in the matrix cell population during this time period, I would perform HITS CLIP analysis. In KRT14-H2B-GFP mice matrix cells are marked by low GFP expression (GFP^{low}) levels and can be sorted away from cells expressing high levels of GFP (Rendl et al., 2008). Matrix cells would be isolated from KRT14-H2B-GFP mice, five days after hair plucking at PD50. At this time point, matrix cells will be rapidly

dividing and I would expect miRNAs that protect the genomic stability in these cells to be actively regulating their mRNA targets.

To first enrich for the matrix GFP^{low} population, I would separate the epidermis from the dermal portion of biopsied skin, by digestion with 2.5% trypsin and mild mechanical removal of the epidermis. Once left with only the dermal portion, which will contain the majority of the hair follicles, I would digest with 1% Collagenase I to produce a single cell suspension. The GFP^{low} expressing cells would then be isolated by FACS sort, and the Ago2 miRNA and mRNA populations would be further isolated and their respective RNAs would be sequenced as described above. I would validate putative miRNA targets by QPCR, Western and/or ISH and IHC using extracts of skin from *Dicer* and *Drosha^{flEx9}* control and mutant littermates induced at PD40, plucked at PD50 and biopsied at PD55, a time point just prior to the stage when an overt DNA damage response is observed in the matrix.

Regulation of the epidermal Notch signaling pathway.

In constitutive epidermal *Dicer* mutant mice, Notch receptor expression was decreased in both the epidermis and the hair follicles (Andl et al., 2006). In Chapter Two, I show that Notch1 receptor expression and its NICD are decreased in *Dicer* and *Drosha^{flEx9f}* mutants following deletion in the embryonic hair follicle growth cycle. In addition to promoting differentiation of the spinous layer, there is evidence that Notch signaling may represses p63 and integrin expression (Blanpain and Fuchs, 2009; Moriyama et al., 2008). If so, loss of Notch1 signaling in the epidermis may contribute to the observed upregulation of

p63 in *Dicer* and *Drosha*^*flEx9* mutant mice. These observations raise the interesting

possibility that epidermal miRNAs might directly regulate the Notch signaling pathway,

for instance by downregulating inhibitors and/or factors involved in negative feedback

regulation of Notch1 expression.

The Notch pathway is a highly conserved signaling pathway, required for numerous

developmental processes, most importantly the determination of cell fate. In mammals

there are four Notch receptors, activated by either the Delta-like family of ligands (DLL1,

DLL3 and DLL4), or the ligands Jagged1 and Jagged 2 (Jag1 and Jag2). In the skin,

Notch receptors 1, 2, and 3 are expressed throughout the epidermis and hair follicles, and

the ligands Jagged 1 and Jagged 2 are differentially expressed. Jagged 2 is expressed in

the basal layer of the epidermis, whereas Jagged 1 is expressed in the suprabasal layers.

Both ligands and receptors are transmembrane proteins that are processed and released

from the membrane, requiring the signaling and receiving cells to be closely apposed.

Once activated by a ligand, the extracellular domain of the Notch receptor is cleaved,

usually by the metalloprotease TACE (a.k.a. ADAM17). The extracellular portion of

Notch is internalized by endocytosis within the cell expressing the ligand, while the

transmembrane portion remains and is available for further processing by gamma-

secretase. Cleaveage by gamma-secretase releases the intracellular signaling domain

(NICD) from the transmembrane domain, and NICD is then free to enter the nucleus

where it interacts with a member of the CSL transcription factor family. Together NICD

and a CSL family member activate transcription of target genes including Myc, p21 and

HES-family members. In the skin HES-1 expression is required for spinous cell

induction in the epidermis and is activated in hair follicle matrix cells as they commit to terminal differentiation (Blanpain et al., 2006).

Inhibition of Notch signaling can occur by direct interactions with a Notch inhibitor such as Nrarp. Nrarp is a unique inhibitor in that its transcription is regulated by NICD and CSL and is therefore part of the Notch synexpression group (Krebs et al., 2001; Lahaye et al., 2002; Lamar et al., 2001). Nrarp has been shown to repress Notch signaling by binding to the NICD portion of Notch in several systems including T-cells; however its function in the skin has not been explored (Lahaye et al., 2002; Lamar et al., 2001; Yun and Bevan, 2003). Intracellular Notch signaling can also be repressed by cis-binding of a Notch family ligand to the Notch receptor(Sakamoto et al., 2002). Ligand-inhibition of Notch signaling occurs during normal Drosophila development to facilitate robust fine-grained patterning, and the programmed intracellular loss of the Notch ligand Delta-like 3 in T-cells is required for reversal of Notch inhibition and for progression of normal T-cell development (Barad et al.; Barad et al., 2010; Hoyne et al., 2011; Sprinzak et al.; Sprinzak et al., 2011). In some systems Fringe, a β4galactosyltransferase, is believed to regulate cis binding of a Notch ligand by glycosolating EGF repeats within Notch (Chen et al., 2001). Evidence that mouse Notch1 is glycosolated in the ligand binding domain suggests an intracellular negative feedback mechanism may occur in mammals. Furthermore overexpression of two Notch ligands in Cos7 cells results in intracellular dominant negative effects on Notch signaling and is proposed to overwhelm Fringe activity, suggesting that Notch ligand expression may be carefully regulated in mammals (Shao et al., 2003). Interestingly in follicle cells of the Drosophila egg chamber, miR-1 is

thought to regulate cis-ligand inhibition by directly inhibiting Delta expression (Kwon et al., 2005; Poulton et al., 2011). Whether miRNAs are involved in cis-ligand inhibition or regulation of intracellular Notch repression in mammalian skin is not known, and will be an interesting area for future studies. I propose possible approaches to this question below.

Are Jag2 and Nrarp directly targeted by a specific set of miRNAs?

HITS CLIP results obtained by Zhengquan Yu in the Millar lab identified miRNA "hits" for two members of the Notch1 signaling pathway, both of which if upregulated could potentially result in reduced Notch1 receptor and cleaved Notch1 protein expression. The first is the Notch ligand Jag2. Complementary seed sequences for several miRNAs enriched in keratinocyte RISC complexes, miR-205, miR-93, miR-18a, miR-324-3p and let-7i, are located in the 3'end of mouse Jag2 mRNA. Jag2 is expressed specifically in the basal layer of the epidermis during development, and has been shown to activate Notch1 in vivo during oral development (Casey et al., 2006). QPCR results presented in Chapter Five (Figure 5.1B) show that Jag2 mRNA expression trends upward in full thickness skin isolated from *Dicer* mutant mice induced from PD1 until PD12 compared with controls (p=0.120). It will be important to repeat these experiments with isolated epidermis to determine whether this apparent upregulation is significant.

The second "hit" was Nrarp, a member of the Notch-Delta synexpression group that is believed to inhibit Notch signaling by binding to, and promoting the loss of NICD protein. Complementary seed sequences for miR-955 and miR-103 are present in the

3'region of mouse NARP mRNA. I hypothesize that inappropriate overexpression of

Jag2 results in cis-ligand mediated repression of Notch activity, and overexpression of

Nrarp directly inhibits the stability of NICD. To test this I will first confirm

overexpression of Jag2 and Nrarp in specific *Dicer* mutant skin populations. I will use

Dicer^{fl/fl}, *rtTA, tetO-Cre* mice caring the *K14-H2B-GFP* transgene, permitting FACS

isolation of GFP high basal and ORS cells and GFP low suprabasal and matrix cells from

Dicer control and mutant mice. QPCR analysis of Jag2 and Nrarp mRNA expression will

be compared in high, or low GFP FACS sorted populations in isolated epidermal and hair

follicle preparations corresponding to the basal, suprabasal, and ORS and matrix, cell

populations respectively. If enough material is available, western blot analysis will be

carried out to investigate miRNA regulation of Jag2 or Nrarp at the protein level.

Future studies to test whether miRNAs directly regulate Jag2 would include co-

expressing a luciferase reporter system including the 3'region of Jag2 mRNA, and

miRNA expression plasmids for miR-93, miR-18a, miR-324-3p or let-7i in tissue culture

cells. Repression of luciferase activity in these cells would suggest direct regulation of

Jag2 expression by miRNAs. Similar studies could be used to explore the regulation of

Nrarp by miR-95 and miR-103.

To test whether one or more of these specific miRNAs directly regulates Jag2 or Nrarp in

vivo, "sponge" constructs designed with multiple repeats of the complementary seed

sequence for the miRNA of interest, engineered with a bulge to prevent RNA

interference–type cleavage and degradation of the construct, would be expressed under a

skin specific promoter (ie KRT14, Involucrin, or Shh). MiRNA sponges have been used

successfully to repress the effects of miR-16, miR-20 and miR-30, are thought to

competitively inhibit binding of miRNAs to their targets resulting in target depression

(Ebert et al., 2007). Therefore, up-regulation of Jag2 or Nrarp in this system would

provide evidence for direct regulation by a given miRNA. Because many miRNAs may

act together to target the same mRNA, it may be necessary to generate transgenic mice

expressing sponges for more then one of these miRNAs, before Jag2 is noticeably de-

repressed. An alternative approach would be to rescue Jag2 expression in the *Dicer* or

Drosha[flEx9] mutant by over-expressing one or more of these miRNAs; however this

would be cumbersome in vivo, even in the constitutive *Dicer* mutant mice, as an

inducible system may be necessary to over-express each miRNA(s) after *Dicer* depletion

is induced. The exact in vivo compartment that the miRNA should be expressed in

should be chosen carefully, since overexpressing the miRNA in a region that it is

normally not active in, may result in additional phenotypes instead of a rescue.

Identification of which arm of the DNA damage pathway is disturbed in Dicer and

***Drosha*[flEx9] deficient mice**

DNA damage occurs normally in rapidly dividing cells, and the DNA damage pathway

functions to either delay cell division until the damage can be fixed, or activate cell death

or senescence. Double stranded breaks (DSB) at replication forks are fairly common

occurrences, as the DNA helix is unwound and exposed during DNA replication. Once a

DSB occurs, DNA damage proteins are recruited to the site of DNA damage. The

method of repair depends on the machinery that is present. DSB are repaired most

commonly in keratinocytes by either homologous recombination or non homologus end

joining (Rapp and Greulich, 2004). Both pathways involve the phosphorylation and

recruitment of pH2A.X, making pH2A.X a good marker for DSB. In addition to

pH2A.X, a complex of DNA damage response proteins including Mre11, Rad50, and

NBS, localizes to DSB. For non homologous end joining, the protein Ku localizes to

DSB with other proteins to form the DNS-PK holoenzyme. This is responsible for the

phosphorylation of proteins, such as XRCC4, a cofactor of Ligase 5, and the replication

factor, A2, which mediate the direct ligation of the two broken ends. During this process

genetic information is almost always lost at the site of the DSB. For homologous

recombination Rad51p binds to the 3' end of the single-stranded DNA on each side of the

DSB, and catalyzes strand-exchange from an adjacent homologous region allowing

recombination to take place. With this method of repair, genetic information is usually

not lost. During this process the protein kinase ATM is recruited and activated at the site

of the DSB, and phosphorylates the cell cycle checkpoint kinases, CHK1 and CHK2 and

p53, leading to inhibited cell cycle progression and/or apoptosis. ATM also

phosphorylates pH2A.X and NSB facilitating DNA damage repair. Once

phosphorylated, pH2A.X recruits chromatin remodelers such as Ino80, Rvb1, NuA4 and

Swr1, cohesin, or members of the Smc5/6 complex, which facilitate both homologous

recombination and non homologous end joining. ATR, which belongs to the same protein

family as ATM, is activated by its own distinct spectrum of DNA damage lesions

typically resulting in stalled replication forks. ATR phosphorylates many of the same

factors as ATM, including CHK1, CHK2 and p53 (reviewed by (Jackson, 2002).

In experiments described in Chapter Four, I observe and overabundance of pH2A.X positive cells in hair follicle matrix regions in *Dicer* and *Drosha^flEx9* mutant mice following hair plucking. This observation would reflect increased sensitivity of mutant matrix cells to DNA damage; an ability of cells to recover from DNA damage; or upregulation of DNA damage response proteins that are normally directly repressed by miRNAs. Below, I outline possible experiments to determine which of these mechanisms occur.

Are Dicer or Drosha^flEx9 deficient matrix cells more susceptible to DNA damage?
Preliminary experiments on UVB treated *Dicer* control and mutant epidermis did not show a difference in the number pH2A.X positive epidermal cells, indicating that mutant epidermis is not more prone to DNA damage compared to control epidermis. However since UVB radiation does not penetrate very deeply into the skin, this experiment did not address whether deficient matrix cells are more susceptible to DNA damage than control matrix cells.

To test if *Dicer* or *Drosha^flEx9* mutant matrix cells, specifically, are more susceptible to DNA damage, mutant and control *Dicer* or *Drosha^flEx9* mice could be treated systemically with low doses of agents that inflict DNA damage, such as fluorouracil or could be subjected to UVA radiation, which penetrates more deeply into the skin then UVB. Treatment would be carried out during telogen (PD50), and skin would be biopsied before initiation of treatment and then at two, four, and six days after treatment. Skin sections from *Dicer* or *Drosha^flEx9* mutants and controls would be analyzed for numbers

of TUNEL and pH2A.X positive cells in the matrix region, to determine whether *Dicer* or

Drosha depletion causes increased apoptosis or DNA damage in response to fluorouracil

or UVA. An increased number of cells positive for pH2A.X in mutants, compared to

littermate controls would indicate a susceptibility to DNA damage. An increase in

TUNEL positive cells alone would indicate that apoptosis is caused by mechanisms other

then a DNA damage response.

If *Dicer* and *Drosha* deficient cells were found to be more susceptible to DNA damage

than controls, this would warrant a closer look at the process of replication, repair and the

S-phase checkpoint. The cell cycle could be followed by analyzing DNA content, using

FACS analysis of propidium iodide stained matrix cells, isolated from K14-H2B-GFP

expressing mice using published protocols (Rendl et al., 2008). To determine whether

matrix cells underwent increased levels of homologous recombination repair or

nonhomologous end joining, activity of these pathways could be analyzed in matrix cells

by assaying for the presence, absence or overabundance of Rad51 and Rad52 or DNA-PK

and Ku70, respectively. These experiments would begin to delineate the mechanisms by

which miRNAs suppress DNA damage in the matrix.

Are Dicer or Drosha deficient cells defective in recovering from DNA damage?
If I found that *Dicer* or *Drosha*[flEx9] deficient matrix cells were not unusually susceptible

to DNA damage, I would then test whether recovery from DNA damage was altered in

the mutants. To test the ability of the mutant matrix population to recover from DNA

damage, *Dicer* and *Drosha*[flEx9] control and mutant mice would be treated with low doses

of Fluorouracil or UVA radiation during telogen, similar to the DNA damage

experiments outlined above. However, matrix cells would be allowed to recover from

this treatment, and skin would instead be biopsied zero, eight, ten, and twelve days after

treatment. Skin sections would be assayed for progression through the DNA damage

pathway by immunostaining for factors recruited by pH2A.X such as the chromatin

remodelers, Ino80, Rvb1, NuA4 and Swr1, the protein, cohesin, or members of the

Smc5/6 complex.

Is a DNA damage response overly sensitive in Dicer or Drosha^{flEx9} mutant matrix cells?

During S-phase, DNA at replication forks is susceptible to formation of double stranded

breaks. These are normally repaired by activation of the ATM pathway and can occur in

any proliferating cell. If *Dicer* or *Drosha^{flEx9}* mutant matrix cells are not more

susceptible to DNA damage or are not defective in recovering from DNA damage during

telogen, another possibility is that these cells have an upregulated response to normal

replicative stress. Interestingly, the DNA damage response marker H2A.X is a direct

target of miR-24 (Lal et al., 2009). To test if overexpression of H2A.X could lead to hair

follicle defects, transgenic mice carrying a KRT5-H2A.X construct would be generated.

The gross phenotype of these mice would be observed, paying particular attention to

formation of the hair coat. If hair loss was observed during early to mid anagen of the

spontaneous or plucking-induced hair follicle growth cycle, I would carry out analysis of

histology, apoptosis and proliferation and differentiation to determine whether this

phenotype was similar to that observed in *Dicer* and *Drosha^{flEx9}* mutants. If similar

phenotypes were observed, I would ask whether forced expression of miR-24 under the

control of a Msx promoter, active in the matrix, could rescue apoptosis and DNA damage in *Drosha*^{flEx9} and *Dicer* mutants. If miR-24 was capable of rescuing H2A.X upregulation and matrix cell death, this would support the notion that it normally suppresses H2A.X expression in matrix cells. The above experiments would delineate whether matrix cells are more sensitive than controls to DNA damage, recover more slowly from DNA damage, or upregulate DNA damage response genes that are directly controlled by miRNAs.

In conclusion, by comparing epidermal-specific *Dicer* and *Drosha* deficient mice we uncovered shared functions for these factors in epidermal maintenance at particular phases of the hair follicle growth cycle. As the phenotypes were essentially the same, this suggests that epidermal Drosha and Dicer predominantly act to process miRNAs. My results indicate that miRNAs function in adult skin at specific time points for normal progression of the hair follicle growth cycle, and that loss of key miRNAs during these phases results in hair shaft malformation, failed entry into catagen, and matrix cell loss.

Future experiments will focus on identifying miRNAs expressed in the appropriate cell types at time points just prior to the appearance of defects in *Dicer* and *Drosha* mutants. In addition, I have identified three miR-205 targets that are overexpressed in *Dicer* mutant skin, and have also observed reduced Notch activity in *Dicer* and *Drosha* mutant skin. Determining how these factors contribute to mutant phenotypes will be an important area for future studies. The *Dicer* and *Drosha* mutant systems along with techniques such as HITS CLIP, should prove to be useful tools to identify essential

miRNAs and their mRNA targets that are involved at specific phases in the hair follicle growth cycle and for epidermal maintenance.

Overall these findings have expanded our understanding of global miRNA function in the epidermis and during the hair follicle growth cycle, and may have implications in other broad processes such as tissue maintenance and tumor development. The Notch signaling pathway regulates many fundamental cellular processes such as proliferation, differentiation and stem cell maintenance and is fine-tuned in both embryonic and adult systems at the transcriptional and chromatin level (Borggrefe and Liefke 2012). miRNA regulation of Notch signaling has just begun to be evaluated in many systems (Capuano et al 2011.; Cichocki et al.2011; de Antonellis et al.2011; Liu et al.2011; Sureban et al.2011; Vallejo et al.2011). Since Notch plays a prominent role in embryonic and adult skin, our finding of downregulated Notch signaling in both *Dicer* and *Drosha* mutants provides a promising future line of inquiry in miRNA regulation of Notch activity.

Similarly our observation that miRNAs play a protective role against DNA damage in the matrix raises many mechanistic questions on the role of miRNAs in promoting genomic stability. MiRNAs are known to regulate key processes involved in tumor evolution such as transcriptional regulation, differentiation, proliferation, and apoptosis (Sotiropoulou et al., 2009). Consistent with this, miRNA genes and clusters are frequently located at or around fragile sites, as well as in regions of loss of heterozygosity, amplification, or common breakpoint regions (Calin et al., 2004; Huppi et al., 2007; Huppi et al., 2008; Lagana et al.; Sevignani et al., 2007). Moreover, all three of the miR-205 target genes

151

that we observed to be upregulated in *Dicer* mutant skin are misregulated in epithelial-derived cancers. Studying their regulation in the skin may provide insight into the etiology of skin carcinomas (Dar et al., 2011; Gregory et al., 2008; Majid et al., 2011). Notch signaling is activated in the majority of cancers and is a target for cancer therapy (Harris et al.2012). The mechanisms by which miRNAs contribute to genomic stability or regulate Notch signaling may shed light on the development of other epithelial-derived carcinomas. The identification of miRNAs and elucidation of their specific functions in skin subpopulations, as proposed above, may therefore identify pharmacodynamic markers and potential therapeutic targets in the study and treatment of epithelial cancers.

BIBLIOGRAPHY

Andl, T., Ahn, K., Kairo, A., Chu, E. Y., Wine-Lee, L., Reddy, S. T., Croft, N. J., Cebra-Thomas, J. A., Metzger, D., Chambon, P. et al. (2004). Epithelial Bmpr1a regulates differentiation and proliferation in postnatal hair follicles and is essential for tooth development. *Development* **131**, 2257-68.

Andl, T., Murchison, E. P., Liu, F., Zhang, Y., Yunta-Gonzalez, M., Tobias, J. W., Andl, C. D., Seykora, J. T., Hannon, G. J. and Millar, S. E. (2006). The miRNA-processing enzyme dicer is essential for the morphogenesis and maintenance of hair follicles. *Curr Biol* **16**, 1041-9.

Antonini, D., Russo, M. T., De Rosa, L., Gorrese, M., Del Vecchio, L. and Missero, C. (2010). Transcriptional repression of miR-34 family contributes to p63-mediated cell cycle progression in epidermal cells. *J Invest Dermatol* **130**, 1249-57.

Barad, O., Rosin, D., Hornstein, E. and Barkai, N. (2010). Error minimization in lateral inhibition circuits. *Sci Signal* **3**, ra51.

Bartel, D. P. (2004). MicroRNAs: genomics, biogenesis, mechanism, and function. *Cell* **116**, 281-97.

Bergeron, L., Jr., Perreault, J. P. and Abou Elela, S. (2010). Short RNA duplexes guide sequence-dependent cleavage by human Dicer. *RNA* **16**, 2464-73.

Bickenbach, J. R. and Mackenzie, I. C. (1984). Identification and localization of label-retaining cells in hamster epithelia. *J Invest Dermatol* **82**, 618-22.

Bindels, S., Mestdagt, M., Vandewalle, C., Jacobs, N., Volders, L., Noel, A., van Roy, F., Berx, G., Foidart, J. M. and Gilles, C. (2006). Regulation of vimentin by SIP1 in human epithelial breast tumor cells. *Oncogene* **25**, 4975-85.

Biton, M., Levin, A., Slyper, M., Alkalay, I., Horwitz, E., Mor, H., Kredo-Russo, S., Avnit-Sagi, T., Cojocaru, G., Zreik, F. et al. (2011). Epithelial microRNAs regulate gut mucosal immunity via epithelium-T cell crosstalk. *Nat Immunol* **12**, 239-46.

Blanpain, C. and Fuchs, E. (2009). Epidermal homeostasis: a balancing act of stem cells in the skin. *Nat Rev Mol Cell Biol* **10**, 207-17.

Blanpain, C., Lowry, W. E., Geoghegan, A., Polak, L. and Fuchs, E. (2004). Self-renewal, multipotency, and the existence of two cell populations within an epithelial stem cell niche. *Cell* **118**, 635-48.

Blanpain, C., Lowry, W. E., Pasolli, H. A. and Fuchs, E. (2006). Canonical notch signaling functions as a commitment switch in the epidermal lineage. *Genes Dev* **20**, 3022-35.

Borggrefe, T. and Liefke, R. (2012). Fine-tuning of the intracellular canonical Notch signaling pathway. *Cell Cycle* **11**.

Braig, S., Mueller, D. W., Rothhammer, T. and Bosserhoff, A. K. (2010). MicroRNA miR-196a is a central regulator of HOX-B7 and BMP4 expression in malignant melanoma. *Cell Mol Life Sci* **67**, 3535-48.

Cai, X., Hagedorn, C. H. and Cullen, B. R. (2004). Human microRNAs are processed from capped, polyadenylated transcripts that can also function as mRNAs. *RNA* **10**, 1957-66.

Calin, G. A., Sevignani, C., Dumitru, C. D., Hyslop, T., Noch, E., Yendamuri, S., Shimizu, M., Rattan, S., Bullrich, F., Negrini, M. et al. (2004). Human microRNA

genes are frequently located at fragile sites and genomic regions involved in cancers. *Proc Natl Acad Sci U S A* **101**, 2999-3004.

Capuano, M., Iaffaldano, L., Tinto, N., Montanaro, D., Capobianco, V., Izzo, V., Tucci, F., Troncone, G., Greco, L. and Sacchetti, L. (2011). MicroRNA-449a Overexpression, Reduced NOTCH1 Signals and Scarce Goblet Cells Characterize the Small Intestine of Celiac Patients. *PLoS One* **6**, e29094.

Casey, L. M., Lan, Y., Cho, E. S., Maltby, K. M., Gridley, T. and Jiang, R. (2006). Jag2-Notch1 signaling regulates oral epithelial differentiation and palate development. *Dev Dyn* **235**, 1830-44.

Chen, J., Feilotter, H. E., Pare, G. C., Zhang, X., Pemberton, J. G., Garady, C., Lai, D., Yang, X. and Tron, V. A. MicroRNA-193b represses cell proliferation and regulates cyclin D1 in melanoma. *Am J Pathol* **176**, 2520-9.

Chen, J., Moloney, D. J. and Stanley, P. (2001). Fringe modulation of Jagged1-induced Notch signaling requires the action of beta 4galactosyltransferase-1. *Proc Natl Acad Sci U S A* **98**, 13716-21.

Chong, M. M., Rasmussen, J. P., Rudensky, A. Y. and Littman, D. R. (2008). The RNAseIII enzyme Drosha is critical in T cells for preventing lethal inflammatory disease. *J Exp Med* **205**, 2005-17.

Cichocki, F., Felices, M., McCullar, V., Presnell, S. R., Al-Attar, A., Lutz, C. T. and Miller, J. S. (2011). Cutting Edge: MicroRNA-181 Promotes Human NK Cell Development by Regulating Notch Signaling. *J Immunol* **187**, 6171-5.

Cotsarelis, G., Sun, T. T. and Lavker, R. M. (1990). Label-retaining cells reside in the bulge area of pilosebaceous unit: implications for follicular stem cells, hair cycle, and skin carcinogenesis. *Cell* **61**, 1329-37.

D'Souza, S. J., Vespa, A., Murkherjee, S., Maher, A., Pajak, A. and Dagnino, L. (2002). E2F-1 is essential for normal epidermal wound repair. *J Biol Chem* **277**, 10626-32.

Dar, A. A., Majid, S., de Semir, D., Nosrati, M., Bezrookove, V. and Kashani-Sabet, M. (2011). miRNA-205 suppresses melanoma cell proliferation and induces senescence via regulation of E2F1 protein. *J Biol Chem* **286**, 16606-14.

de Antonellis, P., Medaglia, C., Cusanelli, E., Andolfo, I., Liguori, L., De Vita, G., Carotenuto, M., Bello, A., Formiggini, F., Galeone, A. et al. (2011). MiR-34a targeting of Notch ligand delta-like 1 impairs CD15+/CD133+ tumor-propagating cells and supports neural differentiation in medulloblastoma. *PLoS One* **6**, e24584.

DeGregori, J. (2002). The genetics of the E2F family of transcription factors: shared functions and unique roles. *Biochim Biophys Acta* **1602**, 131-50.

Degregori, J. (2011). A new role for E2F1 in DNA repair: all for the greater good. *Cell Cycle* **10**, 1716.

Demehri, S. and Kopan, R. (2009). Notch signaling in bulge stem cells is not required for selection of hair follicle fate. *Development* **136**, 891-6.

Demehri, S., Liu, Z., Lee, J., Lin, M. H., Crosby, S. D., Roberts, C. J., Grigsby, P. W., Miner, J. H., Farr, A. G. and Kopan, R. (2008). Notch-deficient skin induces a lethal systemic B-lymphoproliferative disorder by secreting TSLP, a sentinel for epidermal integrity. *PLoS Biol* **6**, e123.

Dry, F. W. (1926). The coat of the mouse (mus musculus). *J. Genet.* **16**, 287-340.

Ebert, M. S., Neilson, J. R. and Sharp, P. A. (2007). MicroRNA sponges: competitive inhibitors of small RNAs in mammalian cells. *Nat Methods* **4**, 721-6.

Field, S. J., Tsai, F. Y., Kuo, F., Zubiaga, A. M., Kaelin, W. G., Jr., Livingston, D. M., Orkin, S. H. and Greenberg, M. E. (1996). E2F-1 functions in mice to promote apoptosis and suppress proliferation. *Cell* **85**, 549-61.

Fuchs, E. (2007). Scratching the surface of skin development. *Nature* **445**, 834-42.

Gossen, M., Freundlieb, S., Bender, G., Muller, G., Hillen, W. and Bujard, H. (1995). Transcriptional activation by tetracyclines in mammalian cells. *Science* **268**, 1766-9.

Gregory, P. A., Bert, A. G., Paterson, E. L., Barry, S. C., Tsykin, A., Farshid, G., Vadas, M. A., Khew-Goodall, Y. and Goodall, G. J. (2008). The miR-200 family and miR-205 regulate epithelial to mesenchymal transition by targeting ZEB1 and SIP1. *Nat Cell Biol* **10**, 593-601.

Gregory, R. I., Yan, K. P., Amuthan, G., Chendrimada, T., Doratotaj, B., Cooch, N. and Shiekhattar, R. (2004). The Microprocessor complex mediates the genesis of microRNAs. *Nature* **432**, 235-40.

Grishok, A., Pasquinelli, A. E., Conte, D., Li, N., Parrish, S., Ha, I., Baillie, D. L., Fire, A., Ruvkun, G. and Mello, C. C. (2001). Genes and mechanisms related to RNA interference regulate expression of the small temporal RNAs that control C. elegans developmental timing. *Cell* **106**, 23-34.

Han, J., Lee, Y., Yeom, K. H., Nam, J. W., Heo, I., Rhee, J. K., Sohn, S. Y., Cho, Y., Zhang, B. T. and Kim, V. N. (2006). Molecular basis for the recognition of primary microRNAs by the Drosha-DGCR8 complex. *Cell* **125**, 887-901.

Harfe, B. D., Scherz, P. J., Nissim, S., Tian, H., McMahon, A. P. and Tabin, C. J. (2004). Evidence for an expansion-based temporal Shh gradient in specifying vertebrate digit identities. *Cell* **118**, 517-28.

Harris, P. J., Speranza, G. and Dansky Ullmann, C. (2012)Targeting embryonic signaling pathways in cancer therapy. *Expert Opin Ther Targets*.

Hener, P., Friedmann, L., Metzger, D., Chambon, P. and Li, M. (2011). Aggravated TSLP-induced atopic dermatitis in mice lacking dicer in adult skin keratinocytes. *J Invest Dermatol* **131**, 2324-7.

Hoyne, G. F., Chapman, G., Sontani, Y., Pursglove, S. E. and Dunwoodie, S. L. (2011). A cell autonomous role for the Notch ligand Delta-like 3 in alphabeta T-cell development. *Immunol Cell Biol* **89**, 696-705.

Hsu, Y. C., Pasolli, H. A. and Fuchs, E. (2011). Dynamics between stem cells, niche, and progeny in the hair follicle. *Cell* **144**, 92-105.

Huppi, K., Volfovsky, N., Mackiewicz, M., Runfola, T., Jones, T. L., Martin, S. E., Stephens, R. and Caplen, N. J. (2007). MicroRNAs and genomic instability. *Semin Cancer Biol* **17**, 65-73.

Huppi, K., Volfovsky, N., Runfola, T., Jones, T. L., Mackiewicz, M., Martin, S. E., Mushinski, J. F., Stephens, R. and Caplen, N. J. (2008). The identification of microRNAs in a genomically unstable region of human chromosome 8q24. *Mol Cancer Res* **6**, 212-21.

155

Hutvagner, G., McLachlan, J., Pasquinelli, A. E., Balint, E., Tuschl, T. and Zamore, P. D. (2001). A cellular function for the RNA-interference enzyme Dicer in the maturation of the let-7 small temporal RNA. *Science* **293**, 834-8.

Ito, M. and Kizawa, K. (2001). Expression of calcium-binding S100 proteins A4 and A6 in regions of the epithelial sac associated with the onset of hair follicle regeneration. *J Invest Dermatol* **116**, 956-63.

Ito, M., Liu, Y., Yang, Z., Nguyen, J., Liang, F., Morris, R. J. and Cotsarelis, G. (2005). Stem cells in the hair follicle bulge contribute to wound repair but not to homeostasis of the epidermis. *Nat Med* **11**, 1351-4.

Jackson, S. P. (2002). Sensing and repairing DNA double-strand breaks. *Carcinogenesis* **23**, 687-96.

Jones, P. H., Harper, S. and Watt, F. M. (1995). Stem cell patterning and fate in human epidermis. *Cell* **80**, 83-93.

Kaufman, C. K., Zhou, P., Pasolli, H. A., Rendl, M., Bolotin, D., Lim, K. C., Dai, X., Alegre, M. L. and Fuchs, E. (2003). GATA-3: an unexpected regulator of cell lineage determination in skin. *Genes Dev* **17**, 2108-22.

Ketting, R. F., Fischer, S. E., Bernstein, E., Sijen, T., Hannon, G. J. and Plasterk, R. H. (2001). Dicer functions in RNA interference and in synthesis of small RNA involved in developmental timing in C. elegans. *Genes Dev* **15**, 2654-9.

Kim, B. M., Woo, J., Kanellopoulou, C. and Shivdasani, R. A. (2011). Regulation of mouse stomach development and Barx1 expression by specific microRNAs. *Development* **138**, 1081-6.

Kuhnert, F., Mancuso, M. R., Hampton, J., Stankunas, K., Asano, T., Chen, C. Z. and Kuo, C. J. (2008). Attribution of vascular phenotypes of the murine Egfl7 locus to the microRNA miR-126. *Development* **135**, 3989-93.

Kulessa, H., Turk, G. and Hogan, B. L. (2000). Inhibition of Bmp signaling affects growth and differentiation in the anagen hair follicle. *EMBO J* **19**, 6664-6674.

Kwon, C., Han, Z., Olson, E. N. and Srivastava, D. (2005). MicroRNA1 influences cardiac differentiation in Drosophila and regulates Notch signaling. *Proc Natl Acad Sci U S A* **102**, 18986-91.

Lagana, A., Russo, F., Sismeiro, C., Giugno, R., Pulvirenti, A. and Ferro, A. Variability in the incidence of miRNAs and genes in fragile sites and the role of repeats and CpG islands in the distribution of genetic material. *PLoS One* **5**, e11166.

Lal, A., Pan, Y., Navarro, F., Dykxhoorn, D. M., Moreau, L., Meire, E., Bentwich, Z., Lieberman, J. and Chowdhury, D. (2009). miR-24-mediated downregulation of H2AX suppresses DNA repair in terminally differentiated blood cells. *Nat Struct Mol Biol* **16**, 492-8.

Lee, J., Basak, J. M., Demehri, S. and Kopan, R. (2007). Bi-compartmental communication contributes to the opposite proliferative behavior of Notch1-deficient hair follicle and epidermal keratinocytes. *Development* **134**, 2795-806.

Lee, Y., Ahn, C., Han, J., Choi, H., Kim, J., Yim, J., Lee, J., Provost, P., Radmark, O., Kim, S. et al. (2003). The nuclear RNase III Drosha initiates microRNA processing. *Nature* **425**, 415-9.

Lee, Y., Hur, I., Park, S. Y., Kim, Y. K., Suh, M. R. and Kim, V. N. (2006). The role of PACT in the RNA silencing pathway. *EMBO J* **25**, 522-32.

Lee, Y., Jeon, K., Lee, J. T., Kim, S. and Kim, V. N. (2002). MicroRNA maturation: stepwise processing and subcellular localization. *EMBO J* **21**, 4663-70.

Lee, Y., Kim, M., Han, J., Yeom, K. H., Lee, S., Baek, S. H. and Kim, V. N. (2004). MicroRNA genes are transcribed by RNA polymerase II. *EMBO J* **23**, 4051-60.

Lena, A. M., Shalom-Feuerstein, R., Rivetti di Val Cervo, P., Aberdam, D., Knight, R. A., Melino, G. and Candi, E. (2008). miR-203 represses 'stemness' by repressing DeltaNp63. *Cell Death Differ* **15**, 1187-95.

Levy, V., Lindon, C., Harfe, B. D. and Morgan, B. A. (2005). Distinct stem cell populations regenerate the follicle and interfollicular epidermis. *Dev Cell* **9**, 855-61.

Lindner, G., Botchkarev, V. A., Botchkareva, N. V., Ling, G., van der Veen, C. and Paus, R. (1997). Analysis of apoptosis during hair follicle regression (catagen). *Am J Pathol* **151**, 1601-17.

Liu, J., Carmell, M. A., Rivas, F. V., Marsden, C. G., Thomson, J. M., Song, J. J., Hammond, S. M., Joshua-Tor, L. and Hannon, G. J. (2004). Argonaute2 is the catalytic engine of mammalian RNAi. *Science* **305**, 1437-41.

Liu, X. S., Chopp, M., Zhang, R. L., Tao, T., Wang, X. L., Kassis, H., Hozeska-Solgot, A., Zhang, L., Chen, C. and Zhang, Z. G. (2011). MicroRNA profiling in subventricular zone after stroke: MiR-124a regulates proliferation of neural progenitor cells through Notch signaling pathway. *PLoS One* **6**, e23461.

Liu, Y., Lyle, S., Yang, Z. and Cotsarelis, G. (2003). Keratin 15 promoter targets putative epithelial stem cells in the hair follicle bulge. *J Invest Dermatol* **121**, 963-8.

Lynch, M. H., O'Guin, W. M., Hardy, C., Mak, L. and Sun, T. T. (1986). Acidic and basic hair/nail ("hard") keratins: their colocalization in upper cortical and cuticle cells of the human hair follicle and their relationship to "soft" keratins. *J Cell Biol* **103**, 2593-606.

Ma, J. B., Ye, K. and Patel, D. J. (2004). Structural basis for overhang-specific small interfering RNA recognition by the PAZ domain. *Nature* **429**, 318-22.

Majid, S., Saini, S., Dar, A. A., Hirata, H., Shahryari, V., Tanaka, Y., Yamamura, S., Ueno, K., Zaman, M. S., Singh, K. et al. (2011). MicroRNA-205 inhibits Src-mediated oncogenic pathways in renal cancer. *Cancer Res* **71**, 2611-21.

Manni, I., Artuso, S., Careccia, S., Rizzo, M. G., Baserga, R., Piaggio, G. and Sacchi, A. (2009). The microRNA miR-92 increases proliferation of myeloid cells and by targeting p63 modulates the abundance of its isoforms. *FASEB J* **23**, 3957-66.

Matsumoto, T., Jiang, J., Kiguchi, K., Ruffino, L., Carbajal, S., Beltran, L., Bol, D. K., Rosenberg, M. P. and DiGiovanni, J. (2003). Targeted expression of c-Src in epidermal basal cells leads to enhanced skin tumor promotion, malignant progression, and metastasis. *Cancer Res* **63**, 4819-28.

McKenna, L. B., Schug, J., Vourekas, A., McKenna, J. B., Bramswig, N. C., Friedman, J. R. and Kaestner, K. H. (2010). MicroRNAs control intestinal epithelial differentiation, architecture, and barrier function. *Gastroenterology* **139**, 1654-64, 1664 e1.

Means, A. L., Xu, Y., Zhao, A., Ray, K. C. and Gu, G. (2008). A CK19(CreERT) knockin mouse line allows for conditional DNA recombination in epithelial cells in multiple endodermal organs. *Genesis* **46**, 318-23.

Meister, G., Landthaler, M., Patkaniowska, A., Dorsett, Y., Teng, G. and Tuschl, T. (2004). Human Argonaute2 mediates RNA cleavage targeted by miRNAs and siRNAs. *Mol Cell* **15**, 185-97.

Michel, S., Schmidt, R., Shroot, B. and Reichert, U. (1988). Morphological and biochemical characterization of the cornified envelopes from human epidermal keratinocytes of different origin. *J Invest Dermatol* **91**, 11-5.

Millar, S. E. (2002). Molecular mechanisms regulating hair follicle development. *J Invest Dermatol* **118**, 216-25.

Mills, A. A., Zheng, B., Wang, X. J., Vogel, H., Roop, D. R. and Bradley, A. (1999). p63 is a p53 homologue required for limb and epidermal morphogenesis. *Nature* **398**, 708-13.

Moriyama, M., Durham, A. D., Moriyama, H., Hasegawa, K., Nishikawa, S., Radtke, F. and Osawa, M. (2008). Multiple roles of Notch signaling in the regulation of epidermal development. *Dev Cell* **14**, 594-604.

Morris, R. J., Liu, Y., Marles, L., Yang, Z., Trempus, C., Li, S., Lin, J. S., Sawicki, J. A. and Cotsarelis, G. (2004). Capturing and profiling adult hair follicle stem cells. *Nat Biotechnol* **22**, 411-7.

Mourelatos, Z. (2008). Small RNAs: The seeds of silence. *Nature* **455**, 44-5.

Muller-Rover, S., Handjiski, B., van der Veen, C., Eichmuller, S., Foitzik, K., McKay, I. A., Stenn, K. S. and Paus, R. (2001). A comprehensive guide for the accurate classification of murine hair follicles in distinct hair cycle stages. *J Invest Dermatol* **117**, 3-15.

Murchison, E. P., Partridge, J. F., Tam, O. H., Cheloufi, S. and Hannon, G. J. (2005). Characterization of Dicer-deficient murine embryonic stem cells. *Proc Natl Acad Sci U S A* **102**, 12135-40.

Murillas, R., Larcher, F., Conti, C. J., Santos, M., Ullrich, A. and Jorcano, J. L. (1995). Expression of a dominant negative mutant of epidermal growth factor receptor in the epidermis of transgenic mice elicits striking alterations in hair follicle development and skin structure. *EMBO J* **14**, 5216-23.

Nakamura, M. and Tokura, Y. (2010). Expression of Snail1 in the fibrotic dermis of postmenopausal frontal fibrosing alopecia: possible involvement of an epithelial-mesenchymal transition and a review of the Japanese patients. *Br J Dermatol* **162**, 1152-4.

Nowak, J. A., Polak, L., Pasolli, H. A. and Fuchs, E. (2008). Hair follicle stem cells are specified and function in early skin morphogenesis. *Cell Stem Cell* **3**, 33-43.

O'Guin, W. M., Sun, T. T. and Manabe, M. (1992). Interaction of trichohyalin with intermediate filaments: three immunologically defined stages of trichohyalin maturation. *J Invest Dermatol* **98**, 24-32.

Oliver, R. F. and Jahoda, C. A. (1988). Dermal-epidermal interactions. *Clin Dermatol* **6**, 74-82.

Olsen, P. H. and Ambros, V. (1999). The lin-4 regulatory RNA controls developmental timing in Caenorhabditis elegans by blocking LIN-14 protein synthesis after the initiation of translation. *Dev Biol* **216**, 671-80.

Oshima, H., Rochat, A., Kedzia, C., Kobayashi, K. and Barrandon, Y. (2001). Morphogenesis and renewal of hair follicles from adult multipotent stem cells. *Cell* **104**, 233-245.

Pan, Y., Lin, M. H., Tian, X., Cheng, H. T., Gridley, T., Shen, J. and Kopan, R. (2004). gamma-secretase functions through Notch signaling to maintain skin appendages but is not required for their patterning or initial morphogenesis. *Dev Cell* **7**, 731-43.

Paterson, E. L., Kolesnikoff, N., Gregory, P. A., Bert, A. G., Khew-Goodall, Y. and Goodall, G. J. (2008). The microRNA-200 family regulates epithelial to mesenchymal transition. *ScientificWorldJournal* **8**, 901-4.

Pierce, A. M., Fisher, S. M., Conti, C. J. and Johnson, D. G. (1998). Deregulated expression of E2F1 induces hyperplasia and cooperates with ras in skin tumor development. *Oncogene* **16**, 1267-76.

Plikus, M. V., Mayer, J. A., de la Cruz, D., Baker, R. E., Maini, P. K., Maxson, R. and Chuong, C. M. (2008). Cyclic dermal BMP signalling regulates stem cell activation during hair regeneration. *Nature* **451**, 340-4.

Potten, C. S. and Morris, R. J. (1988). Epithelial stem cells in vivo. *J Cell Sci Suppl* **10**, 45-62.

Poulton, J. S., Huang, Y. C., Smith, L., Sun, J., Leake, N., Schleede, J., Stevens, L. M. and Deng, W. M. (2011). The microRNA pathway regulates the temporal pattern of Notch signaling in Drosophila follicle cells. *Development* **138**, 1737-45.

Rapp, A. and Greulich, K. O. (2004). After double-strand break induction by UV-A, homologous recombination and nonhomologous end joining cooperate at the same DSB if both systems are available. *J Cell Sci* **117**, 4935-45.

Rendl, M., Lewis, L. and Fuchs, E. (2005). Molecular dissection of mesenchymal-epithelial interactions in the hair follicle. *PLoS Biol* **3**, e331.

Rendl, M., Polak, L. and Fuchs, E. (2008). BMP signaling in dermal papilla cells is required for their hair follicle-inductive properties. *Genes Dev* **22**, 543-57.

Reynolds, A. J. and Jahoda, C. A. (1992). Cultured dermal papilla cells induce follicle formation and hair growth by transdifferentiation of an adult epidermis. *Development* **115**, 587-93.

Rosenquist, T. A. and Martin, G. R. (1996). Fibroblast growth factor signalling in the hair growth cycle: expression of the fibroblast growth factor receptor and ligand genes in the murine hair follicle. *Dev Dyn* **205**, 379-86.

Ryan, D. G., Oliveira-Fernandes, M. and Lavker, R. M. (2006). MicroRNAs of the mammalian eye display distinct and overlapping tissue specificity. *Mol Vis* **12**, 1175-84.

Sakamoto, K., Ohara, O., Takagi, M., Takeda, S. and Katsube, K. (2002). Intracellular cell-autonomous association of Notch and its ligands: a novel mechanism of Notch signal modification. *Dev Biol* **241**, 313-26.

Satzger, I., Mattern, A., Kuettler, U., Weinspach, D., Voelker, B., Kapp, A. and Gutzmer, R. MicroRNA-15b represents an independent prognostic parameter and is correlated with tumor cell proliferation and apoptosis in malignant melanoma. *Int J Cancer* **126**, 2553-62.

Sevignani, C., Calin, G. A., Nnadi, S. C., Shimizu, M., Davuluri, R. V., Hyslop, T., Demant, P., Croce, C. M. and Siracusa, L. D. (2007). MicroRNA genes are frequently located near mouse cancer susceptibility loci. *Proc Natl Acad Sci U S A* **104**, 8017-22.

Shao, L., Moloney, D. J. and Haltiwanger, R. (2003). Fringe modifies O-fucose on mouse Notch1 at epidermal growth factor-like repeats within the ligand-binding site and the Abruptex region. *J Biol Chem* **278**, 7775-82.

Siomi, H. and Siomi, M. C. (2010). Posttranscriptional regulation of microRNA biogenesis in animals. *Mol Cell* **38**, 323-32.

Song, J. J., Smith, S. K., Hannon, G. J. and Joshua-Tor, L. (2004). Crystal structure of Argonaute and its implications for RISC slicer activity. *Science* **305**, 1434-7.

Sonkoly, E., Wei, T., Janson, P. C., Saaf, A., Lundeberg, L., Tengvall-Linder, M., Norstedt, G., Alenius, H., Homey, B., Scheynius, A. et al. (2007). MicroRNAs: novel regulators involved in the pathogenesis of psoriasis? *PLoS One* **2**, e610.

Sotiropoulou, G., Pampalakis, G., Lianidou, E. and Mourelatos, Z. (2009). Emerging roles of microRNAs as molecular switches in the integrated circuit of the cancer cell. *RNA* **15**, 1443-61.

Sprinzak, D., Lakhanpal, A., LeBon, L., Garcia-Ojalvo, J. and Elowitz, M. B. (2011). Mutual inactivation of Notch receptors and ligands facilitates developmental patterning. *PLoS Comput Biol* **7**, e1002069.

Sureban, S. M., May, R., Mondalek, F. G., Qu, D., Ponnurangam, S., Pantazis, P., Anant, S., Ramanujam, R. P. and Houchen, C. W. (2011). Nanoparticle-based delivery of siDCAMKL-1 increases microRNA-144 and inhibits colorectal cancer tumor growth via a Notch-1 dependent mechanism. *J Nanobiotechnology* **9**, 40.

Taki, M., Verschueren, K., Yokoyama, K., Nagayama, M. and Kamata, N. (2006). Involvement of Ets-1 transcription factor in inducing matrix metalloproteinase-2 expression by epithelial-mesenchymal transition in human squamous carcinoma cells. *Int J Oncol* **28**, 487-96.

Teta, M., Rankin, M. M., Long, S. Y., Stein, G. M. and Kushner, J. A. (2007). Growth and regeneration of adult beta cells does not involve specialized progenitors. *Dev Cell* **12**, 817-26.

Tumbar, T., Guasch, G., Greco, V., Blanpain, C., Lowry, W. E., Rendl, M. and Fuchs, E. (2004). Defining the epithelial stem cell niche in skin. *Science* **303**, 359-63.

Tuttle, A. H., Rankin, M. M., Teta, M., Sartori, D. J., Stein, G. M., Kim, G. J., Virgilio, C., Granger, A., Zhou, D., Long, S. H. et al. (2010). Immunofluorescent detection of two thymidine analogues (CldU and IdU) in primary tissue. *J Vis Exp*.

Vallejo, D. M., Caparros, E. and Dominguez, M. (2011). Targeting Notch signalling by the conserved miR-8/200 microRNA family in development and cancer cells. *EMBO J* **30**, 756-69.

Vandewalle, C., Comijn, J., De Craene, B., Vermassen, P., Bruyneel, E., Andersen, H., Tulchinsky, E., Van Roy, F. and Berx, G. (2005). SIP1/ZEB2 induces EMT by repressing genes of different epithelial cell-cell junctions. *Nucleic Acids Res* **33**, 6566-78.

Vauclair, S., Nicolas, M., Barrandon, Y. and Radtke, F. (2005). Notch1 is essential for postnatal hair follicle development and homeostasis. *Dev Biol* **284**, 184-93.

Wilson, C., Cotsarelis, G., Wei, Z. G., Fryer, E., Margolis-Fryer, J., Ostead, M., Tokarek, R., Sun, T. T. and Lavker, R. M. (1994a). Cells within the bulge region of mouse hair follicle transiently proliferate during early anagen: heterogeneity and functional differences of various hair cycles. *Differentiation* **55**, 127-36.

Wilson, C. L., Sun, T. T. and Lavker, R. M. (1994b). Cells in the bulge of the mouse telogen follicle give rise to the lower anagen follicle. *Skin Pharmacology* **0007**, 8-11.

Wu, H., Xu, H., Miraglia, L. J. and Crooke, S. T. (2000). Human RNase III is a 160-kDa protein involved in preribosomal RNA processing. *J Biol Chem* **275**, 36957-65.

Xin, H. B., Deng, K. Y., Shui, B., Qu, S., Sun, Q., Lee, J., Greene, K. S., Wilson, J., Yu, Y., Feldman, M. et al. (2005). Gene trap and gene inversion methods for conditional gene inactivation in the mouse. *Nucleic Acids Res* **33**, e14.

Yagi, R., Waguri, S., Sumikawa, Y., Nada, S., Oneyama, C., Itami, S., Schmedt, C., Uchiyama, Y. and Okada, M. (2007). C-terminal Src kinase controls development and maintenance of mouse squamous epithelia. *EMBO J* **26**, 1234-44.

Yang, A., Schweitzer, R., Sun, D., Kaghad, M., Walker, N., Bronson, R. T., Tabin, C., Sharpe, A., Caput, D., Crum, C. et al. (1999). p63 is essential for regenerative proliferation in limb, craniofacial and epithelial development. *Nature* **398**, 714-8.

Ye, D., Guo, S., Al-Sadi, R. and Ma, T. Y. (2011). MicroRNA regulation of intestinal epithelial tight junction permeability. *Gastroenterology* **141**, 1323-33.

Yi, R., O'Carroll, D., Pasolli, H. A., Zhang, Z., Dietrich, F. S., Tarakhovsky, A. and Fuchs, E. (2006). Morphogenesis in skin is governed by discrete sets of differentially expressed microRNAs. *Nat Genet* **38**, 356-62.

Yi, R., Pasolli, H. A., Landthaler, M., Hafner, M., Ojo, T., Sheridan, R., Sander, C., O'Carroll, D., Stoffel, M., Tuschl, T. et al. (2009). DGCR8-dependent microRNA biogenesis is essential for skin development. *Proc Natl Acad Sci U S A* **106**, 498-502.

Yi, R., Poy, M. N., Stoffel, M. and Fuchs, E. (2008). A skin microRNA promotes differentiation by repressing 'stemness'. *Nature* **452**, 225-9.

Youssef, K. K., Van Keymeulen, A., Lapouge, G., Beck, B., Michaux, C., Achouri, Y., Sotiropoulou, P. A. and Blanpain, C. (2010). Identification of the cell lineage at the origin of basal cell carcinoma. *Nat Cell Biol* **12**, 299-305.

Yu, J., Ryan, D. G., Getsios, S., Oliveira-Fernandes, M., Fatima, A. and Lavker, R. M. (2008). MicroRNA-184 antagonizes microRNA-205 to maintain SHIP2 levels in epithelia. *Proc Natl Acad Sci U S A* **105**, 19300-5.

Zhang, L., Stokes, N., Polak, L. and Fuchs, E. (2011). Specific microRNAs are preferentially expressed by skin stem cells to balance self-renewal and early lineage commitment. *Cell Stem Cell* **8**, 294-308.